

**Surface Modification and Microwave-Assisted Synthesis of  
NiO/CNTs Composite as Chemical Sensitive Materials**

**PAPITCHAYA WOONTRANONT**

**A THESIS SUBMITTED IN PARTIAL FULFILLMENT  
OF THE REQUIREMENT FOR THE DEGREE OF  
MASTER OF SCIENCE IN NANOSCIENCE AND NANOTECHNOLOGY  
COLLEGE OF NANOTECHNOLOGY  
KING MONGKUT'S INSTITUTE OF TECHNOLOGY LADKRABANG**

**2012**

**KMITL-2012-NT-M-001-006**

การปรับปรุงสมบัติพื้นผิวของท่อนาโนคาร์บอนและการสังเคราะห์วัสดุคอมโพสิต  
เทคนิคเกลอออกไซด์และท่อนาโนคาร์บอนด้วยคลื่นไมโครเวฟเพื่อเป็นวัสดุไว  
สารเคมี

**Surface Modification and Microwave-Assisted Synthesis of  
NiO/CNTs Composite as Chemical Sensitive Materials**

ปพิชญา วูอินทรานนท์

**PAPITCHAYA WOINTRANONT**

วิทยานิพนธ์นี้สำหรับการศึกษาตามหลักสูตรปริญญาวิทยาศาสตรมหาบัณฑิต

สาขาวิชานาโนวิทยาและนาโนเทคโนโลยี

วิทยาลัยนาโนเทคโนโลยีพระจอมเกล้าลาดกระบัง

สถาบันเทคโนโลยีพระจอมเกล้าเจ้าคุณทหารลาดกระบัง

พ.ศ. 2555

**KMITL-2012-NT-M-001-006**

**Surface Modification and Microwave-Assisted Synthesis of  
NiO/CNTs Composite as Chemical Sensitive Materials**

**PAPITCHAYA WOINTRANONT**

**A THESIS SUBMITTED IN PARTIAL FULFILLMENT  
OF THE REQUIREMENT FOR THE DEGREE OF  
MASTER OF SCIENCE IN NANOSCIENCE AND NANOTECHNOLOGY  
COLLEGE OF NANOTECHNOLOGY  
KING MONGKUT'S INSTITUTE OF TECHNOLOGY LADKRABANG**

**2012**

**KMITL-2012-NT-M-001-006**

**COPYRIGHT 2012**

**COLLEGE OF NANOTECHNOLOGY**

**KING MONGKUT'S INSTITUTE OF TECHNOLOGY LADKRABANG**

<b>Thesis Title</b>	Surface Modification of Carbon Nanotubes and Microwave-Assisted Synthesis of NiO/CNTs Composite as Chemical Sensitive Materials
<b>Student</b>	Ms. Papitchaya Woontranont
<b>Student ID</b>	52670251
<b>Degree</b>	Master of Science
<b>Program</b>	Nanoscience and Nanotechnology
<b>Year</b>	2012
<b>Thesis Advisor</b>	Assoc. Prof. Dr. Wisanu Pecharapa

### ABSTRACT

In this thesis, the surface modification of carbon nanotubes and microwave-assisted synthesis of NiO/CNTs composite as chemical sensitive materials was conducted. The surface modification was carried out by three different methods including surfactant treatment, UV-ozone exposure and acid treatment. Series of treated-carbon nanotubes were characterized by UV-Visible Spectroscopy, the chemical properties of the nanocomposites were observed by Fourier transform infrared spectroscopy (FTIR) and Raman spectroscopy (Raman). The results indicated that, among three treatment methods, the UV-ozone treatment of CNTs greatly improves the dispersion stability and functionalization. After that, the mixture of Nickel chloride hexahydrate and treated CNTs was heated with different microwave irradiation powers at 150, 300 and 450 watts. The structural properties of the samples was determined by powder X-ray diffraction (XRD). The fine structure of the composite was investigated by Transmission Electron Microscopy (TEM) and scanning electron microscope (SEM) and the element analytical was characterized by Energy-dispersive X-ray spectroscopy (EDX). The result reveal that the NiO/UV-ozone treated CNTs have most distribution uniformity of NiO on the CNTs surface compared to another treatment method and the formation of NiO were tends to increase in accordance with the increasing of irradiation power. NiO/CNTs nanocomposites were applied as chemical sensitive electrodes for detecting hydrogen peroxide by Potentiostat and applied as alcohol gas sensor. The results suggests that the NiO/UV-ozone treated heated with microwave irradiation powers at 450 watts have more efficiency compared to the other conditions.

**Keywords:** Composite, Carbon nanotubes, Nickel Oxide, Microwave assisted

หัวข้อวิทยานิพนธ์	การปรับปรุงสมบัติพื้นผิวของท่อนาโนคาร์บอนและการสังเคราะห์วัสดุคอมโพสิตนิกเกิลออกไซด์และท่อนาโนคาร์บอนด้วยคลื่นไมโครเวฟเพื่อเป็นวัสดุไวสารเคมี
นักศึกษา	นางสาวปัทมา วุฒินทรานนท์
รหัสประจำตัว	52670251
ปริญญา	วิทยาศาสตร์มหาบัณฑิต
สาขาวิชา	นาโนวิทยาและนาโนเทคโนโลยี
พ.ศ.	2555
อาจารย์ที่ปรึกษาวิทยานิพนธ์	รศ.ดร.วิษณุ เพชรภา

### บทคัดย่อ

งานวิจัยนี้ได้ทำการปรับปรุงสมบัติพื้นผิวของท่อนาโนคาร์บอนและการสังเคราะห์วัสดุคอมโพสิตนิกเกิลออกไซด์และท่อนาโนคาร์บอนด้วยคลื่นไมโครเวฟเพื่อเป็นวัสดุไวสารเคมีโดยเริ่มจากการศึกษาผลกระทบและสมบัติของท่อนาโนคาร์บอนผนังหลายชั้นที่ได้รับการปรับปรุงพื้นผิวด้วยวิธีต่างๆ เช่น กรดซัลฟูริกกับกรดไนตริก สารละลายโซเดียมโอดีซิลซัลเฟตซึ่งเป็นสารลดแรงตึงผิว และการอบยูวีโอโซน จากนั้นนำไปวิเคราะห์สมบัติการกระจายตัวด้วยเครื่องวัดการดูดกลืนรังสียูวี (UV-Vis) และวิเคราะห์เชิงเคมีด้วยเครื่องวัดฟูเรียร์ทรานส์ฟอร์มอินฟราเรดสเปกโตรสโคปี (FTIR) และรามานสเปกโตรสโคปี (Raman) พบว่าการปรับปรุงพื้นผิวของท่อนาโนคาร์บอนด้วยวิธีอบโอโซน มีประสิทธิภาพในการกระจายตัวและการเกิดหมู่ฟังก์ชันที่ดีกว่าเมื่อเปรียบเทียบกับการใช้สารลดแรงตึงผิวและกรด จากนั้นนำไปสังเคราะห์วัสดุคอมโพสิตนิกเกิลออกไซด์/ท่อนาโนคาร์บอน ภายใต้ความร้อนจากคลื่นไมโครเวฟที่ค่ากำลัง 150 วัตต์ 300 วัตต์ และ 450 วัตต์ ซึ่งวัสดุคอมโพสิตที่ได้จะนำไปทำการวัดและวิเคราะห์เชิงโครงสร้างด้วยเครื่องวิเคราะห์การเลี้ยวเบนรังสีเอ็กซ์ (XRD) กล้องจุลทรรศน์อิเล็กตรอนแบบเลือนกราด (SEM) กล้องจุลทรรศน์อิเล็กตรอนแบบส่องผ่าน (TEM) และวิเคราะห์เพื่อยืนยันชนิดของธาตุด้วยเครื่องวิเคราะห์ธาตุด้วยการกระจายพลังงานรังสีเอ็กซ์ (EDX) ซึ่งจากผลการวิเคราะห์พบว่าการกระจายตัวของอนุภาคนิกเกิลออกไซด์บนพื้นผิวของท่อนาโนคาร์บอนที่ปรับปรุงพื้นผิวท่อนาโนคาร์บอนด้วยการอบยูวีโอโซนมีความสม่ำเสมอ และไม่เกิดการทำลายโครงสร้างของท่อนาโนคาร์บอนเมื่อเปรียบเทียบกับการใช้สารลดแรงตึงผิวและกรด นอกจากนี้ค่าการพอร์มตัวเป็นผลึกของอนุภาคนิกเกิลออกไซด์บนพื้นผิวของท่อนาโนคาร์บอนยังมีแนวโน้มที่เพิ่มขึ้นตามกำลังที่เพิ่มขึ้นของไมโครเวฟ เมื่อนำวัสดุคอมโพสิตที่ได้มาประยุกต์เป็นชิ้นงานสำหรับการวัดการเกิดปฏิกิริยาทางไฟฟ้าเคมีที่มีต่อสารละลายไฮโดรเจนเพอรอกไซด์ด้วยเครื่องวิเคราะห์ทางไฟฟ้าเคมี (Potentiostat) และประยุกต์ใช้เพื่อเป็นตัวตรวจวัดก๊าซแอลกอฮอล์ซึ่งพบว่าชิ้นงานไฟฟ้าทำงานและตัวตรวจวัดที่ทำจากวัสดุคอมโพสิตนิกเกิลออกไซด์และท่อนาโนคาร์บอนที่ปรับปรุงพื้นผิวด้วยการอบยูวีโอโซนภายใต้ความร้อนจากคลื่นไมโครเวฟที่ค่ากำลัง 450 วัตต์ มีประสิทธิภาพในการตรวจวัดดังกล่าวดีที่สุดเมื่อเทียบกับเงื่อนไขอื่นๆ

**คำสำคัญ :** วัสดุคอมโพสิต, นิกเกิลออกไซด์, ท่อนาโนคาร์บอน, การสังเคราะห์ด้วยคลื่นไมโครเวฟ

# ACKNOWLEDGMENT

This thesis is a product of two and a half years of my work in Nanomaterials Research Laboratory at College of Nanotechnology, King Mongkut's Institute of Technology Ladkrabang. Here, I was blessed that I met so many wonderful people who made my study and research enjoyable. First and foremost I would like to thank my advisor, Associate Professor Dr. Wisanu Pecharapa who believed in my potential from the very beginning and constantly supported me in my research. His readiness to help, openness for questions, and caring about his students makes him an outstanding graduate advisor. The respect and trust of my best advisor made me stronger and confident.

Second, I would like to thank the chair of my committee Dr. Sirapat Pratontep and my committee members, Dr. Winadda Wongwiriyan and Asst. Prof. Dr. Ratchapak Chitaree for taking time to critically review my Thesis. They were also in my proposal committee and I am very pleased and appreciate their efforts. They reviewed my proposal and actively discussed it with me.

I am indebted to the many people who influenced, helped and had fun in working with me when preparing this thesis, especially Miss Russameeruk Noonuruk. My profound thanks are conveyed to members of the Nanomaterials Research Laboratory who gave me so much assistance. Special thanks go to my vein group, who cheered, relaxed, helped and encouraged me.

I wish to acknowledge King Mongkut's Institute of Technology Ladkrabang for financial support.

Finally, I wish to dedicate this thesis to my beloved parents, Mr. Witaya and Mrs. Creuawan Wointranont and my beloved sister Miss Tananya and Miss Kulasub for their support, understanding, patience and constant love. Definitely, I can't finish my thesis without them.

Papitchaya Wointranont

# TABLE OF CONTENTS

	<b>Page</b>
<b>ABSTRACT (ENGLISH)</b>	I
<b>ABSTRACT (THAI)</b>	II
<b>ACKNOWLEDGMENT</b>	III
<b>LIST OF TABLES</b>	VIII
<b>LIST OF FIGURES</b>	VIII
<b>CHAPTER 1 INTRODUCTION</b>	
1.1 Introduction	1
1.2 Objectives of this work	3
1.3 Scope of this work	3
1.4 Expected Results	3
<b>CHAPTER 2 RELATED THEORY</b>	
2.1 Carbon Nanotubes	4
2.1.1 The Structure of Carbon nanotubes	4
2.1.2 Growth of Carbon Nanotubes	6
2.1.2.1 Arc-Discharge Technique	6
2.1.2.2 Laser-Ablation Technique	7
2.1.2.3 Chemical Vapor Deposition Technique	8
2.1.3 Electronic Properties of CNTs	9
2.1.4 Chemical and Electrochemical Properties	10
2.1.5 Chemical Fuctionalization in Carbon Nanotubes	11
2.1.6 Electrochemical and Gas sensor	13
2.2 Nickel Oxide	14
2.2.1 Nickel oxide applications	15
2.3 Nanocomposite	16
2.4 Microwave Assisted Process	18
2.5 Characterization Techniques in this research	19
2.5.1 Ultraviolet – Visible Spectrophotometer	19

# TABLE OF CONTENTS

	<b>Page</b>
2.5.2 X - ray Diffractometer	20
2.5.3 Scanning Electron Microscope	23
2.5.4 Transmission Electron Microscope	24
2.5.5 Infrared Spectroscopy	25
2.5.6 Raman Spectroscopy	27
2.5.7 Gas sensing Characterization	29
2.5.8 Voltammetry Technique	29
2.5.8.1 Cyclic Voltammetry	29
2.5.8.2 Chronoamperometry	30
2.6 Literature Reviews	31
 <b>CHAPTER 3 RESEARCH METHODOLOGY</b>	
3.1 Treatment Process of Carbon Nanotubes	33
3.1.1 Acid Treatment Procedure	33
3.1.1.1 Chemicals and Materials	33
3.1.1.2 Methodology	33
3.1.2 Surfactant Treatment Procedure	34
3.1.2.1 Chemicals and Materials	34
3.1.2.2 Methodology	34
3.1.3 UV Ozone Treatment Procedure	35
3.1.3.1 Chemicals and Materials	35
3.1.3.2 Methodology	35
3.2 Preparation of NiO/MWNTs composites	36
3.2.1 Chemicals and Materials	36
3.2.2 Methodology	36
3.3 Applications	37
3.3.1 NiO/MWNTs gas sensors fabrications	37
3.3.1.1 Chemicals and Materials	37
3.3.1.2 Methodology	37

# TABLE OF CONTENTS

	<b>Page</b>
3.3.2 Modification of NiO/MWNTs/FTO electrode	38
3.3.2.1 Chemicals and Materials	38
3.3.2.2 Methodology	39
3.4 Characterizations	39
3.4.1 The Dispersion stability	39
3.4.2 Ultraviolet Visible Spectrophotometer	39
3.4.3 X - ray Diffractometer	40
3.4.4 Scanning Electron Microscope	41
3.4.5 Transmission Electron Microscope	41
3.4.6 Fourier Transform Infrared Spectroscopy	41
3.4.7 Raman Spectroscopy	42
3.4.8 Gas sensing	42
3.4.9 Electrochemistry Characterization	43
 <b>CHAPTER 4 RESULTS AND DISCUSSION</b>	
4.1. Surface Modification of Multiwall Carbon nanotubes	44
4.1.1. The dispersion stability of surface modified MWNTs	44
4.1.2. The Fourier transform infrared spectroscopy results	46
4.1.3. The Raman spectroscopy results	47
4.2. NiO/MWNTs nanocomposites	49
4.2.1. NiO/surface modified MWNTs nanocomposites	49
4.2.1.1. XRD results	49
4.2.1.2. The Scanning Electron Microscopy results	50
4.2.1.3. The Energy-dispersive X-ray spectroscopy results	55
4.2.1.4. The Transmission Electron Microscopy results	56
4.2.2. NiO/UV-Ozone treated MWNTs nanocomposites with various irradiation powers	61
4.2.2.1. XRD results	61

4.2.2.2. The Scanning Electron Microscopy results	62
4.3.Applications of the NiO/MWNTs composite as chemical sensing materials	66
4.3.1. Gas sensing	66
4.3.2. Modified electrode	72
4.3.2.1. Cyclic Voltammetry measurement of NiO/MWNTs/FTO modified electrode	72
4.3.2.2. The electrocatalytic reduction of NiO/MWNTs /FTO modified electrode	74
<b>CHAPTER 5 CONCLUSIONS</b>	<b>75</b>
5.1. Surface Modification of Multiwall Carbon nanotubes	75
5.2. NiO/MWNTs nanocomposites	75
5.3. Applications	76
<b>REFERENCES</b>	<b>77</b>
<b>AUTHOR BIOGRAPHY</b>	<b>82</b>

# LIST OF TABLES

<b>Table</b>	<b>Page</b>
2.1. Properties of Nickel oxide	15
4.1. Raman data collected at room temperature on the different series of surface modified MWNTs	44

# LIST OF FIGURES

Figure	Page
2.1. (a) Single-walled carbon nanotubes (b) Multi-walled carbon nanotubes	4
2.2. All possible structures of CNT	5
2.3. Schematics of an arc-discharge apparatus	6
2.4. Schematics of laser ablation	8
2.5. Schematic diagram of the CVD apparatus	9
2.6. Different types of carbon nanotubes functionalization	13
2.7. Nickel oxide powder	14
2.8. Nickel oxide Structure	15
2.9. Typologies of the composite material orientation (a) continuous (b) discontinuous (c) random	17
2.10. Preparation of conventional heating and microwave heating	18
2.11. Schematic of microwave system	19
2.12. Ultraviolet-visible spectrophotometer system diagram	20
2.13. Ultraviolet-visible spectrophotometer	20
2.14. Schematic of X-ray diffractometer arrangement	21
2.15. X-ray diffractometers	22
2.16. Schematic of scanning electron microscopy	23
2.17. Field-emission scanning electron microscope	24
2.18. Schematic of transmission electron microscope	25
2.19. Schematic of fourier transform infrared spectroscopy	26
2.20. Fourier transform infrared spectroscopy	27
2.21. Schematic of Raman spectroscopy	28
2.22. Raman spectroscopy	29
2.23. (a) CV wave form (b) Cyclic voltammogram	30
3.1. Reflux system	33
3.2. Ultrasonication	34
3.3. UV-Ozone generator	35
3.4. Magnetic Sterrer	36
3.5. Microwave	37

# LIST OF FIGURES

Figure	Page
3.6. Interdigitated Electrode	37
3.7. SEM Images of (a) bare electrode (b) modified electrode using as-prepared composites	38
3.8. Ultraviolet Visible Spectrophotometer	39
3.9. X-ray diffractometer	40
3.10. Field Emission Scanning Electron Microscopy	41
3.11. Raman Spectroscopy	42
3.12. Diagram of sensor measurement system	42
3.13. Potentiostat	43
4.1. Dispersion stability of MWNTs with different treatment-method in DI water for various times	45
4.2. Absorption spectra of Raw MWNTs and the surface-modified MWNTs	45
4.3. FTIR spectra of saw MWNTs and the surface-modified MWNTs using three different processes	46
4.4. Raman spectra of Raw MWNTs and the surfac-modified MWNTs	47
4.5. Schematic of the carbon nanotubes with COOH group	48
4.6. XRD patterns of NiO/MWNTs nanocomposites prepared with different treatment method	50
4.7. The morphology of NiO/Raw-treated MWNTs illustrated by (a) Low magnification images of SEM (b) High magnification images of SEM	51
4.8. The morphology of NiO/Acid-treated MWNTs illustrated by (a) Low magnification images of SEM (b) High magnification images of SEM	52
4.9. The morphology of NiO/SDS-treated MWNTs illustrated by (a) Low magnification images of SEM (b) High magnification images of SEM	53

# LIST OF FIGURES

<b>Figure</b>	<b>Page</b>
<b>4.10.</b> The morphology of NiO/UV-treated MWNTs illustrated by (a) Low magnification images of SEM (b) High magnification images of SEM	54
<b>4.11.</b> EDX spectrum of NiO/MWNTs nanocomposite	55
<b>4.12.</b> EDX elemental mapping of Carbon, Oxygen and Nickel	55
<b>4.13.</b> The fine structure of (a) Low magnification of NiO/Raw-treated MWNTs (b) High magnification TEM image of NiO/Raw-treated MWNTs (c) HRTEM image of NiO/Raw-treated MWNTs nanocomposites	57
<b>4.14.</b> The fine structure of (a) Low magnification of NiO/Acid-treated MWNTs (b) High magnification TEM image of NiO/ Acid -treated MWNTs (c) HRTEM image of NiO/ Acid -treated MWNTs nanocomposites	58
<b>4.15.</b> The fine structure of (a) Low magnification of NiO/SDS-treated MWNTs (b) High magnification TEM image of NiO/Raw-treated MWNTs (c) HRTEM image of NiO/Raw-treated MWNTs nanocomposites	59
<b>4.16.</b> The fine structure of (a) Low magnification of NiO/UV ozone-treated MWNTs (b) High magnification TEM image of NiO/ UVozone -treated MWNTs (c) HRTEM image of NiO/ UVozone -treated MWNTs nanocomposites	60
<b>4.17.</b> XRD patterns of NiO/MWNTs composites prepared at different microwave irradiation powers	62
<b>4.18.</b> SEM images of NiO/MWNTs nanocomposite prepared at 150 watts	63
<b>4.19.</b> SEM images of NiO/MWNTs nanocomposite prepared at 300 watts	64
<b>4.20.</b> SEM images of NiO/MWNTs nanocomposite prepared at 450 watts	65
<b>4.21.</b> Sensing Performance of MWNTs, NiO and NiO/MWNTs nanocomposite	70

## LIST OF FIGURES

Figure	Page
4.22. Sensing Performance of NiO/surface modified MWNTs nanocomposites	71
4.23. Sensing Performance of NiO/UV-O <sub>3</sub> treated MWNTs nanocomposites with various irradiation powers	72
4.24. Cyclic voltammograms of bare electrode and modified electrode heat with irradiation powers	73
4.25. Amperometric response of the FTO electrode and NiO/MWCNT/FTO modified electrodes from successive 10mL additions of H <sub>2</sub> O <sub>2</sub> at 0.5V in 0.1M phosphate buffer solution with a stirring rate of ~300 rpm	74

# CHAPTER 1

## INTRODUCTION

### 1.1. Introduction

Carbon nanotubes (CNTs) has recently been among the most distinguished functional materials in modern science and engineering and has become an extensively studied and widely used material. Different forms of carbon ranging from carbon fibers and/or glassy carbon have been used for diverse electrochemical applications. Since first discovery, CNTs has received great attentions from scientists and technologists owing to their unique electrical, mechanical, and chemical properties. CNTs has been utilized as a novel functional material in various kinds of applications including biosensor, supercapacitor, field emission device and energy storage. To further improve their properties, one of the most effective techniques is suggested by modifying the functionalization of the surface of CNTs with a variety of organic, inorganic and metallic low-dimensional materials attached to the surface of CNTs. Carbon nanotubes has been suggested as a support material for the dispersion and stabilization of metal and semiconductor nanoparticles. Recently, there have been a number of researches emphasized on the synthesis of nanocomposites of metal oxide/CNTs as potentially applicable materials in optics, electronics and chemistry. In electrochemical applications, CNTs has been usually used as compatible material for metal oxide based composites. Among metal oxide nanostructures, nickel oxide is known as potential functional material in wide range of applications such as catalyst, fuel cell, magnetic-based devices, electrochemical batteries, accompanying its outstanding properties including excellent chemical stability, fascinating optical, magnetic and electrical properties. However, due to the chemical stability and highly hydrophobic nature of CNTs, surface modification of CNTs is the first important step for developing high-performance CNTs/metal oxide composites and increasing their dispersion stability. Chemical functionalization is method that can improve its functionalized properties to ensure good physical and electrical contact between the CNTs and metal oxide nanoparticles. Acid-treated CNTs generally contain carboxylic acid and hydroxyl groups, which are the most commonly functional groups on CNTs. Although this process can increase the dispersion property, it can also have a detrimental effect on the conductivity of the composites because of the morphological

damage. Several studies have pioneered to study the effects of surfactant on dispersibility and other related properties of CNTs. On the other hand, UV-Ozone dry treatment is found to be an effective and relatively simple surface modification process. It has been reported that insignificant severe morphological damages commonly observed in the case of a conventional acid treatment such as shortening or sharp bending were observed after UV-ozone treatment. It has also been reported that NiO/MWNTs composite nanostructures have been synthesized by various methods such as chemical precipitation, direct thermal decomposition, and chemical vapor deposition and exhibited excellent functional properties for practical applications. However, for an economical purpose, a facile, effective, rapid, and low-cost technique to synthesize the composite systems is mandatory. Because of significant advantages over conventional heating such as non-contact, instantaneous and rapid heating rate resulting in the reduction of reaction time, and uniform heat transfer, microwave irradiation as an energy source has been successfully utilized to synthesize various kinds of functional materials such as nanocrystalline structures, nanoparticles, and composite materials.

In this work, the surface modification of CNTs including acid mixtures, surfactant and UV-Ozone on were conducted and investigated. the synthesis of NiO/MWNTs nanocomposites by microwave-assisted method using as-modified CNTs for starting material. The effects of surface modification methods and microwave irradiation power on relevant properties of CNTs and as-prepared composites were scrutinized.. Moreover, as-synthesized composites were utilized as modified materials of electrochemical working electrode and their electrocatalytic activities towards hydrogen peroxide were performed. The gas sensing performance of as-prepared composites toward alcohol gas was additionally carried out and the sensing mechanisms are proposed and discussed.

## 1.2. Objectives of this work

This research is conducted in order to

1. Study the effects of surface modification on the dispersion and the existence of functional groups on carbon nanotubes.
2. Study the effects of surface modification of carbon nanotubes on the formation of NiO/MWNTs nanocomposites.
3. Study the effects of microwave irradiation powers on significant properties of the composites.
4. Study chemical sensing properties of as-prepared composites.

## 1.3. Scope of this work

The scope of this study is as follows,

1. Study on the theory of major materials (carbon nanotubes, nickel oxide).
2. Study on the effects of surface modification on the physical and structural properties of carbon nanotubes.
3. Study on the influence of surface modification method on the formation of NiO/MWNTs nanocomposites.
4. Investigate the chemical sensing performance of as-synthesized composites prepared under various conditions.
5. Study on the performance of the modified working electrode and modified gas sensor using NiO/MWNTs nanocomposites for detecting hydrogen peroxide and alcohol gas, respectively.

## 1.4. Expected Results

1. Important theories of major materials and their functionalities will be clearly understood.
2. Effects of surface modification on the important properties of carbon nanotubes and the formation of NiO/MWNTs nanocomposites will be acknowledged.
3. Potential advantages of NiO/MWNTs nanocomposites are utilized.
4. Optimized preparation condition of the composites for practical applications can be notified.

## CHAPTER 2

# THEORETICAL BACKGROUND

### 2.1. Carbon Nanotubes

Carbon nanotubes (CNTs) are hexagonal shape arrangement of carbon atoms that are rolled into tubes. They are one of the most attractive materials with extraordinary properties being discovered in the last decade. The unique structure of carbon nanotubes provides fascinating structure with extraordinary mechanical and electrical properties. The outstanding properties that these materials have opened new interesting research areas in nanoscience and nanotechnology.

#### 2.1.1. Structure of Carbon Nanotubes

Carbon nanotubes can be visualized as a modified form of graphite. Graphite is formed from many layers of carbon atoms that are bonded in hexagonal pattern in flat sheets, with weak bonds between the sheets and strong bonds within them. Carbon nanotubes can be thought as a sheet or sheets of graphite that have been rolled up into tube structure. Carbon nanotubes can be formed as Single Walled Carbon Nanotubes (SWNT) (Fig. 2.1(a)), as if a single sheet had been rolled up, or Multi Walled Carbon Nanotubes (MWNT) (Fig. 2.1(b)), similar in appearance to a number of sheets rolled together [1].

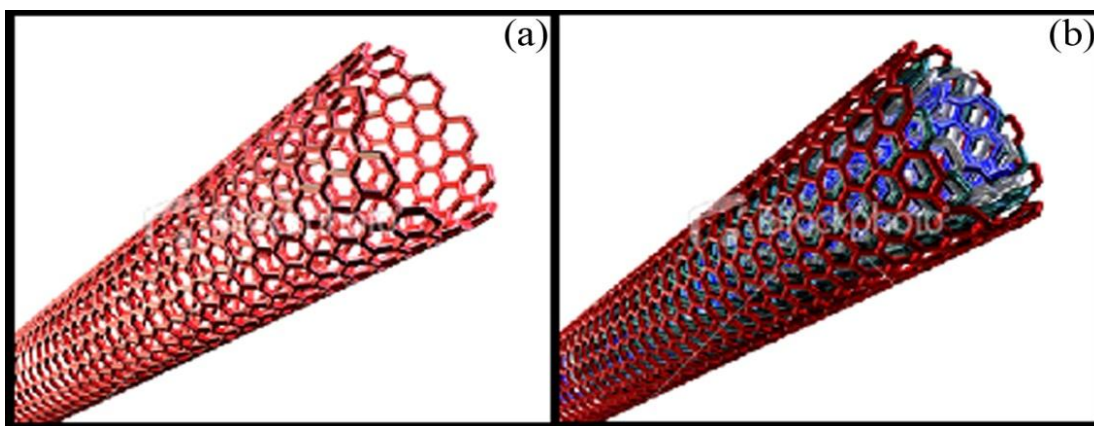


**Figure 2.1** (a) Single-walled carbon nanotubes (b) Multi-walled carbon nanotubes [2-3]

The simplest way to specify structure of an individual tube is in terms of a vector labeled as  $C$  joining two equivalent points on the original graphene lattice. The cylinder is produced by rolling up the sheet such that two end-points of the vector are superimposed. Because of the symmetry of the honeycomb lattice, many of the cylinders produced in this way will be equivalent but there is an ‘irreducible wedge’ comprising one-twelfth of the graphene lattice within which unique tube structures are defined. Figure 2.2 shows a small part of this irreducible wedge with points on the lattice. Each pair of integers  $(n,m)$  represents a possible tube structure. Thus the vector  $C$  can be expressed as

$$C = na_1 + ma_2 \quad (2.1)$$

Where  $a_1$  and  $a_2$  are the unit cell base vectors of the graphene sheet and  $n \geq m$ . As seen in Figure 2.2,  $m = 0$  for all zigzag tubes while  $n = m$  for all armchair tubes. The electronic behavior of carbon nanotubes depends on their chirality. Armchair tubes are metallic, while other tubes are semiconductors. In addition, the degree of conductivity or semiconductivity can be typically controlled by doping.

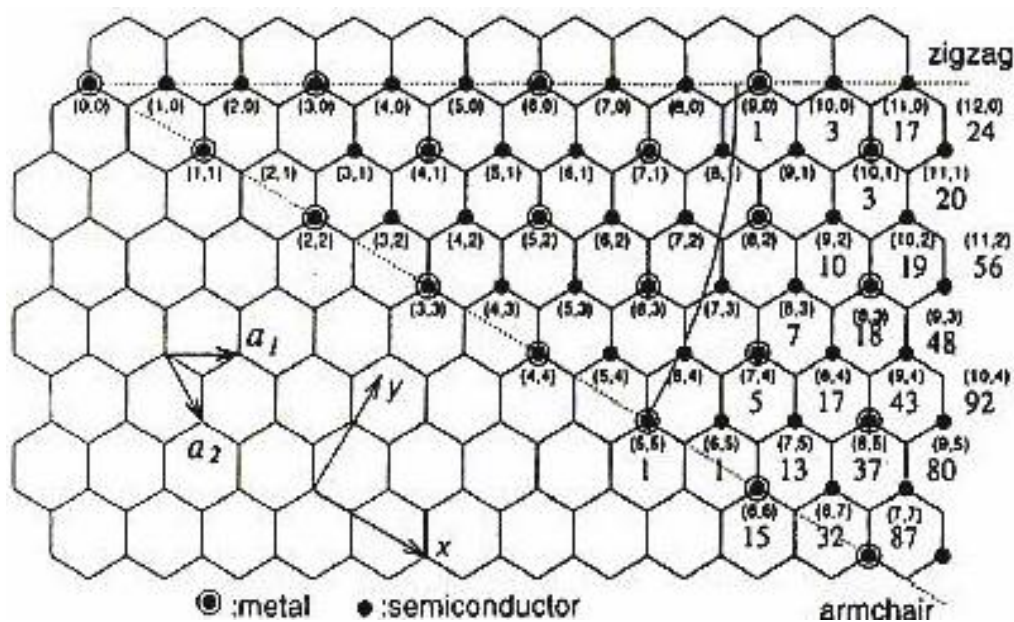


**Figure 2.2** All possible structures of CNTs [4]

## 2.1.2. Growth of Carbon Nanotubes

### 2.1.2.1. Arc-Discharge Technique

Two carbon electrodes are generally used in the carbon arc-discharge technique to generate an arc by DC current. The electrodes are kept in a vacuum chamber and an inert gas is supplied to the chamber as illustrated in Fig. 2.3. The purpose of the inert gas is to increase the speed of carbon deposition. Initially, the two electrodes are kept independent and separately. Once the pressure is stabilized, the power supply is turned on (about 20 V) and the cathode is then gradually brought closer to the anode to generate an electric arc. On arcing, the electrodes become red hot and a plasma forms. Once the arc stabilizes, the rods are kept about a millimeter apart while the CNTs deposition is initiated on the negative electrode. The power supply is cut-off and the machine is left for cooling while a specific length is reached. The most important parameters to be concerned with in this method are: (i) the control of arcing current and (ii) the optimal selection of inert gas pressure in the chamber. Typically, Arc-discharge technique produces high quality CNTs. While SWNTs can only be grown in presence of a catalyst, MWNTs do not need a catalyst for growth. MWNTs can be obtained by controlling the pressure of inert gas in the discharge chamber and the arcing current. Normally, the by-products of MWNTs are polyhedron shaped multi-layered graphitic particles. The MWNTs produced by arc-discharge method were highly crystalline and were bound together by strong van der Waals forces. SWNTs with diameters  $\sim 1$  nm were synthesized by Ijima and Ichihashi using a gas mixture of 10 Torr methane and 40 Torr Argon at current of 200 A and a voltage of 20 V [5].

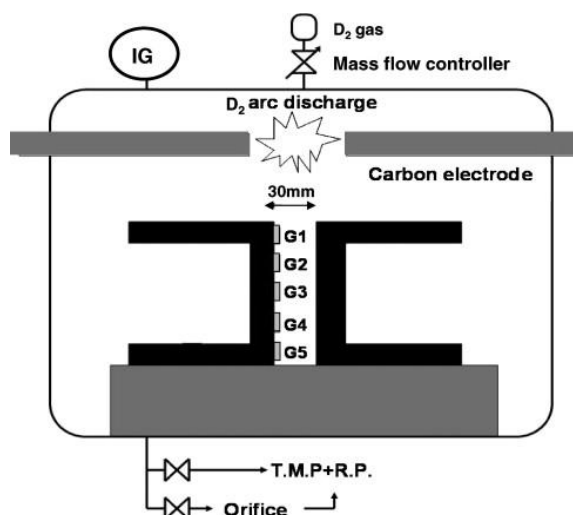


**Figure 2.3** Schematics of an arc-discharge apparatus [6]

### **2.1.2.2. Laser-Ablation Technique**

Laser ablation is the process of removing material from a solid (or occasionally liquid) surface by irradiating it with a laser beam. At low laser flux, the material is heated by the absorbed laser energy and evaporates or sublimates. At high laser flux, the material is typically converted to a plasma. Usually, laser ablation refers to the removal of material with a pulsed laser, but it is possible to ablate material with a continuous wave laser beam if the laser intensity is high enough. The depth over which the laser energy is absorbed, and thus the amount of material removed by a single laser pulse, depend on the material's optical properties and laser wavelength. Laser pulses can vary over a wide range of duration (millisecond to femtosecond) and fluxes, can be precisely controlled. This makes laser ablation very valuable for both research and industrial applications. The simplest application of laser ablation is to remove material from a solid surface in a controlled fashion. Laser machining and particularly laser drilling are examples; pulsed lasers can drill extremely small, deep holes through very hard materials. Very short laser pulses remove material so quickly that the surrounding material absorbs very little heat, so laser drilling can be done on delicate or heat-sensitive materials, including tooth enamel. Also, laser energy can be selectively absorbed by coatings, particularly on metal, so CO<sub>2</sub> or Nd:YAG pulsed lasers can be used to clean surfaces, remove paint or coating, or prepare surfaces for painting without damaging the underlying surface. High power lasers clean a large spot with a single pulse. Lower power lasers use many small pulses which may be scanned across designated area. The advantages of this technique are no solvents, so it is environmentally friendly and operators are not exposed to chemicals. It is relatively easy to automate, e.g., by using robots. The running costs are lower than dry media or CO<sub>2</sub> ice blasting, although the capital investment costs are much higher. The process is gentler than abrasive techniques, e.g. carbon fibers within a composite material are not damaged. Heating of the target is minimal. Another class of applications uses laser ablation to proceed removal process of the material into new forms either not possible or difficult to produce by other means [7].

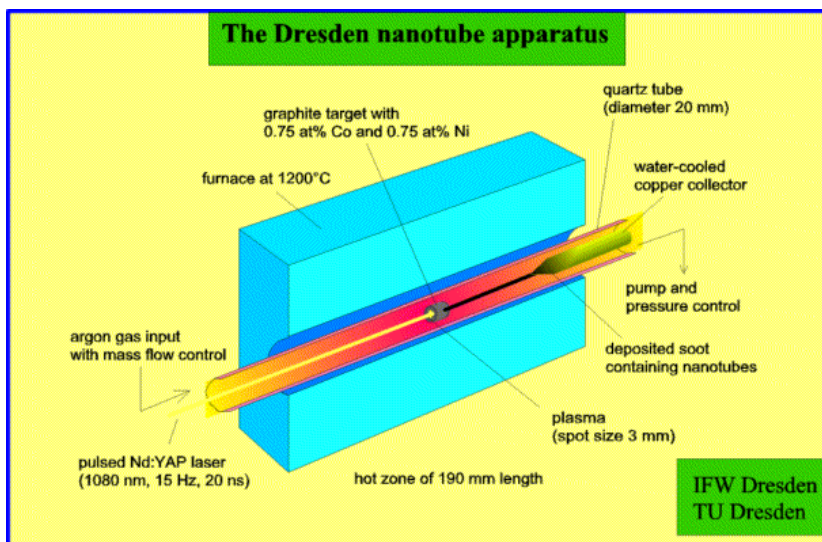


**Figure 2.4** Schematics of Laser ablation [8]

### 2.1.2.3. Chemical Vapor Deposition Technique

Chemical vapor deposition (CVD) synthesis is achieved by putting a carbon source in the gas phase and using an energy source, such as plasma or a resistively heated coil, to transfer energy to a gaseous carbon molecule. Commonly used gaseous carbon sources include methane, carbon monoxide and acetylene. The energy source is used to "crack" the molecule into reactive atomic carbon [9]. Then, the carbon diffuses towards the substrate, which is heated and coated with a catalyst (usually a first row transition metal such as Ni, Fe or Co) where it will bind. Carbon nanotubes will be formed if the proper parameters are maintained. Excellent alignment, as well as positional control on nanometer scale, can be achieved by using CVD. Control over the diameter, as well as the growth rate of the nanotubes can also be maintained. The appropriate metal catalyst can preferentially grow single rather than multiwalled nanotubes.

CVD carbon nanotubes synthesis is essentially a two-step process consisting of a catalyst preparation step followed by the actual synthesis of the nanotubes. The catalyst is generally prepared by sputtering a transition metal onto a substrate and then using either chemical etching or thermal annealing to induce catalyst particle nucleation. Thermal annealing results in cluster formation on the substrate, from which the nanotubes will grow. Ammonia may be used as the etchant. The temperatures for the synthesis of nanotubes by CVD are generally within the 600-1200 °C range. Typical yield for CVD is approximately 30%.

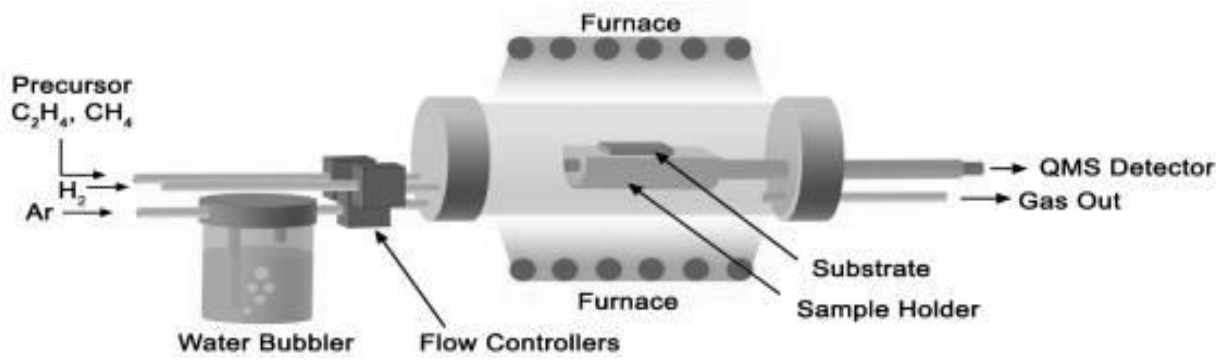


**Figure 2.5** Schematic diagram of the CVD apparatus [10]

A comparison among these three CNTs synthesis techniques indicates that arc-discharge and laser-ablation methods produce high yields (>70%) of SWNTs, and the cost of producing CNTs by arc-discharge method is much cheaper. However, the main disadvantages with these processes are tangled CNTs that make the purification and applications of CNTs difficult and these processes rely on evaporation of carbon atoms at temperatures >3000 °C. In addition to materials scale-up, CVD technique offers controlled synthesis of aligned and ordered CNTs. Although the microstructure of the CNTs tips synthesized by CVD technique have well-formed caps compared to other techniques, they often have interrupted graphite layers. In applications such as scanning probe microscopy, tips are very important. Although CVD process appears technologically easier, the required quality of tips can be made by arc-discharge method.

### 2.1.3. Electronic Properties of CNTs

Electronic properties of nanotubes have received great attention in nanotubes research and applications. Extremely small size and the highly symmetric structure allow remarkable quantum effects and electronic, magnetic, and lattice properties of the nanotubes [11].

In the simplest model, the electronic properties of a nanotubes can be derived from the dispersion relation of a graphite sheet with the wave vectors ( $k_x, k_y$ )

$$E(k_x, k_y) = \pm \gamma \left\{ 1 + 4 \cos \left( \frac{\sqrt{3} k_x a}{2} \right) \cos \left( \frac{k_y a}{2} \right) + 4 \cos^2 \left( \frac{k_y a}{2} \right) \right\}^{1/2} \quad (2.2)$$

Where  $\gamma$  is the nearest neighbor-hopping parameter and  $a$  is lattice constant.  $\gamma = 2.5\text{-}3.2$  eV from different sources and  $a = 0.246$  nm. When the graphite is rolled over to form a nanotubes, a periodic boundary condition is imposed along the tube circumference or the C direction. This condition quantizes the two-dimensional wave vector  $k = (k_x, k_y)$  along this direction.

More theoretical attention has been paid to the electronic properties of heterogeneous nanotubes, especially bent and branched structures. There are three main features for these structures. First, these structures are molecular mimics of 2- or 3-terminal heterojunctions that connect two or three different nanotubes in the form of A-B or A-B-C in which A, B or C can be a metallic or semiconducting tube. Second, localized states appear in the junction interface containing pentagons and heptagons. Third, the interface may or may not be conducted, depending on how tubes are connected. For example, a (9,0)(6,3) tube junction is not conducted for symmetric match but conducted for asymmetric match. The symmetric match retains straight tube geometry, which is difficult to be observed experimentally. Asymmetric match leads to a bend structure. Localized states are originated from pentagons and heptagons incorporated in a hexagonal network. They are also observed in capped SWNT and MWNT ends. These localized states are responsible for enhanced field emission and interface states at nanotubes junctions.

The novel electronic properties of nanotubes have attracted great interest in nanoelectronics applications. Much of the effort to date has been made in using individual semiconductor SWNTs for transistors, memories and logic devices. The striking feature of these nanoelectronic devices are in higher mobility and stronger field effect. In addition, nanotubes junctions such as sharp bends and T and Y branches have been studied as nanoelectronics devices. Furthermore, the electronic properties have been correlated with mechanical, chemical, biological, thermal and magnetic interactions with nanotubes.

#### **2.1.4. Chemical and Electrochemical Properties**

Small radius, large specific surface and  $\sigma$ - $\pi$  rehybridization make CNTs very attractive in chemical and biological applications because of their strong sensitivity to chemical or environmental interactions. However, it also presents challenges in characterization and understanding of other properties. The chemical

properties of interest include chemical and biological separation, purification, sensing and detection, energy storage and electronics. The nanotubes end is more reactive than the sidewall because of the presence of pentagons or metallic catalysts sitting on the opened ends and greater curvature. Many approaches have been used to open nanotubes ends. For example, vapor phase oxidation, plasma etching and chemical reaction using acids such as  $\text{HNO}_3$  and  $\text{H}_2\text{SO}_4$ . The opened end is terminated with different functional groups such as carboxyl.

Nanotubes are hydrophobic and do not show wetting behavior for most aqueous solvents. It is reported that various organic solvents,  $\text{HNO}_3$ ,  $\text{H}_2\text{SO}_4$ , S, Cs, Rb, Se and various oxides such as Pb and  $\text{Bi}_2\text{O}_2$  can wet nanotubes. A nanotubes provides a capillary pressure that is proportional to  $1/D$ . Therefore, these wetting agents can be driven to fill inside the nanotubes by the capillary pressure. It is also likely to fill non-wetting agents inside nanotubes by applying pressure that is higher than the capillary pressure. An effectively alternative method is to use wetting agents such as  $\text{HNO}_3$  to assist filling of non-wetting agents inside the nanotubes.

#### **2.1.5. Chemical Functionalization in Carbon Nanotubes**

Many of the Carbon nanotubes proposed applications in composite materials, molecular electronics, sensors, etc require an understanding and control of the chemistry or chemical reactivity of carbon nanotubes which have been shown to be strongly dependent on the development of strategies for functionalizing because their surface is rather inert, rendering very difficult any type of the mentioned mechanisms. The several approaches for functionalization of CNTs that have been developed can be classified as defect-site chemistry, covalent side-wall functionalization and non-covalent functionalization (Figure 2.6).

The efficiency of the chemical bonding of the end caps or the sidewalls of carbon nanotubes will determine where the chemically sensitive reactions occur and how these change the mechanical or electrical properties. The defect-side chemistry exploits the intrinsic defect sites both at the end and on the sidewalls of the CNTs as a result of the synthesis process. In addition, the purification process of the CNTs involves the use of strong acids to remove the catalytic particles necessary for the synthesis, due to their oxidative reaction. This process ends up in holes with oxygenated functional groups like carboxylic acids or alcohol groups which are promising starting points for the attachment of particles on the sidewalls of CNTs.

The functionalization on the sidewalls of carbon nanotubes can be used to increase bonding or linking of nanotubes on the nanotubes-matrix composite material and can also be used for chemical or gas sensor application.

The covalent sidewall functionalization is one of the promising methods of modifying electric properties of carbon nanotubes for many applications which is based on the chemical reactivity of the CNTs, related with the sp<sup>2</sup>-hybridized carbon atoms and the  $\pi$ -orbital misalignment between adjacent carbon atoms which are scaled inversely with tube diameter and become more reactive tubes as decreasing their diameter. This agrees with the fact that fullerenes have a higher reactivity surface which depends strongly on their curvature compared to CNTs which have no strongly curved regions that could serve for direct additions. This statement also explains why side-functionalization of CNTs by covalent-bond formation needs highly reactive reagent.

The endohedral functionalization comprises the use of the inner cavity of the CNTs for the storage of molecules or compounds since their interaction takes place with the inner surface of the sidewalls, very convenient for confined reactions inside the CNTs.

The non-covalent functionalization comprises the dispersion of CNTs in solution by means of surface active molecules as sodium dodecylsulfate (SDS) which accommodates the CNTs in their hydrophobic interiors or sometimes by strong  $\pi$ - $\pi$  – stacking interactions with the CNTs sidewall if the hydrophobic part contains an aromatic group and/or by wrapping them with polymers which implies an association of the polymers with the sides of the CNTs based on the hydrophobic thermodynamic preference of CNTs-polymer interactions compared to CNTs-water interactions, thereby suppressing the hydrophobic surface of the CNTs.

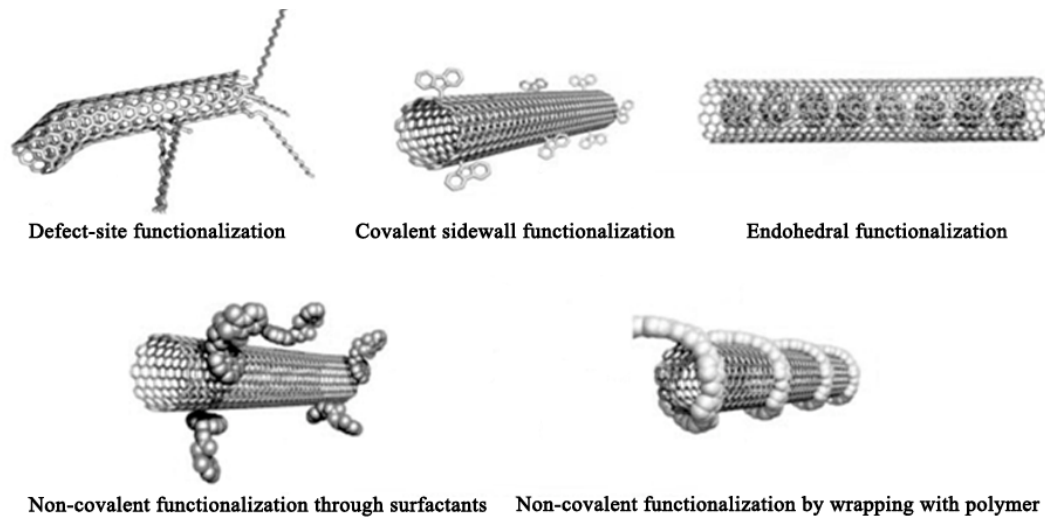


**Figure 2.6** Different types of Carbon nanotubes functionalization [12]

### 2.1.6. Electrochemical and Gas sensor

Electrochemistry implies the transfer of charge from one electrode to another electrode. This means that at least two electrodes constitute an electrochemical cell to form a closed electrical circuit. Another important aspect of electrochemical sensors is that the charge transport within the transducer part of the whole circuit is always electronic [13]. On the other hand, the charge transport in the sample can be electronic, ionic or both. Due to the curvature of carbon graphene sheet in nanotubes, the electron clouds change from a uniform distribution around the C-C backbone in graphite to an asymmetric distribution inside and outside the cylindrical sheet of the nanotubes. Because the electron clouds are distorted, a rich  $\pi$ -electron conjugation forms outside the tube, therefore making the CNTs electrochemically active. Electron donating and withdrawing molecules such as  $\text{NO}_2$ ,  $\text{NH}_3$ ,  $\text{O}_2$  will either transfer electrons to or withdraw electrons from single-walled carbon nanotubes (SWNTs), thereby giving SWNTs more charge carriers or holes, respectively, which increases or decreases the SWNTs conductance. Typical electrochemical interaction may denoted as :



where  $\delta$  is a number that indicates the amount of charge transferred during the interaction.

## 2.2. Nickel Oxide

Nickel oxide is the chemical compound with the formula NiO. It is notable as being the only well characterized oxide of nickel. The mineralogical form of NiO, bunsenite, is very rare. It is classified as a basic metal oxide. Several million kilograms are produced in varying quality annually, mainly as an intermediate in the production of nickel alloys. Nickel oxide can be prepared by multiple methods. Upon heating above 400 °C, nickel powder reacts with oxygen to give nickel oxide. In some commercial processes, green nickel oxide is made by heating a mixture of nickel powder and water at 1000 °C, the rate for this reaction can be increased by the addition of nickel oxide. The simplest and most successful method of preparation is through pyrolysis of a nickel(II) compounds such as the hydroxide, nitrate, and carbonate, which yield a light green powder. Synthesis from the elements by heating the metal in oxygen can yield grey to black powders which indicates nonstoichiometry [13].

Nickel oxide adopts the NaCl structure, with octahedral Ni(II) and O<sup>2-</sup> sites. The conceptually simple structure is commonly known as the rock salt structure. Like many other binary metal oxides, Nickel oxide is often non-stoichiometric, meaning that the Ni:O ratio deviates from 1:1. In nickel oxide this non-stoichiometry is accompanied by a color change, with the stoichiometrically correct NiO being green and the non-stoichiometric NiO being black.



**Figure 2.7** Nickel oxide powder [14]

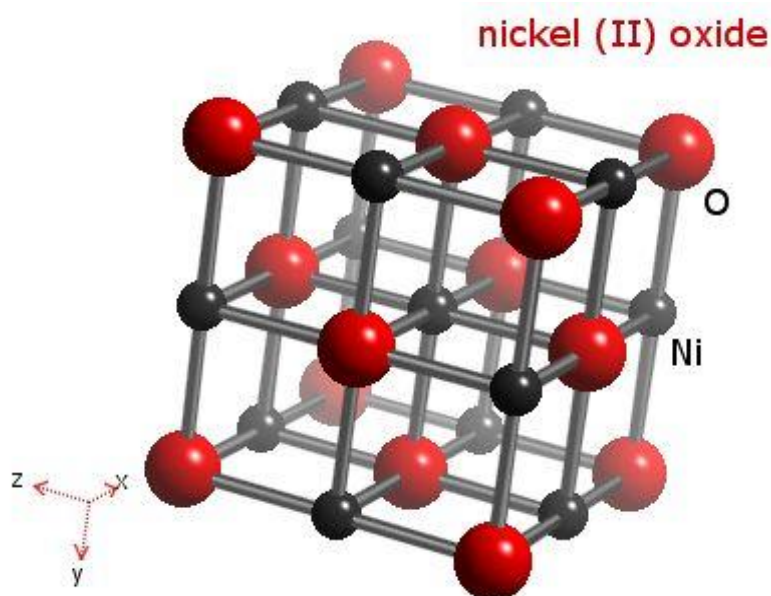


**Figure 2.8** Nickel oxide structure [15]

**Table 2.1** Properties of Nickel oxide

<b>IUPAC name</b>	Nickel(II) oxide
<b>Other names</b>	Nickel monoxide
<b>Molecular formula</b>	NiO
<b>CAS number</b>	1313-99-1
<b>Molar mass</b>	74.6928 g/mol
<b>Appearance</b>	green crystalline solid
<b>Density</b>	6.67 g/cm <sup>3</sup>
<b>Melting point</b>	1955 °C, 2228 K, 3551 °F
<b>Geometry of nickel:</b>	6 coordinate: octahedral
<b>Crystal system</b>	Cubic
<b>Crystal structure:</b>	Rock salt-type structure

### 2.2.1. Nickel oxide applications

NiO has a variety of specialized applications and general applications distinguished between chemical which is relatively pure material for specialty applications and metallurgical grade which is mainly used for the production of alloys. It is used in the ceramic industry to make frits, ferrites, and porcelain glazes.

The sintered oxide is used to produce nickel steel alloys. NiO was also a component in the Nickel-iron battery, also known as the Edison Battery, and is a component in fuel cells. It is the precursor to many nickel salts, for use as specialty chemicals and catalysts. More recently, NiO was used to make the NiCd rechargeable batteries found in many electronic devices until the development of the environmentally superior Lithium Ion battery. About 4000 tons of chemical grade NiO are produced annually. Black NiO is the precursor to nickel salts, which arise by treatment with mineral acids. NiO is a versatile hydrogenation catalyst. Heating nickel oxide with either hydrogen, carbon, or carbon monoxide reduces it to metallic nickel. It combines with the oxides of sodium and potassium at high temperatures ( $>700$  °C) to form the corresponding nickelate.

### **2.3. Nanocomposite**

Nanocomposite is a matrix which nanoparticles are added to improve the properties of the material. The definition of nanocomposite material has significantly broadened to encompass a large variety of systems such as one-dimensional, two-dimensional, three-dimensional and amorphous materials, made of distinctly dissimilar components and mixed at the nanometer scale. The significant effort of nanocomposite is focused on the ability to obtain control of the nanoscale structures via innovative synthetic approaches. The properties of nanocomposite materials depend not only on the properties of their individual main material but also on the morphology and interfacial characteristics which generated many exciting new materials with novel properties that can be derived by combining properties from the parent constituents into a single material. There is also the possibility of new properties which are unknown in the parent constituent materials [16].

The orientation of the guest material relative to the concentration and the distribution which have a significant influence on the strength and other properties of composites. With respect to the orientation, there are two extremes are possible, the first is a parallel alignment of the longitudinal axis of the material in a single direction and the second is a totally random alignment. The continuous composite material are normally aligned (Figure 2.9a), whereas discontinuous composite material may be aligned (Figure 2.9b), randomly oriented (Figure 2.9c). When the composite material orientation is random, short and discontinuous composite material are used. The

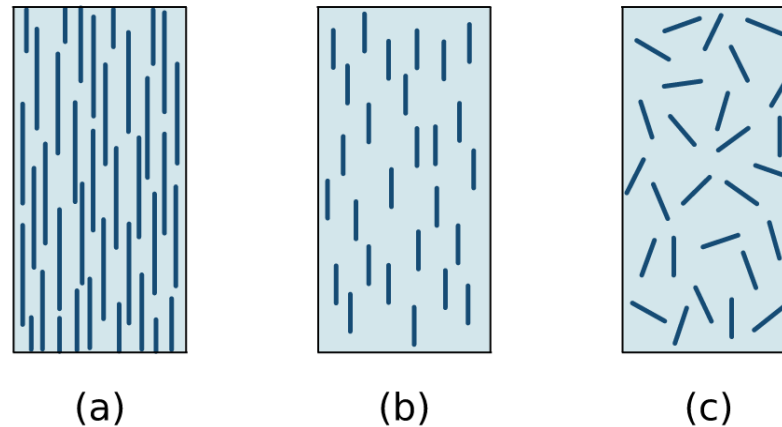


**Figure 2.9** Typologies of the composite material orientation (a) continuous (b) discontinuous (c) random

schematically of this type are demonstrated in Figure 2.9c. Under these circumstances, a "rule-of-mixtures" expression for the elastic modulus similar to equation 15.10a may be utilized, as follows:

$$E_{cd} = KE_f V_f + E_m V_m \quad (2.3)$$

In this expression,  $K$  is a composite material efficiency parameter, which depends on  $V_f$  and the  $E_f/E_m$  ratio. The magnitude will be less than unity and usually in the range 0.1 to 0.6. Thus, for random composite material (as with oriented), the modulus increases in some proportion of the volume fraction of composite material.

One of the important nanocomposites is carbon nanotubes nanocomposite which emerging new material that are being developed to take advantage of the high tensile strength and electrical conductivity of carbon nanotubes materials such as carbon nanotubes and metal oxide nanocomposites which possessing microstructure, electrical conductivity and mechanical properties [17]. The "no defect" description of CNTs is probably sparked an interest in developing nanotubes-metal oxide composites. Carbon nanotubes have been plagued with bonding and reaction issues in metal oxide, and the absence of defects suggests these issues may be evaded. Three main processing routes to produce the composites are being explored and are directed toward producing nanotubes nanostructures, advanced alloys, nanocrystalline materials, coatings, and bulk composites. To promote the development of the composites of various types and sizes, wetting and adhesion of metals to the

nanotubes are very important. Therefore, various routes for improving the wetting are necessary in order to achieve strong interactions between the nanotubes and the matrix. Even with identified ways to promote interactions, many of the processing modes used to date involve processing of the metals when in contact with the nanotubes to provide for nanotubes stability.

## 2.4. Microwave Assisted Process

The microwave-assisted process (MAP) is a simple technology that can be readily understood in terms of the operating step to be performed. MAP also be a relatively novel method of extracting soluble products into a fluid from a wide range of materials using microwave. It offers many advantages over currently used technologies that involve solvent extraction such as reduced energy consumption, smaller volumes of chemical solvents, use of less toxic solvents, and smaller quantity of waste products [18].

Recently, a microwave-assisted synthesis is an enabling technology that has been extensively used in organic synthesis. Microwave-assisted modification of CNTs is non-invasive, simple, fast, environmentally friendly, and clean method as compared to traditional methods. Usually, the use of the microwave facilitates and accelerates reactions, often improving relative yields. In case of microwave-assisted functionalization of CNTs, microwave irradiation of CNTs reduces the reaction time and gives rise to products with higher degrees of functionalization than those obtained by the conventional thermal methods.

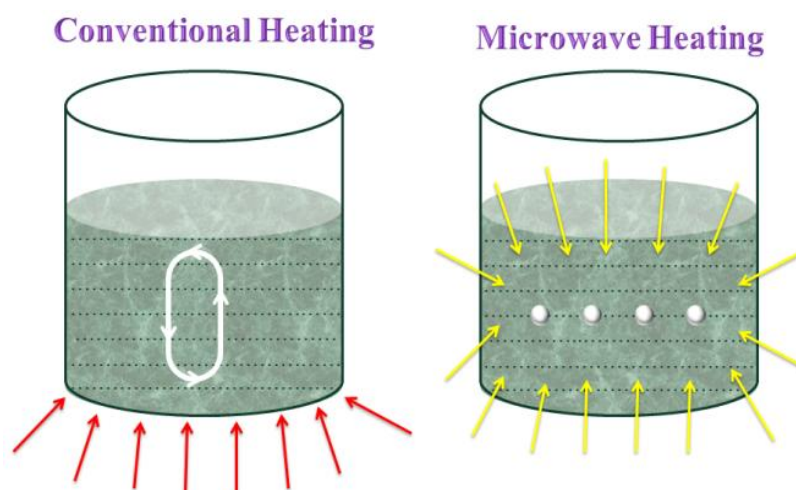


**Figure2.10** Preparation of conventional heating and microwave heating

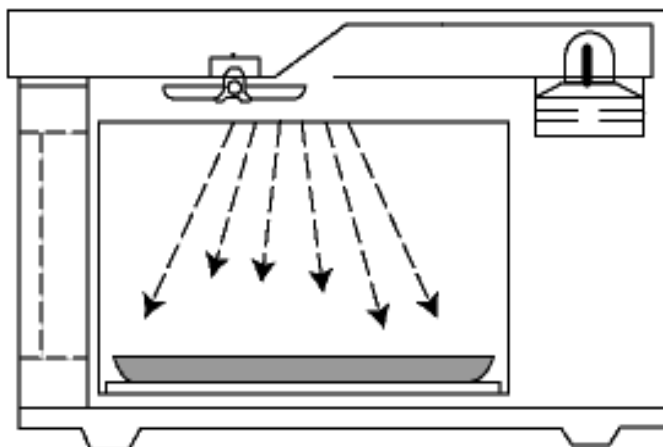


**Figure2.11** Schematic of microwave system

## 2.5. Characterization Techniques in this research

### 2.5.1. Ultraviolet – Visible Spectrophotometer (UV-Vis)

The range covered by UV-visible spectrophotometers generally extends at its lower end down to between 165-210 nm. The upper limit is never less than about 650 nm and may reach 1000 nm or even further. The double beam design provides two equivalent paths for radiation, both originating with the same source. The monochromatic beam of radiation is split or chopped into two components, usually of equal radiant power. One beam passes through the sample and the other through a reference solution or blank. However, the radiant power in the reference beam varies with the source energy, monochromator transmission, reference material transmission and detector response, all of which vary with wavelength. If the output of the reference beam can be kept constant, then the transmittance of the sample can be recorded directly as the output of the sample beam.

The relation of the double beam can be clarified by the Beer's law :

$$A = \log \frac{P_0}{P} \quad (2.3)$$

Where  $A$  is the absorbance value, corrected for absorbance in the reference material.  $P_0$  is the power of the beam coming from the source.  $P$  represents the power transmitted through the sample and reference.

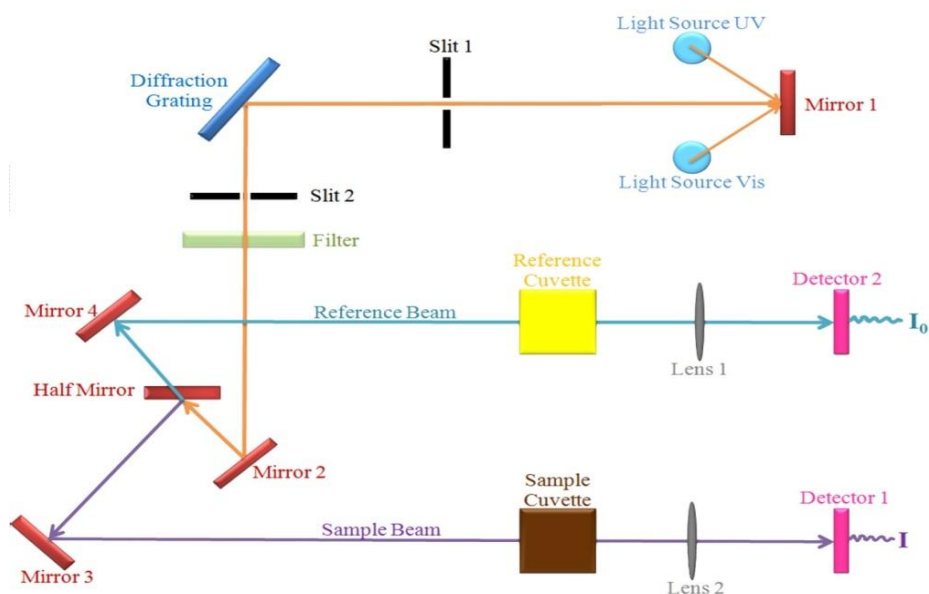


**Figure 2.12** Ultraviolet-visible spectrophotometer system diagram



**Figure 2.13** Ultraviolet-visible spectrophotometer

### 2.5.2. X - ray Diffractometer (XRD)

X-ray diffraction was discovered by Max Von Laue in 1912. It has provided a wealth of important information to science and industry. In addition, such studies have led a much clearer understanding of the physical properties such as composites materials, metals, polymeric materials, and other solids. XRD also provides a convenient and practical means for the qualitative identification of crystalline compounds. XRD is a very important experimental technique in revealing the crystal structure of materials.

X-rays are electromagnetic waves, which radiate with typical photon energies in the range of 100 eV – 100 keV. For diffraction application, only short wavelength x-ray (hard X-ray) in the range of a few angstroms to 0.1 angstrom (1 keV – 120 keV) are used. X-rays are generally produced by either x-ray tubes or synchrotron radiation. In an X-ray tube, which is the primary X-ray source used in X-ray instruments laboratory, X-rays are generated when a focused electron beam accelerated across a high voltage field bombards a stationary or rotating solid target. As electrons collide with atoms in the target and slow down, a continuous spectrum of X-rays are emitted, which are termed Bremsstrahlung radiation. The high energy electron fills the shell, an X-ray photon with energy characteristic of the target material is emitted. Common targets used in X-ray tubes include Cu and Mo, which emits 8 keV and 14 keV X-rays with corresponding wavelengths of 1.54 Å and 0.8 Å, respectively. Because the wavelength of X-rays is comparable to the size of atoms, they are ideally suited for probing the structural arrangement of atoms and molecules in a wide range of materials. The energetic X-rays can penetrate deep into the materials and provide information about the bulk structure.

The crystal information can be obtained from the characteristic of x-ray diffraction peak. The resulting diffraction pattern of a crystal, comprising both the positions and intensities of the diffraction effects, is a fundamental physical property of the material. Analysis of the positions of the diffraction effect leads immediately to a knowledge of the size, shape and orientation of the unit cell.

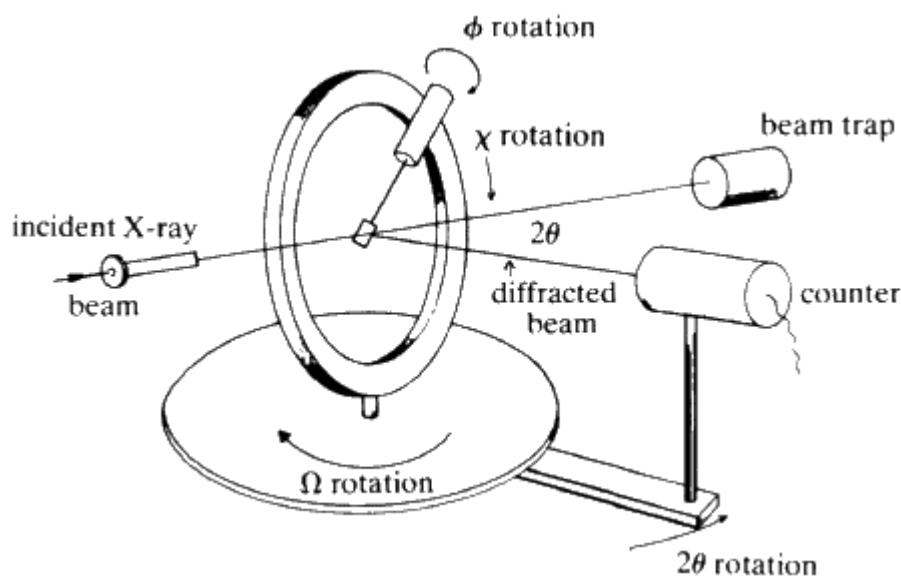


**Figure 2.14** Schematic of X-ray diffractometer arrangement [19]

In order to characterize the structure of the materials, three important parameters should be obtained from the diffraction pattern as the position of the peak, the height of the peak and the full width at half maximum (FWHM) height of the peak. The distance between the two lattice planes is derived from the experimental peak position by Bragg's Law :

$$n\lambda = 2d \sin \theta \quad (2.4)$$

where  $n$  is an integer representing the order of diffraction peak,  $\lambda$  is the wavelength of measured X-ray,  $d$  is the distance between parallel consecutive atomic planes from the experimental peak position and  $\theta$  is the angle between these planes and the incident beam.



**Figure2.15** X-ray diffractometer

### 2.5.3. Scanning Electron Microscopy (SEM)

The scanning electron microscopy (SEM) uses electrons rather than light to create an image. In a scanning electron microscope, a beam of electron is produced at the top of the microscope by field-emission electron source (Tungsten), as shown in Fig.2.14. The electron beam follows a vertical path through the column of the microscope. It makes its way through electromagnetic lenses which focus and direct the beam down towards the sample. Once it hits the sample, other electrons (backscattered or secondary) are ejected from the sample. Detectors collect the secondary or backscattered electrons, and convert them to a signal that is sent to a monitor producing an image.

SEM is surface imaging of solid using electron-beam generated secondary electrons. The primary beam may be focused to a spot size lower than 50 Å in diameter. Upon interaction with the solid, secondary electrons are generated which are utilized to image the surface. As the high energy primary electrons penetrate the solid, they undergo scattering which increases the interaction volume. Some of the primary electrons will be backscattered toward the surface with little or no loss in energy. Energetic primary electrons ionize atoms in the solid producing X-ray which are characteristic of the elements that are presented. With suitable detectors, the X-ray may be detected to provide elemental analysis, known as Energy Disperse X-ray Spectroscopy (EDX).

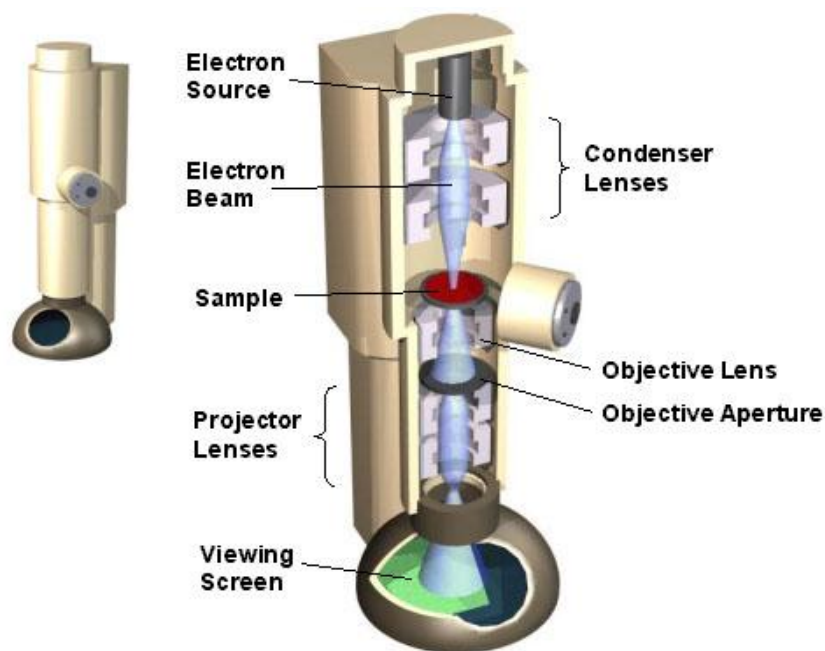


**Figure2.16** Schematic of scanning electron microscopy [20]



**Figure 2.17** Field-Emission Scanning Electron Microscope

#### **2.5.4. Transmission Electron Microscope (TEM)**

The transmission electron microscopy (TEM) is a microscopy technique which operates on the same basic principles as the light microscope by use the electrons instead of light. The beam of electrons is transmitted through the thin specimen and interacting with the specimen as it passes through. The image is magnified and focused onto an imaging device. Compared to light microscope, TEM uses electrons as "light source" and there have much lower wavelength to make the possible to get a better resolution which enables the instrument's user to examine fine detail. The TEM image contrast is due to absorption of electrons in the material which due to the thickness and composition of the material.

The conventional TEM typically operates at voltages exceeding 60, 100, 120 or 200 kV are most common for inorganic samples. The electron lens configuration in the TEM is also different from SEM. The electron ray path through a TEM is analogous to the visible light ray path through the ground glass lenses in an optical microscope configured to operate in the transmitted light mode. A focused electron beam is incident on a thin sample. The signal in TEM is obtained from both undeflected and deflected electrons that penetrate the sample thickness. A series of

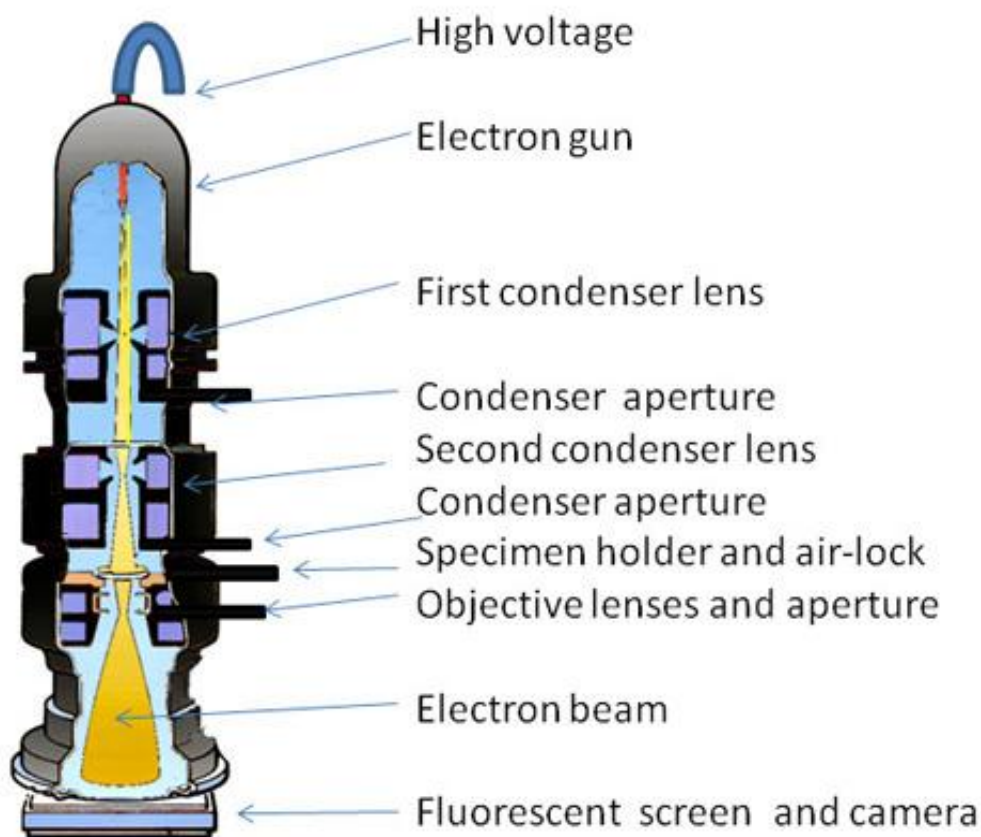


**Figure 2.18** Schematic of Transmission electron microscope [21]

magnetic lenses below the sample position are responsible for delivering the signal to a detector. The remarkable magnification range is facilitated by the small wavelength of the incident electrons and the key to the unique capabilities associated with TEM analysis.

### 2.5.5. Infrared Spectroscopy

The infrared region of the electromagnetic spectrum extends from the red end of the visible spectrum to the microwave region. The region includes radiation at wavelengths between 0.7 and 500  $\mu\text{m}$  or in wave numbers between 14000 and 20  $\text{cm}^{-1}$ . The spectral range used mostly is the mid-infrared region which covers frequencies from 4000 and 20  $\text{cm}^{-1}$  (2.5 and 50  $\mu\text{m}$ ). Infrared spectroscopy involves examination of twisting, bending, rotating and vibrational motions of atoms in a molecule. Upon interaction with infrared radiation, portions of the incident radiation are absorbed at specific wavelengths. The multiplicity of vibrations occurring simultaneously produces a highly complex absorption spectrum that is unique characteristic of the

functional groups that make up the molecule and of the overall configuration of the molecule as well.

Fourier Transform Infrared Spectroscopy (FTIR) is one of effective infrared technique which provides the information about the molecular structure or the chemical bonding of materials and can indicate the amount of elements contained in the molecules of unknown sample. The FTIR works on the fact that bonds and groups of bonds vibrate at characteristic frequencies. FTIR analysis can be applied to minute quantities of materials, whether solid, liquid, or gaseous. When the library of FTIR spectral patterns does not provide an acceptable match, individual peaks in the FTIR plot may be used to yield partial information about the specimen. The advantages of this technique is the entrance slit is replaced by an iris furnishing a better signal to the detector which receives more energy and the signal to noise ratio is much higher to the sequential method since it can be improved by the accumulation of successive scans.

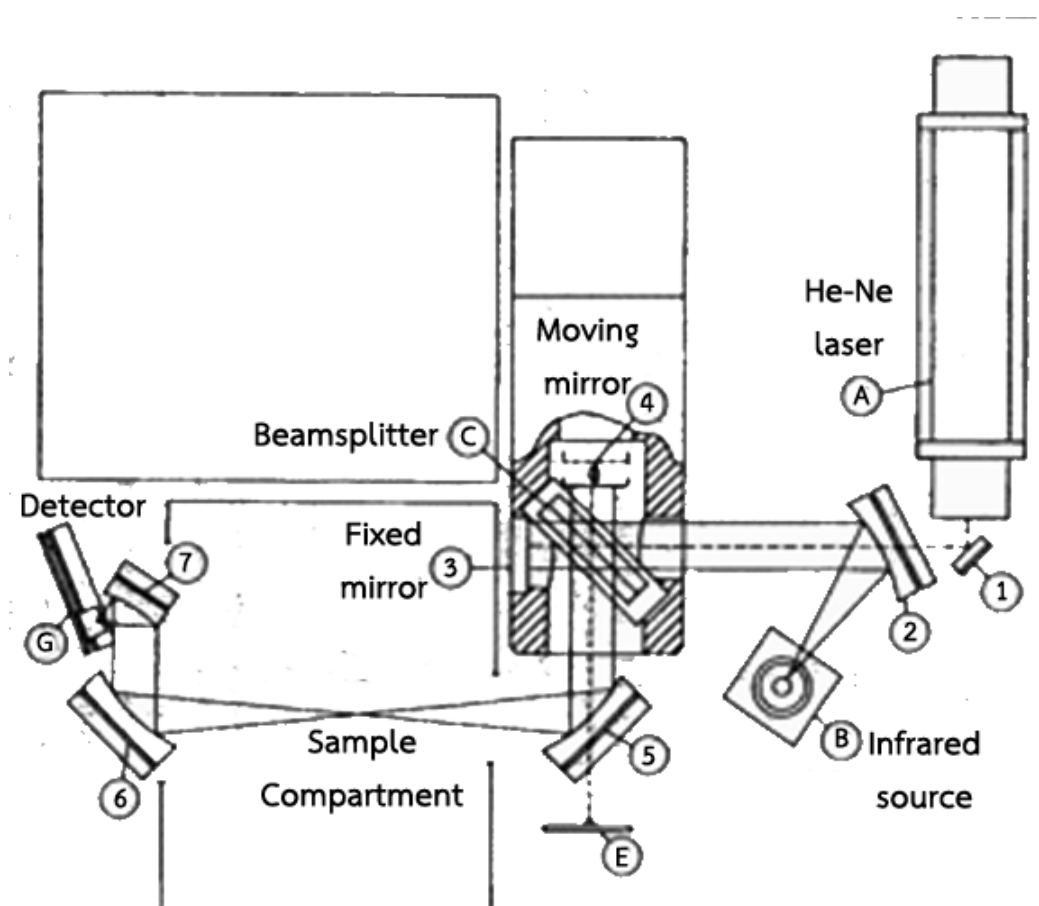


**Figure 2.19** Schematic of Fourier Transform Infrared Spectroscopy [22]



**Figure 2.20** Fourier Transform Infrared Spectroscopy

### 2.5.6. Raman Spectroscopy

Raman spectroscopy is a powerful, multifaceted technique with wide-ranging application in carbon nanotubes studies. As a vibrational spectroscopy, it has been demonstrated to be invaluable for characterization of nanotubes diameter distributions for monitoring production methods. Facile evaluation of nanotubes diameters is made possible by the presence of the radial breathing mode (RBM) which appears in the low frequency ( $100\text{--}400\text{ cm}^{-1}$ ) region of the nanotubes Raman spectrum and has an inverse dependence on nanotubes diameter. This ease of sample characterization has made Raman spectroscopy attractive for real time monitoring of nanotubes processing and various separation methods. Raman is also capable of identifying nanotubes electronic nature through analysis of the nanotubes G-band, found near  $1600\text{ cm}^{-1}$ . Semiconducting nanotubes produce a two peak G-band structure (G+ and G- band) with Lorentzian line shapes, while the G- peak in metallic types shows a pronounced broadening with Breit-Wigner-Fano (BWF) line shape. In addition, measurement of the nanotubes D-band (found near  $1300\text{ cm}^{-1}$ ) can provide an evaluation of the defect density occurring in a sample and provides a useful tool for monitoring the extent of covalent sidewall modification in nanotubes functionalization chemistry. It relies on inelastic scattering or Raman scattering of

monochromatic light usually from a laser in the visible, near infrared or near ultraviolet range. The laser light interacts with molecular vibrations, phonons or other excitations in the system, resulting in the energy of the laser photons being shifted up or down. The shift in energy gives information about the vibrational modes in the system. Infrared spectroscopy yields similar, but complementary information. Figure 2.19 shows a schematic of a Raman spectrometer. A laser source is used to provide high power light at a specific wavelength with a highly focused beam. The beam is focused on the sample through the microscope lens. The lens then collects the scattered light. It passes through a notch filter which removes all the Rayleigh scattered light of the same wavelength. It is then focused on a grating which separates all the wavelengths of light, and then focused on a charge coupled device detector (CCD). The CCD counts the number of photons at each wavelength and sends the information to the computer.

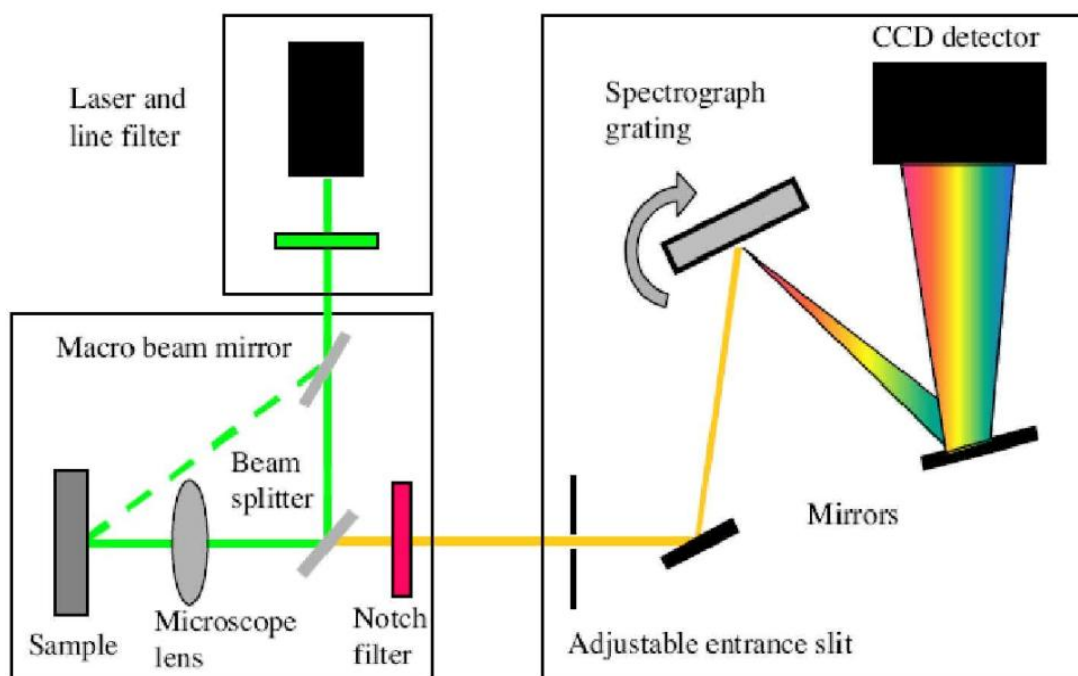


**Figure2.21.** Schematic of Raman Spectroscopy [23]

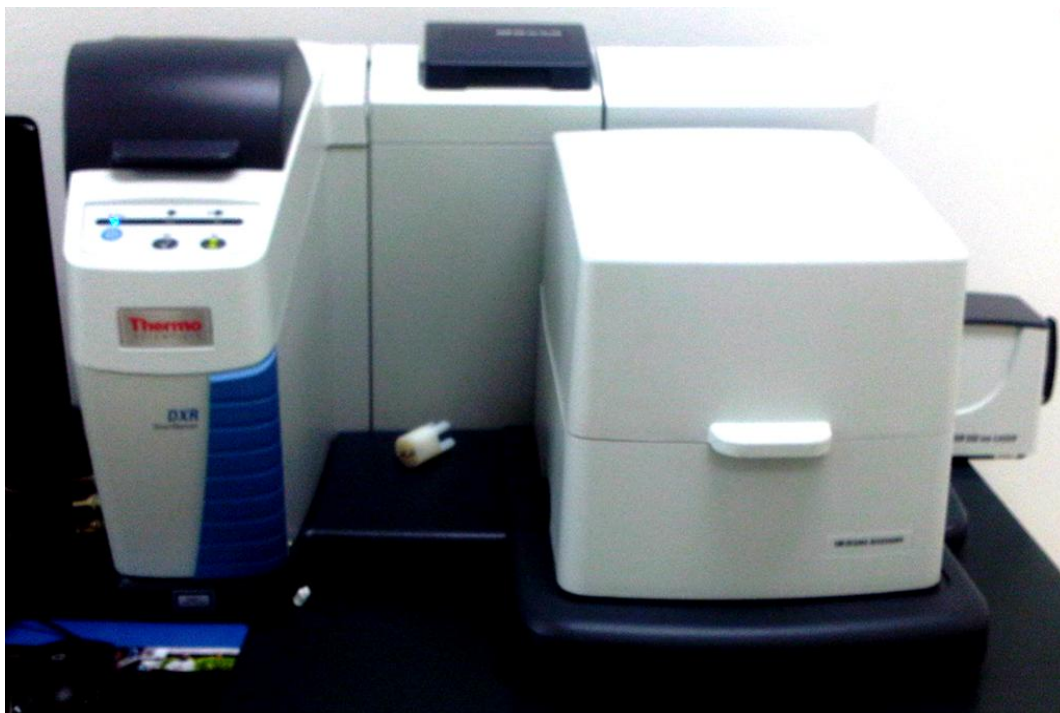


**Figure 2.22.** Raman Spectroscopy

### **2.5.7. Gas sensing Characterization**

The basic principles of gas sensor usually use an electrical response by adsorption of gas molecules on surface of an active layer (in this case is surface of Nickel oxides) which causes the electron transfer between gas molecules and material, leading to the alternation of conductivity (or resistivity) of the material. The conductivity of semiconductor oxides consisted to the conductivity of bulk, grain boundary and especially on surface. Surface area exposed to the first reaction area to gases. Therefore, the nano-structured have more specific materials area to detected gas molecules.

### **2.5.8. Voltammetry Technique**

#### **2.5.8.1. Cyclic Voltammetry (CV)**

Cyclic Voltammetry is a modification of the rapid scan technique wherein the direction of scanning is reversed following the reduction of interested sample. To accomplish, a triangular wave voltage were applied to the cell as shown in Figure 2.21(a), this triangular potential excitation signal sweeps the potential of the working electrode back and forth between two designated values called the switching potentials. The triangle returns at the same speed and permits the display of a-

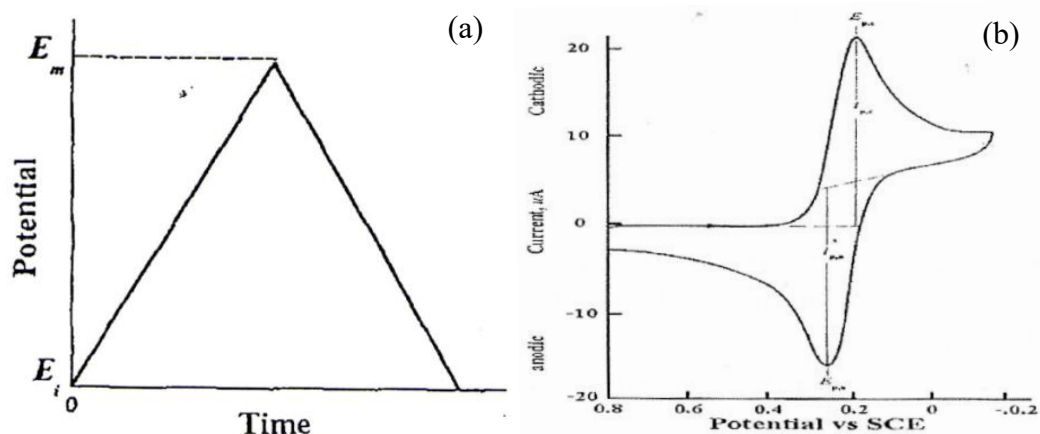


**Figure 2.23.** CV wave form (b) Cyclic Voltammogram [24]

complete voltammogram with cathodic (reduction) and anodic (oxidation) waveforms one above the other. A typical voltammogram was shown in Figure 2.21(b). The potential scan is frequently terminated at the end of the first cycle, it can be continued for any number of cycles. Both the scan rate and the switching potentials are easily varied.

A characteristic of voltammetric instrumentation is a potentiostatic control of working electrode potential. In the three electrode potentiostat, a reference electrode is positioned as close as possible to the working (indicator) electrode. The auxiliary (counter) electrode is the third electrode in the electrochemical cell. The function of the potentiostat is to observe the potential of the working electrode (either cathode or anode) against the reference electrode which sense the potential of working electrode when the potential of the reference electrode is constant.

### 2.5.8.2. Chronoamperometry (CA)

Chronoamperometry is one of electrochemical techniques in which the potential of the working electrode is stepped and the current in the faradic processes will be monitored as a function of time. The identity of the electrolyzed species can be obtained from the ratio of the peak oxidation current versus the peak reduction current. However, as all pulsed techniques, CA generates high charging currents, which decay exponentially with time as any RC circuit. The Faradaic current, which is due to the electron transfer and most often the current component of interest, decays much more slowly than the charging decay cells with no supporting electrolyte are notable exceptions. Since the current is integrated over relatively longer time

intervals, the CA gives a better signal to noise ratio in comparison to other amperometric technique.

## 2.6. Literature Reviews

Parka, O.K. et. al. reported on the effects of surface modification on the dispersion and electrical conductivity of carbon nanotubes/polyaniline composites [25]. The surface of the CNTs was modified with acid mixtures, potassium persulfate (KPS) and sodium dodecylsulfate. They found that the surface modification of the CNTs had a strong influence on the dispersion stability and electrical conductivity of the resulting composites. It can be concluded that the acid mixture treatment of CNTs greatly improves the dispersion stability and FE-TEM images of the composites showed that the KPS treatment of the CNTs enhanced the coating ability of PANi.

Najafi, E. et. al. reported on UV-ozone treatment of multi-walled carbon nanotubes for enhanced organic solvent dispersion [26]. They demonstrated that UV-ozone treatment under ambient conditions could have a dramatic effect on the nature of the surface oxidation of MWNTs. During a 60 min exposure time, compared to a raw CNTs, the solubility in polar organic solvents was improved by as much as 320%, which was comparable to vigorous acid treatment. Interestingly, the UVO exposure had no effect on the aspect ratio of the CNTs and due to their preserved higher aspect ratio, UVO modified CNTs induced a higher electrical conductivity in polymer matrices.

Flahaut, E. et. al. reported on carbon nanotubes-metal oxide nanocomposites : microstructure, electrical conductivity and mechanical properties [27]. Carbon nanotubes – metal oxide composites were prepared by hot-pressing the corresponding composite powders, in which the carbon nanotubes were very homogeneously dispersed between the metal–oxide grains. The carbon nanotubes–metal–oxide composites are electrical conductors with an electrical conductivity in the range 0.2–4.0 S/cm<sup>-1</sup> owing to the percolation of the CNTs. The values of the electrical conductivity were fairly well correlated to the relative quantity of CNTs.

Prasek, J. et. al. reported on nanopatterned working electrode with carbon nanotubes improving electrochemical sensors [28]. The screen printed thick film amperometric sensor were fabricated using Ag based paste for leads. The thick film technology sensor was fabricated using screen printing techniques. The CNTs were

grown on substrates placed at various distances and the thin nickel layer deposited by magnetron sputtering was used as a catalyst. The buffer results indicated that residues of nickel from CNTs growing process did not influence the sensor response because of no any other peaks. The sensors were able to detect the concentrations of 106  $\mu\text{mol/L}$  of  $\text{CdCl}_2$ .

Xing, W. et. al. reported on synthesis and electrochemical properties of mesoporous nickel oxide [29]. The mesoporous  $\text{Ni}(\text{OH})_2$  were synthesized using sodium dodecyl sulfate as a template. The cyclic voltammetry indicated good capacitive behavior for mesoporous NiO samples and that this behaviour improved with increase in calcination temperature. NiO calcined at 300 °C possessed the highest surface redox reactivity. Compared with NiO prepared by dip-coating and cathodic deposition methods, mesoporous NiO could be used to fabricate electrodes for capacitors in a much larger mass and, at the same time, maintained a high value of specific capacitance and good capacitive behavior.

Liao, X.N. et. al. reported on preparation of NiO/MWNTs nanocomposites by a simple chemical precipitation method [30]. The NiO/MWNTs nanocomposites were prepared by a simple and efficient chemical precipitation method with the aid of sodium dodecyl sulfate (SDS). They found that NiO nanoparticles with the size of less than 9 nm were well-dispersed on the outside of MWNTs functionalized with SDS and showed high catalytic activity for benzene hydrogenation after reduction with hydrogen gas.

J.Y. Lee, et. al. gave a report on nickel oxide/carbon nanotubes nanocomposite for electrochemical capacitance [31]. They fabricated supercapacitor electrodes with nickel oxide/carbon nanotubes nanocomposite formed by a simple chemical precipitation method. The CNTs were treated by acid. SEM image indicated that the CNTs were damaged to some extent and the originally bundled CNTs were dispersed into individual CNTs during the reflux and sonication process. The presence of CNTs network in the NiO significantly improved the electrical conductivity of the host NiO by the formation of conducting network of CNTs and the active sites for the redox reaction of the metal oxide by increasing its specific surface area.

## CHAPTER 3

# RESEARCH METHODOLOGY

### 3.1. Treatment Process of Carbon Nanotubes

#### 3.1.1. Acid Treatment Procedure

##### 3.1.1.1. Chemicals and Materials

1. Multiwall Carbon nanotubes (MWNTs)
2. Acetone ( $C_3H_6O$ )
3. Sodium Hydroxide (NaOH)
4. Deionized Water (DI)
5. Sulfuric Acid ( $H_2SO_4$ )
6. Nitric Acid ( $HNO_3$ )

##### 3.1.1.2. Methodology

Multiwall carbon nanotubes were washed in acetone and then the filtered MWNTs were immersed in NaOH for an hour under stirring at room temperature ( $\sim 25^\circ C$ ). After washing to neutral with DI water and dried at  $100^\circ C$  for an hour, MWNTs were immersed in 8 ml of a mixture of  $HNO_3$  and  $H_2SO_4$ . The suspension was stirred for 15 min before being refluxed at  $160^\circ C$  for 60 min. After cooling to room temperature, the MWNTs were washed with DI water until pH 7 was obtained. The treated MWNTs were separated by centrifuge and dried in oven at  $100^\circ C$  for 24 hours.



**Figure 3.1** Reflux system

### 3.1.2. Surfactant Treatment Procedure

#### 3.1.2.1. Chemicals and Materials

1. Multiwall Carbon nanotubes (MWNTs)
2. Sodium Dodecyl Sulfate (SDS)
3. Deionized Water (DI)

#### 3.1.2.2. Methodology

Multiwall carbon nanotubes were dispersed in 1 wt% SDS aqueous solution to modify the MWNTs surface by sonication for 1 h. The interaction between MWNTs and SDS due to hydrophobic interactions through the  $-CH_3$  groups is identified to be effective for modifying the surface of MWNTs. After that, the MWNTs were washed with deionized water and separated by centrifuge before dried in oven at 100 °C for an hour.



**Figure 3.2** Ultrasonication

### 3.1.3. UV-Ozone Treatment Procedure

#### 3.1.3.1. Chemicals and Materials

1. Multiwall Carbon nanotubes (MWNTs)
2. Ethanol (C<sub>2</sub>H<sub>6</sub>O)

#### 3.1.3.2. Methodology

Prior to UV-Ozone treatment, as produced multiwall carbon nanotubes were washed in ethanol for an hour to clean MWNTs from foreign objects that might attach on their surfaces. Then, MWNTs were placed in a commercial UV-Ozone generator (Sen SUV200GS-14) in ambient laboratory air for 60 min with a distance of 10 mm from the lamp.



Figure 3.3 UV-ozone generator

## 3.2. Preparation of NiO/MWNTs composites

### 3.2.1. Chemicals and Materials

1. Multiwall Carbon nanotubes (MWNTs)
2. Sodium Hydroxide (NaOH)
3. Deionized Water (DI)
4. Nickel chloride hexahydrate ( $\text{NiCl}_2 \cdot 6\text{H}_2\text{O}$ )

### 3.2.2. Methodology

The surfaces of MWNTs were modified by treatment methods mentioned in section 3.1.1-3.1.3. The treated MWNTs were immersed in 0.1 M Nickel chloride hexahydrate ( $\text{NiCl}_2 \cdot 6\text{H}_2\text{O}$ ) solution under stirring at room temperature ( $\sim 25^\circ\text{C}$ ). 0.1 M NaOH solution was then added dropwise to the mixture until the pH 12.00 was reached. After reaction of 24 h, products were washed with deionized water. After that, the mixture was heated with different microwave irradiation powers at 150, 300 and 450 watts for 5 min. Finally, as-synthesized products were dried for 2 h to obtain the NiO/MWNTs composites.



**Figure 3.4** Magnetic Sterrer



**Figure 3.5** Microwave

### **3.3.Applications**

#### **3.3.1. NiO/MWNTs gas sensors fabrications**

##### **3.3.1.1. Chemicals and Materials**

1. Multiwall Carbon nanotubes (MWNTs)
2. Dimethylformamide (DMF)
3. Deionized Water (DI)
4. Interdigitated electrodes

##### **3.3.1.2. Methodology**

The NiO/MWNTs were dispersed in DMF and sonicated for 30 min to form a suspension. NiO/MWNTs-DMF solution was deposited onto the interdigitated area of the electrodes and heat until DMF evaporated. Finally, the modified sensor was dried at 100°C for 24 hours.



**Figure 3.6** Interdigitated Electrode

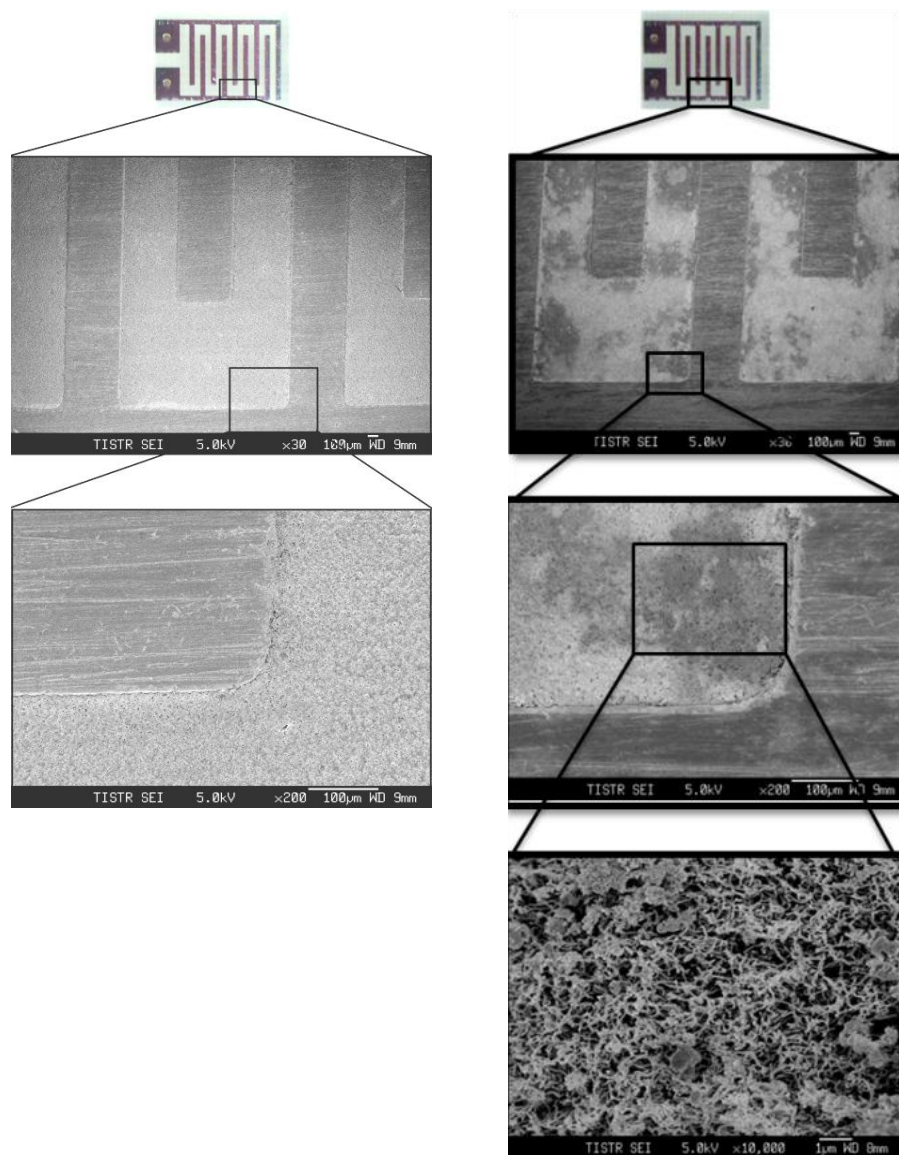


**Figure 3.7** SEM Images of (a) bare electrode (b) modified electrode using as-prepared composites

### 3.3.2. Modification of NiO/MWNTs/FTO electrode

#### 3.3.1.1. Chemicals and Materials

1. Multiwall Carbon nanotubes (MWNTs)
2. Nafion ( $C_7HF_{13}O_5S \cdot C_2F_4$ )
3. Deionized Water (DI)
4. Ethanol ( $C_2H_6O$ )
5. Fluorine-doped tin oxide (FTO)

### 3.3.1.2. Methodology

Before modification, the FTO surface was sonicated successively in ethanol and deionized water for 5 min. The preparation of the suspension NiO/MWNTs concentration of 20 ml NiO/MWNTs with 0.5% nafion 0.5 ml sonicated for 30 min was performed until a black suspension was obtained. Then, drop 10 $\mu$ L of suspension by micropipette onto the surface of a FTO and left until dry.

## 3.4.Characterizations

### 3.4.1. The Dispersion stability

The dispersion stability of MWNTs is an important factor in fabricating uniformly dispersed CNTs composites. MWNTs were dispersed in DI water using an ultrasonic bath for 30 min then left for 1h, 4h and 6h.

### 3.4.2. Ultraviolet Visible Spectrophotometer (UV-Vis)

Ultraviolet-visible spectroscopy (PG Instrument T90) which is double beam spectrometer operated in wavelength range of 300-800 nm.were used to obtain the absorbance spectra of MWNTs. MWNTs were dispersed in DI water before sonication for 30 min and measured every 5 min for an hour.



**Figure 3.8** Ultraviolet Visible Spectrophotometer

### 3.4.3. X - ray Diffractometer (XRD)

The structure of the samples was determined by X-ray diffraction (X'Pert Pro MPD8 PW3040/60) which is a non-destructive technique that reveals detailed information about the chemical composition and crystallographic structure of natural and manufactured materials. The MWNTs or NiO/MWNTs composites were ground into fine powder and poured into the plate. The sample were placed into the sample holder with scan rate of 2 degree/min at 20-80 degree and using Cu  $K_{\alpha}$  with wavelength of 1.5046 Å as a X-ray source.



**Figure 3.9** X-ray diffractometer

#### 3.4.4. Scanning Electron Microscope (SEM)

The morphology of as-synthesized NiO/MWNTs was investigated by Field Emission Scanning Electron Microscope (JEOL JSM-6340F). MWNTs were sprinkle on a carbon tape and blow off excess with compressed air.



**Figure 3.10** Field Emission Scanning Electron Microscopy (FE-SEM)

#### 3.4.5. Transmission Electron Microscope (TEM)

To ascertain morphology of obtained sample, NiO/MWNTs composites were further characterized and confirmed by Transmission Electron Microscope (JEOL JEM-2010). The Samples being characterized were prepared by adding small amount of MWNTs in ethanol and sonicated to obtain well-dispersed particles follow by drop on the copper grid before left until dry.

#### 3.4.6. Fourier Transform Infrared Spectroscopy (FT-IR)

The functional groups of the NiO/MWNTs composites prepared by three different modification methods were monitored by Fourier transform infrared spectroscopy (Spectrum GX FTIR System T904019) in the range of  $400\text{--}4000\text{ cm}^{-1}$ . MWNTs were ground in a mortar to reduce the average particle size to 1 to 2 microns. About 5 to 10 mg of finely ground sample were placed on the potassium bromide (KBr) plate to form a very fine powder. This powder was then compressed into a thin pellet which can be analyzed.

### 3.4.7. Raman Spectroscopy

The structure and electronic properties of carbon nanotubes materials were observed by Raman spectroscopy (DXR Raman Microscope) with minimal sample preparation in the range of  $1000\text{-}1800\text{ cm}^{-1}$ .



**Figure 3.11** Raman Spectroscopy

### 3.4.8. Gas sensing

The electrical resistance of the prepared sample was measured using a multimeter program (UT71C\_D\_E) which was connected to computer. This measurement was carried out in a glass chamber with 200 ml of ethanol and methanol.

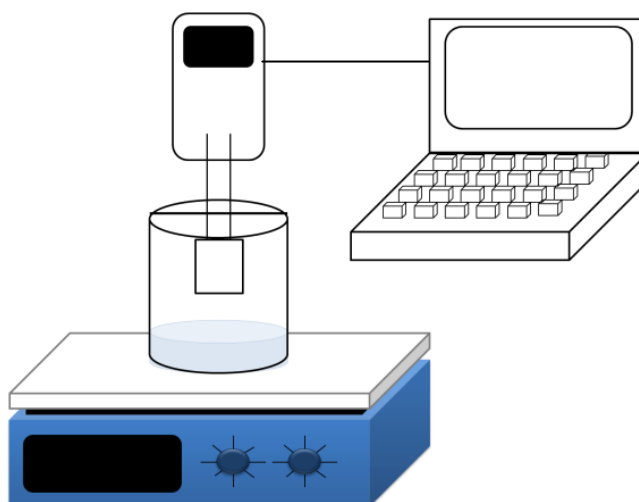


**Figure 3.12** Diagram of sensor measurement system

### 3.4.9. Electrochemistry Characterization

The working electrode was characterized electrochemically in 1 mM  $K_3Fe(CN)_6$  solution by potentiostat (PGSTAT302). A three electrode system were employed using NiO/MWCNT/FTO as working electrode, an Ag/AgCl (saturated potassium chloride) as reference electrode and a platinum as counter electrode. The amperometric response for  $H_2O_2$ , repeatability and stability of the NiO/MWCNT/FTO electrode were also studied on successive additions 10  $\mu L$  of hydrogen peroxide at applied potential of 0.5 V.

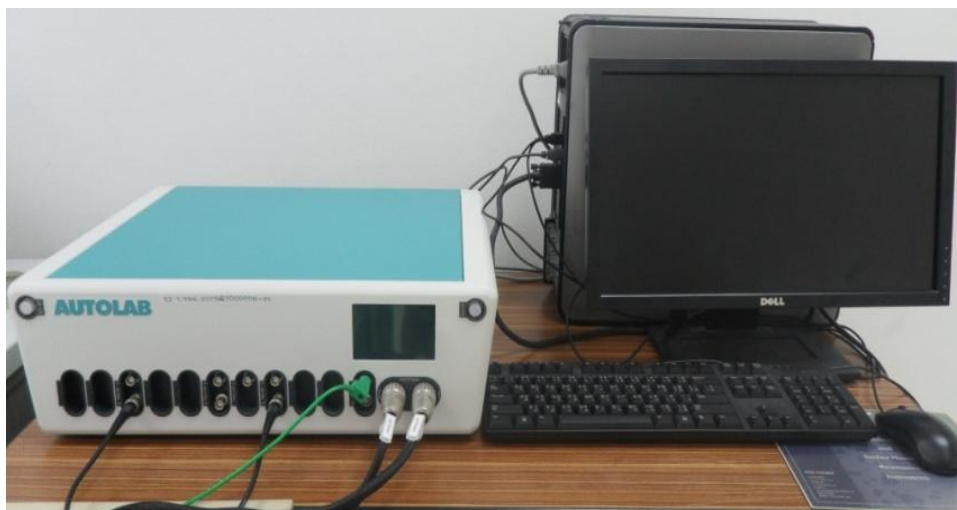


**Figure 3.13** Potentiostat

## CHAPTER 4

### Results and Discussion

#### 4.1. Surface Modification of Multiwall Carbon nanotubes

##### 4.1.1. The dispersion stability of surface modified MWNTs

The comparison of the dispersion stability of surface modified MWNTs in a solvent is one of the most direct means to understand the effects of treatment method and also be an important factor for fabrication of uniformly dispersed CNTs composites. The electrochemical properties of the resulting composites will also be strongly influenced by the dispersion stability of the nanotubes. The dispersion stability of MWNTs in DI water under sonication after 1 h, 4 h and 6 h are shown in Figure 4.1. It is clearly seen that the suspension of the raw MWNTs agglomerates and lodges to the base of the bottle whereas the solutions of the surface modified MWNTs exhibits better dispersion stability. With increasing time, treated MWNTs with SDS and UV/Ozone were slowly precipitated, accompanying the slower precipitation of UV/Ozone treated MWNTs. After 6 h, the acid-treated MWNTs suspensions were still homogeneous and scarce sedimentation was observed which may due to the fact that the defect side walls of the MWNTs carry more dissociated carboxyl groups after oxidization with the acid mixture.

The dispersibility of CNTs could be quantified by measuring the absorbance of visible light at 635 nm which is in the typical absorption range of pristine MWNTs [32]. The corresponding results were shown in Figure 4.2. As seen in the figure, the dispersion of the raw MWNTs, SDS-treated MWNTs and UV/Ozone-treated MWNTs show a significant decrease in their absorbance compared to that value of raw MWNTs, which is in good agreement with the pictures in Figure 4.1. The result clearly indicates that the surface modification of MWNTs can drastically improve the dispersion stability. On the other hand, the absorbance of acid treated MWNTs still remains constant or even decreases slightly with increasing time, that is in contrast to raw MWNTs whose absorbance spectrum decreases rapidly with increasing time. Meanwhile, the absorbance of UV/Ozone-treated MWNTs and SDS-treated MWNTs are in similar characteristic. It is obvious that the absorbance of UV/Ozone-treated MWNTs decreases slower than that of SDS-treated MWNTs as time increases up to 1 h. The results strongly indicate that MWNTs can be well functionalized by either acid

treatment or UV-Ozone treatment, accompanying the comparably good dispersibility by both method.

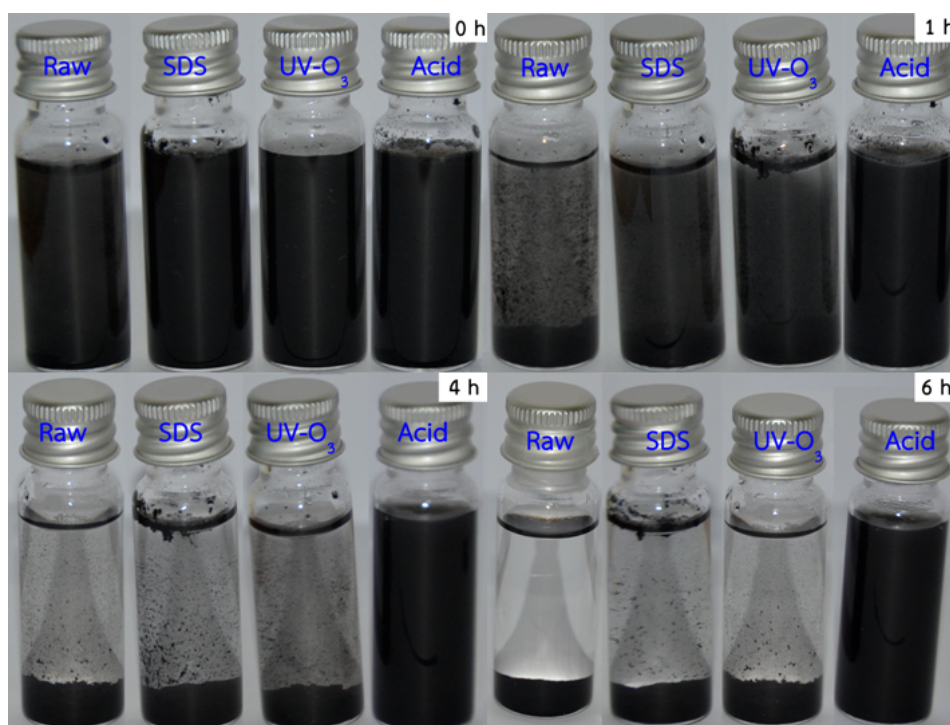


**Figure 4.1** Dispersion stability of MWNTs with different treatment method in DI-water for various time.

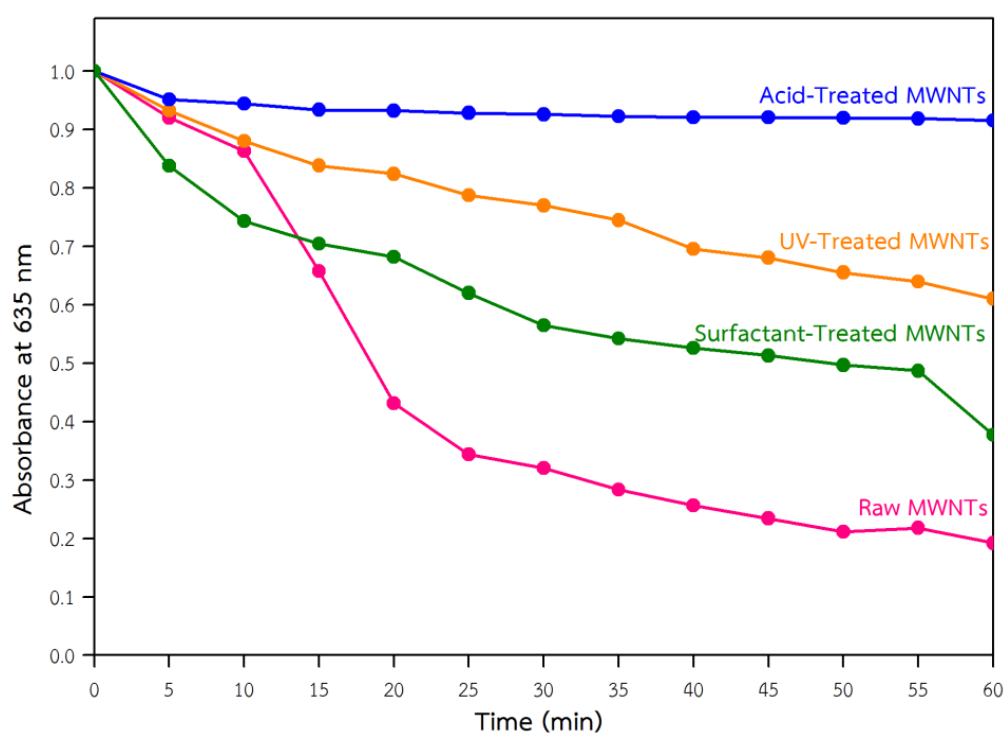


**Figure 4.2** Absorption spectra of Raw MWNTs and the surface-modified MWNTs.

#### 4.1.2. The Fourier transform infrared spectroscopy results

FT-IR measurements of MWNTs modified with three different processes were carried out in the range of 400-4000  $\text{cm}^{-1}$  and the corresponding results are shown in Fig. 4.3. The chemical composition of MWNTs was scrutinized by correlating the developed peaks in the spectrum to the bond, vibration, or stretching of various functional groups. The band located at 1020  $\text{cm}^{-1}$  is typically assigned to nickel oxygen interaction and Ni-O-CO<sub>2</sub> group which may originate from Ni catalyst used in synthesis process [33]. For UV/ozone-treated MWNTs, the band at 1220  $\text{cm}^{-1}$  and 1754  $\text{cm}^{-1}$  can be assigned to the stretching vibration of C-OH groups and the stretching of C=O bond located near the oxygen containing group, respectively. It is suggested that the MWNTs are functionalized with the hydroxyl groups and carboxyl group by UV/ozone treatment, that is the major functional groups to initiate the formation of functional metal-oxide nanoparticles on the CNT surface. The noticeable band at about 1590  $\text{cm}^{-1}$ , 2310  $\text{cm}^{-1}$ , 2944  $\text{cm}^{-1}$  appeared in all samples generally attributes to the C=C aromatic stretching, CO<sub>2</sub> stretching, H-C=O stretching, respectively. The FTIR spectrum of acid-treated sample of additionally indicates the strongest peak at 3437  $\text{cm}^{-1}$  which is peak of O-H stretching that can be generated due to adsorbed water in peak of acid treated MWNTs.

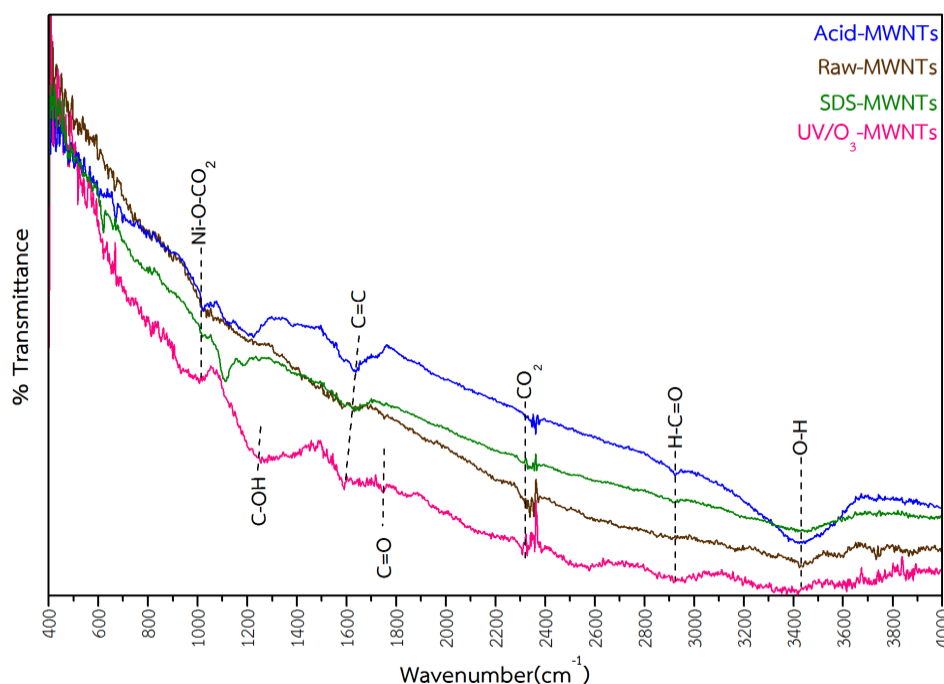


**Figure 4.3** FTIR spectra of saw MWNTs and the surface-modified MWNTs using three different processes.

### 4.1.3. The Raman spectroscopy results

Figure 4.4 shows Raman spectra of the MWNTs with different surface modified methods. All samples have similar Raman scattering patterns. Two distinct peaks were observed showing the characteristics of CNTs. The defects of the structure, named D band locates at  $1339\text{ cm}^{-1}$  and another band situated at about  $1570\text{-}1590\text{ cm}^{-1}$  is the graphite band (G band). After modifications, a significant decrease in the intensity of D-band can be observed in Raman spectra. This is because the perfect two-dimensional graphitization is altered to a more disordered structure by carboxylation [34]. The relatively high intensity ratio of D band to G band suggests the existence of high concentration of defects in the MWNTs. The intensity ratio of D-band to G-band ( $I_D/I_G$ ) is typically considered as a key parameter to assess the degree of disorder of CNTs and calculated for characterizing the surface modified MWNTs and the correlated results is shown in table 4.1. According to the obtained ratios, the result can be proposed as the indication of the formation of defects on MWNTs after treatment process. As a result, it is clearly noticed that the acid-treated MWNTs contain more amount of defects than the MWNTs treated by other processes. Meanwhile, the defects of MWNTs treated by UV-Ozone are more than the MWNTs treated by SDS. The defects on MWNTs achieved by surface modification consequently play a key role on the formation of nanoparticles on the surface of MWNTs.

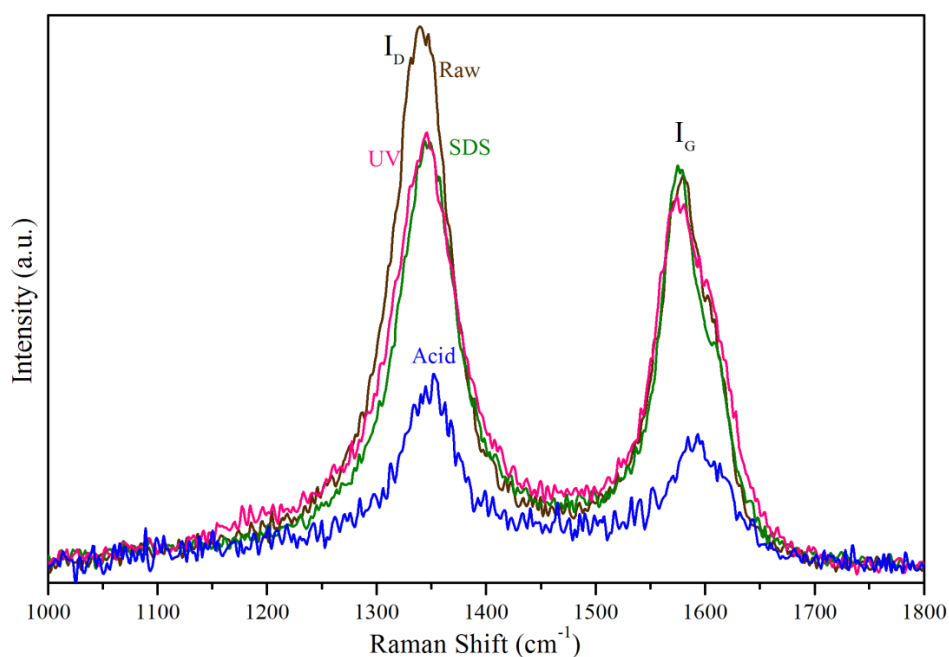


**Figure 4.4** Raman spectra of raw MWNTs and the surface-modified MWNTs.

**Table 4.1** Raman data collected at room temperature on the different series of surface modified MWNTs

Sample	$I_D$ (a.u.)	$I_G$ (a.u.)	$I_D/I_G$
SDS Treated	107.82	101.61	1.06
UV Treated	110.04	91.39	1.20
Raw CNTs	135.13	99.19	1.36
Acid Treated	48.35	33.03	1.46

The surface modification of CNTs is the first important step for developing high-performance CNT/metal oxide composites and increasing their dispersion stability. The major mechanism responsible for the functionalization by UV-ozone treatment is proposed. Under intense UV radiation, the molecules on the MWNTs are dissociated by absorbing short-wavelength UV radiation. Consequently the carbon atoms at the defect sites on the nanotubes either owing to the UV radiation or originally existed react with the atomic oxygen from the continuous dissociation of the oxygen molecules and the generation of the ozone molecules for the carboxylation reaction as shown in Figure 4.5. This feature leads to the increase of the dispersion stability of surface treated MWNTs. According to the FTIR and Raman spectra, the result indicates the formation of defects or functional groups on MWNTs after treatment process which will affect to the formation of NiO on the surface of MWNTs in synthesis process of NiO/MWNTs nanocomposites.

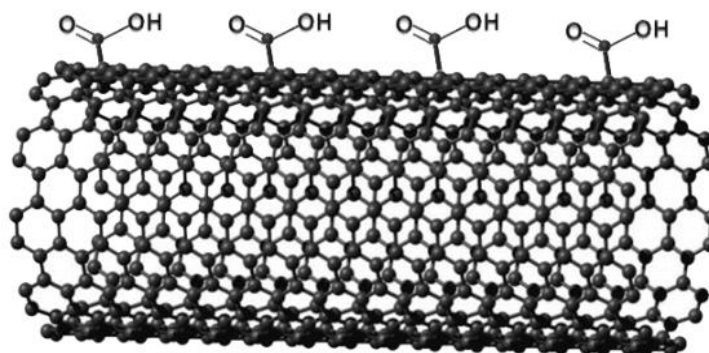


**Figure 4.5** Schematic of the carbon nanotubes with COOH group [35].

## 4.2. NiO/MWNTs nanocomposites

### 4.2.1. NiO/surface modified MWNTs nanocomposites

#### 4.2.1.1. XRD results

The XRD patterns of raw MWNTs and NiO/surface modified MWNTs composites are illustrated in Figure 4.6. The peak situated at  $26.4^\circ$  observed in all samples is referred to (002)  $d$ -spacing of the CNTs (JCPDS-ICDD No.751621) whereas the peaks at  $44.6^\circ$ ,  $51.9^\circ$  and  $75.7^\circ$  correspond to the FCC structure of the Ni catalyst used in CNTs synthesis process. For as-synthesized composites, the peaks positioned at  $2\theta = 37.3^\circ$ ,  $43.1^\circ$ , and  $62.8^\circ$  attribute to (111), (200), and (220) orientation planes of cubic NiO, respectively (JCPDS-ICDD No.895881). XRD results firmly indicate that all composites are mixtures of two phases of NiO and CNT. Moreover, comparing to UV-ozone treated MWNTs and surfactant treated MWNTs samples, the intensity of (002) reflection of MWNTs of acid treated MWNTs sample significantly decreases, implying that acid-treated method may cause the structural destruction or the shortening of MWNTs.

The grain size of NiO crystallites was calculated from major reflection (111) using the well-known Scherrer's formula:

$$D = \frac{K\lambda}{\beta \cos \theta} \quad (4.1)$$

Where  $D$  is the grain diameter,  $K$  is the shape factor (0.9),  $\lambda$  is the X-ray wavelength ( $1.5406 \times 10^{-10}$  m),  $\beta$  is the full-width at half maximum and  $\theta$  is the Bragg angle. The calculated average particle sizes of NiO obtained by this method are approximately 6 – 8 nm.

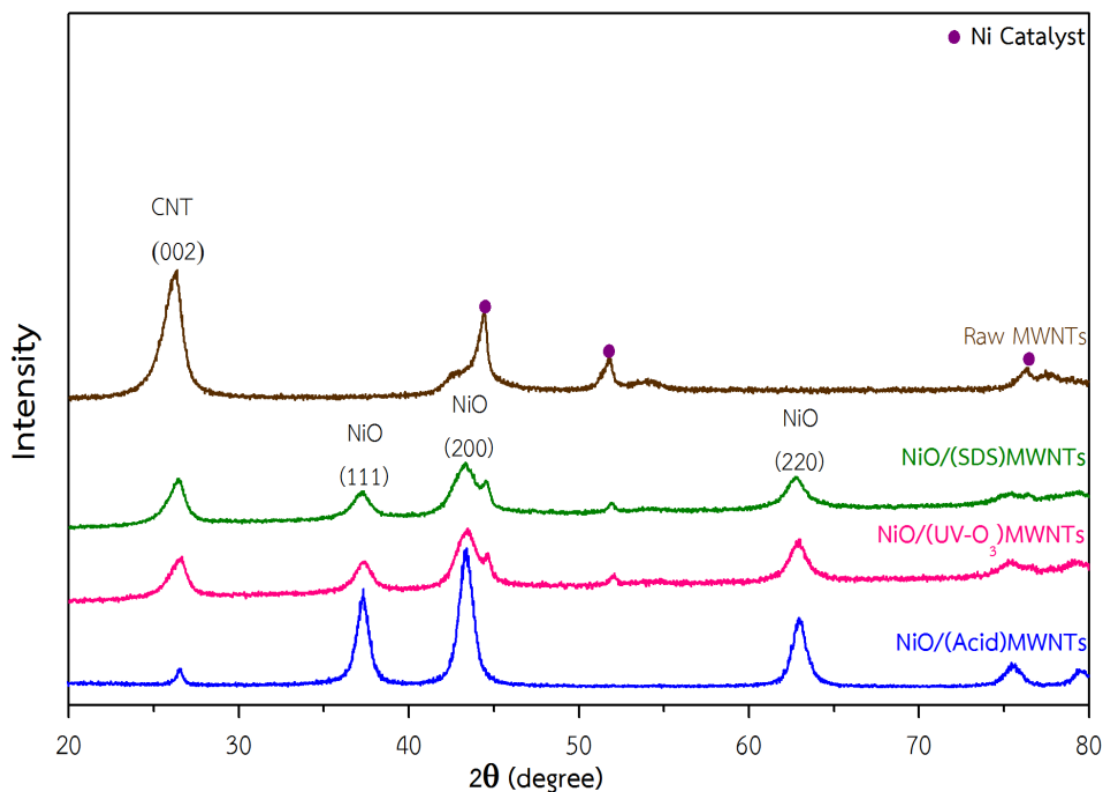


**Figure 4.6** XRD patterns of NiO/MWNTs nanocomposites prepared with different treatment method

#### 4.2.1.2. The Scanning Electron Microscopy results

The morphologies of as-synthesized NiO/MWNTs nanocomposite were investigated by SEM. The SEM images clearly indicate the existence of NiO nanostructure formed over the surface of modified MWNTs. Figure. 4.7 illustrates the SEM images of NiO/unmodified MWNTs nanocomposite which shows rather poor distribution of NiO nanoparticles and MWNTs. Meanwhile, as shown in Figure. 4.8, the SEM image of acid treated MWNTs sample exhibits the shortening of MWNTs. Furthermore, the formation of NiO on MWNTs treated by SDS as seen in Figure. 4.9 is not rather uniform, that may due to the ineffective surface treatment by SDS. As seen in Figure. 4.10, the SEM image reveals that the MWNTs treated with the UV-Ozone have more uniform coating ability of NiO compared to the CNTs treated with SDS and acid mixture. This manner is originated from the fact that the UV-Ozone treatment does not significantly alter the surface morphologies of CNTs but effectively functionalized their wall surfaces, accompanying the drastically improved dispersion properties in solution. This result is consistent with previously work reported on effects of conventional acid treatment on CNT structure [36].

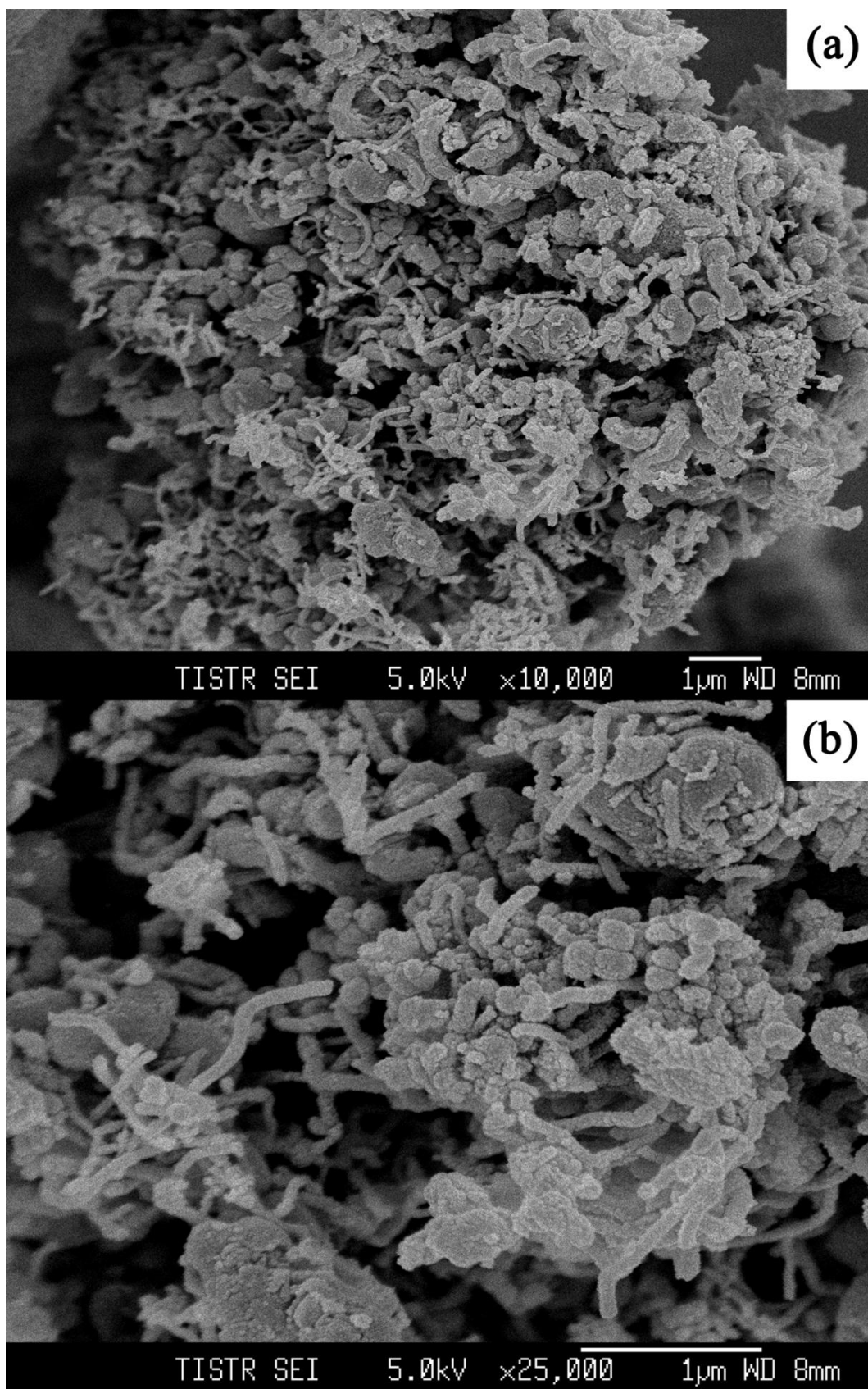


**Figure 4.7** The morphology of NiO/Raw-treated MWNTs illustrated by (a) Low magnification images of SEM (b) High magnification images of SEM.

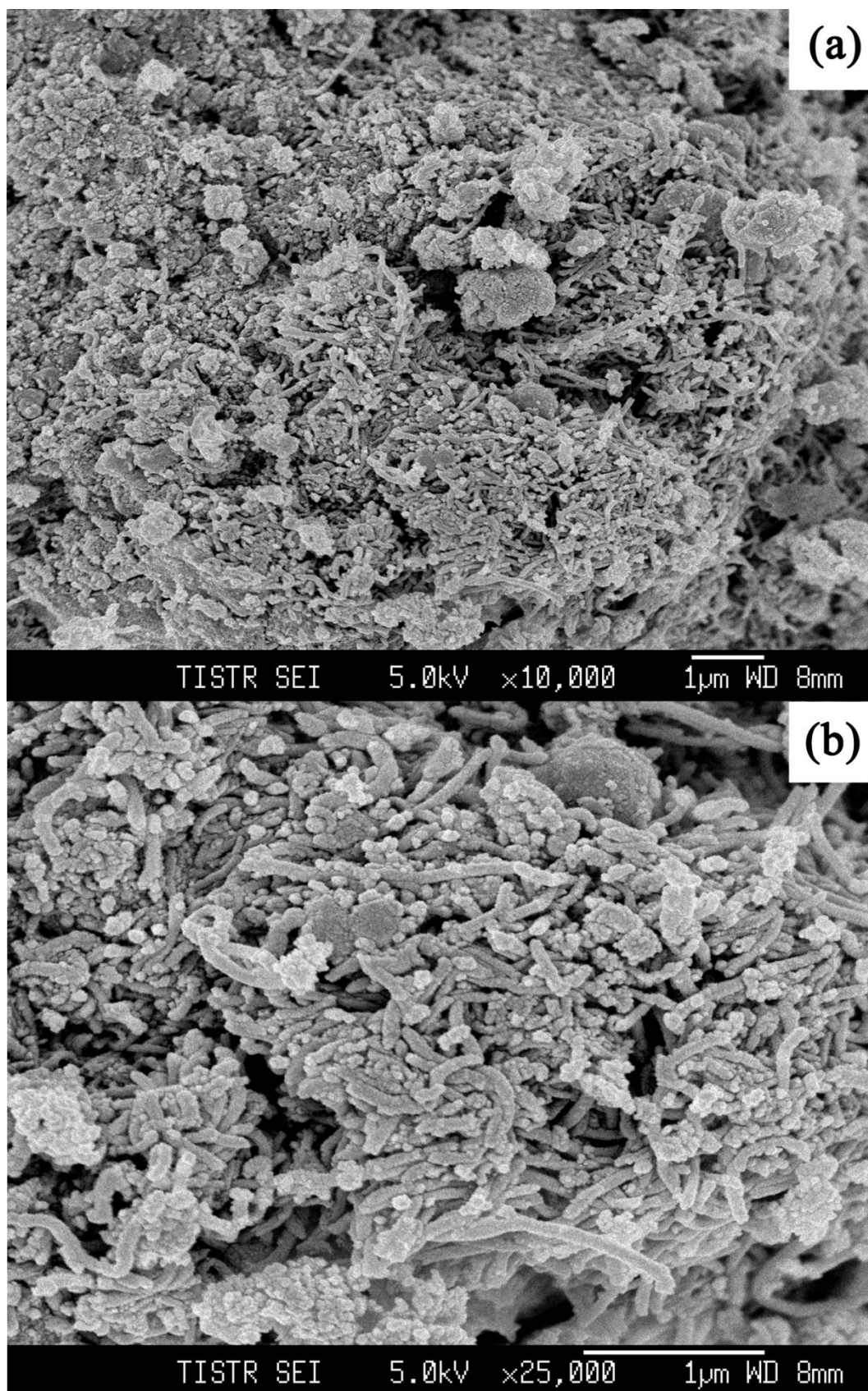


**Figure 4.8** The morphology of NiO/Acid-treated MWNTs illustrated by (a) Low magnification images of SEM (b) High magnification images of SEM.

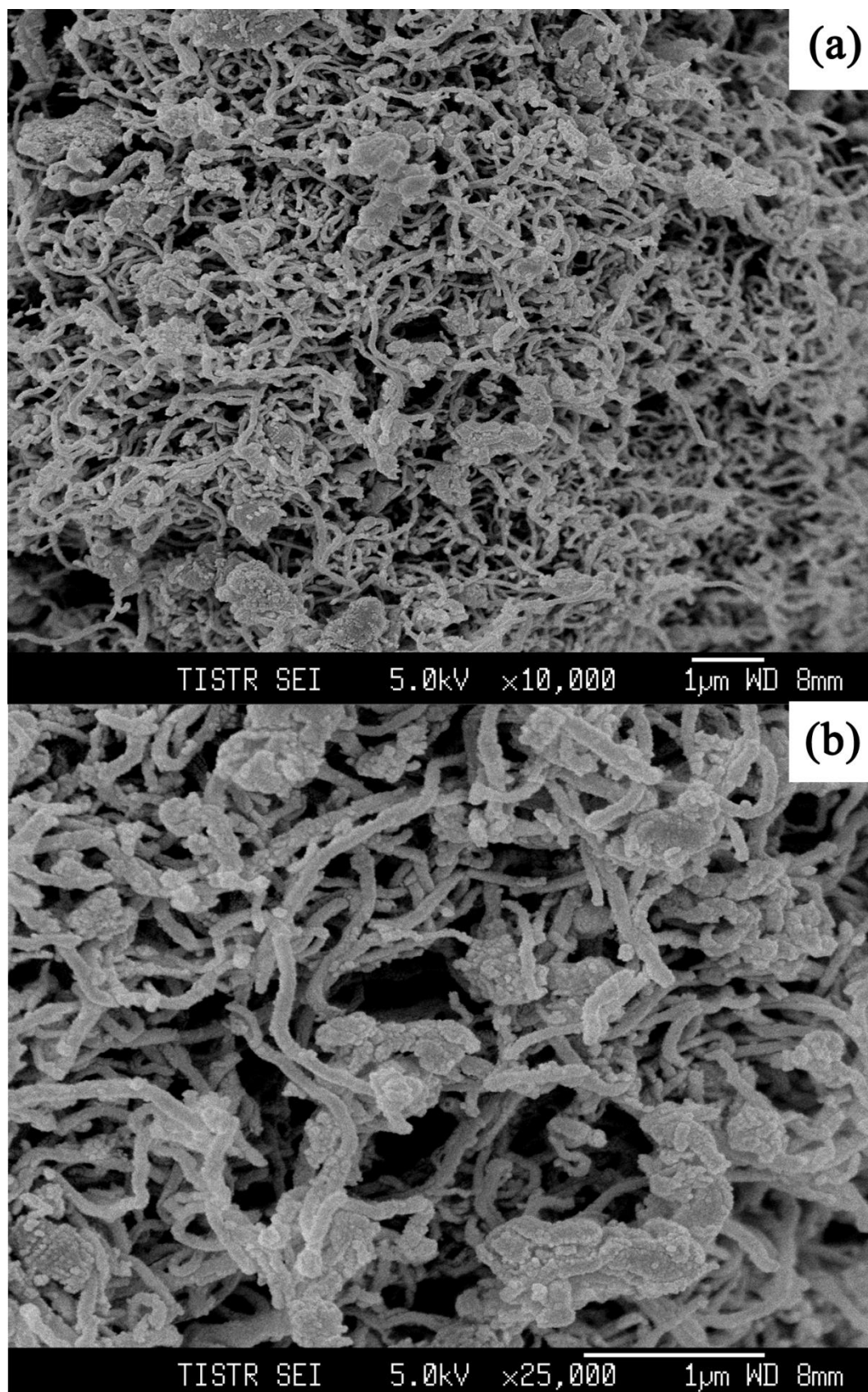


**Figure 4.9** The morphology of NiO/SDS-treated MWNTs illustrated by (a) Low magnification images of SEM (b) High magnification images of SEM.

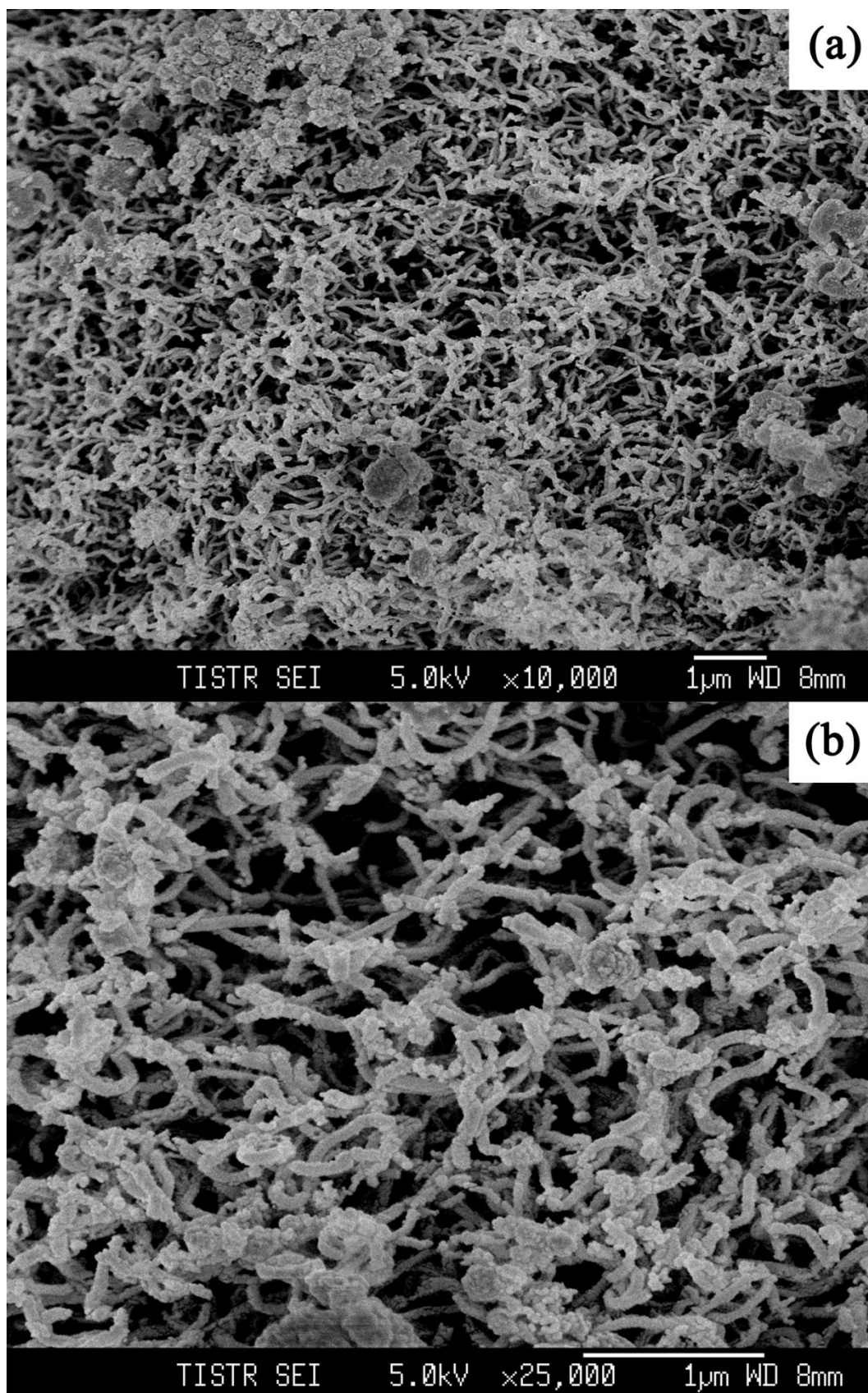


**Figure 4.10** The morphology of NiO/UV-ozone-treated MWNTs illustrated by (a) Low magnification images of SEM (b) High magnification images of SEM

#### 4.2.1.3. The Energy-dispersive X-ray spectroscopy results

The quantitative microanalysis of C and Ni as major elements for the NiO/UV-Ozone treated MWNTs nanocomposite was performed by Energy-dispersive X-ray spectroscopy (EDX). The EDX spectra of NiO/MWNTs nanocomposite are shown in Figure 4.11. The spectra exhibit the presence a major elements of C with Ni and O peaks which confirms the nanoparticles absorbed on MWNTs are NiO phase. The numerical result of EDX quantitative microanalysis of C: Ni: O is about 77: 12: 11. The distribution of major elements including C, O and Ni was also carried and the corresponding results are illustrated in Figure 4.12, which firmly exhibits the uniform distribution of NiO on CNTs.

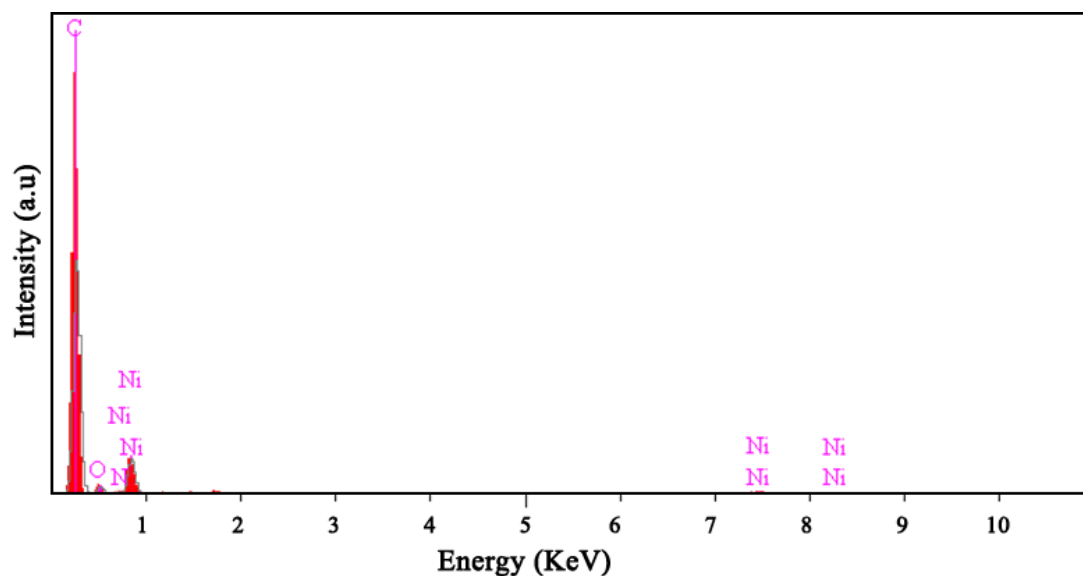


Figure 4.11 EDX spectra of NiO/MWNTs nanocomposite

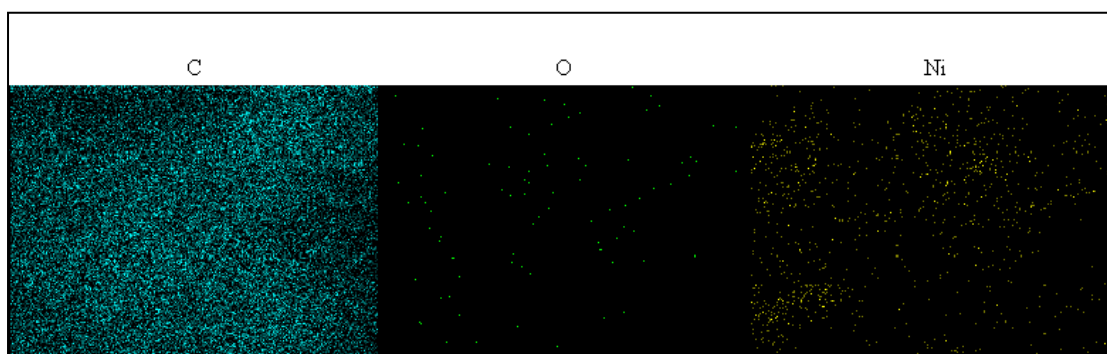
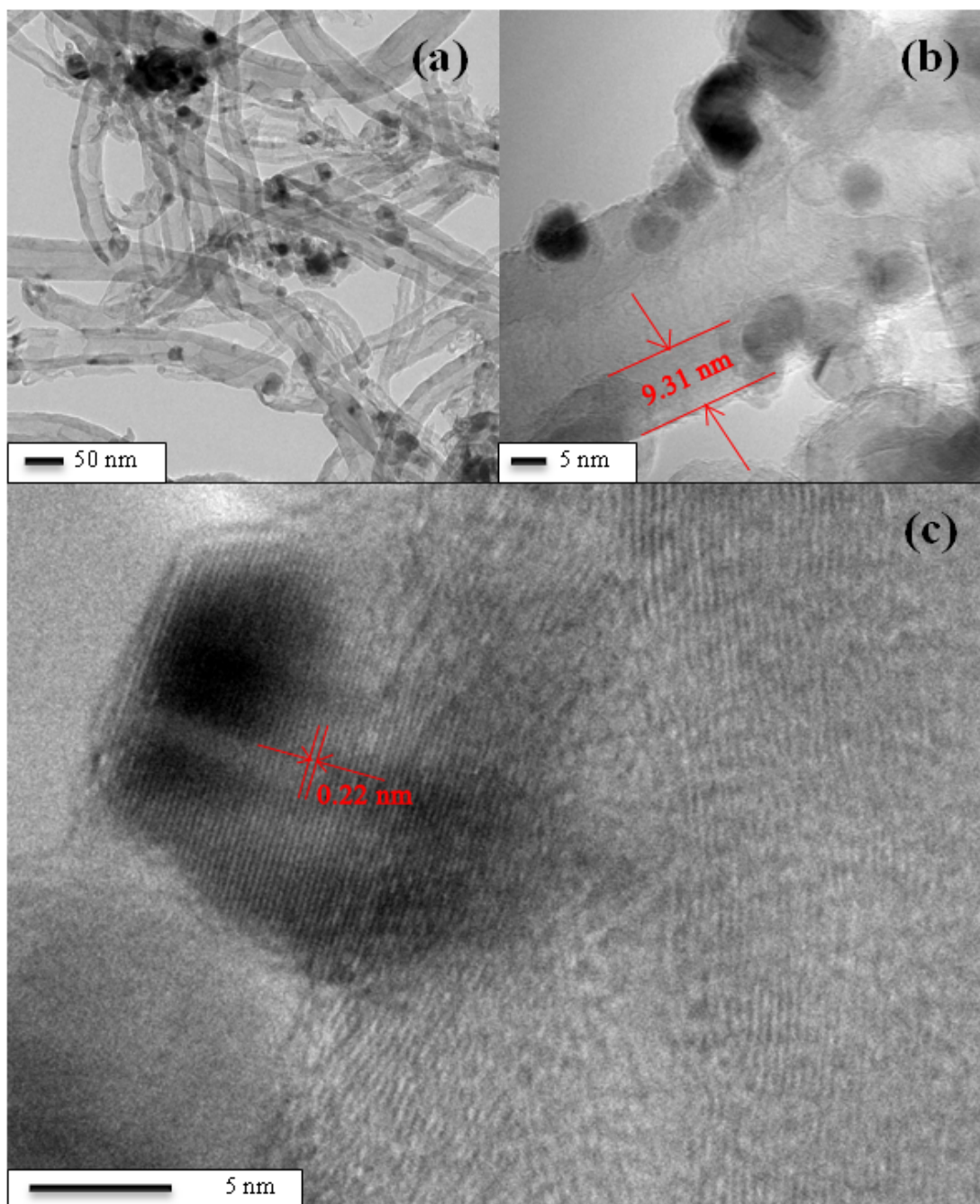


Figure4.12 EDX elemental mapping of Carbon, Oxygen and Nickel

#### 4.2.1.4. The Transmission Electron Microscopy results

To ascertain morphology of obtained samples, NiO/surface modified MWNTS nanocomposite were further characterized and confirmed by TEM. The TEM image of the NiO/surface modified MWNTs exhibits in Figure 4.12 for NiO/raw MWNTs, Figure 4.13 for NiO/acid-treated MWNTs, Figure 4.14 for NiO/SDS-treated MWNTs and Figure 4.15 for NiO/UV-ozone-treated MWNTs. As observed in low-magnified TEM images, the MWNTs exhibits Bamboo-like structure [37]. All TEM images except Figure 4.14 clearly indicate the formation of NiO nanoparticles which are intimately adhered to the MWNTs walls in the combination of nanoparticles and quasi-spherical shape structure. The results also indicate that the NiO/UV-ozone treated MWNTs have more uniform coating ability of NiO compared to the NiO/raw MWNTs which the amount NiO on wall of MWNTs are less. Additionally, NiO/acid-treated MWNTs which the deposition of NiO on wall of MWNTs was resembled as clusters forms with bad distribution whereas NiO/SDS treated MWNTs which shows nanorod-like structure of NiO coating over the wall of MWNTs. The average particle size of NiO is less than 12 nm, which is consistent with the values obtained from the XRD results. The High resolution (HR) TEM images clearly show the patterns of the MWNTs with wall thickness of 8-14 nm and the lattice pattern of NiO corresponding to (111) plane of reflection. Based on overall results, the UV-ozone treatment is determined as the suitable process to treat and functionalize the MWCNTs for the synthesis of NiO/CNTs. The possible mechanisms involved in the formation of NiO onto MWNTs may be described. Firstly, UV treatment may modify the wall of MWNTs with oxygen-containing functional groups which are more reactive than defect-free CNTs. When introduced into treated CNT matrix,  $\text{Ni}^{2+}$  would likely react on the sidewall of CNTs with the assistance of these defects resulting to intermediate product such as  $\text{Ni}(\text{OH})_2$ . During uniformly heating under microwave irradiation, NiO caused by the dehydration of  $\text{Ni}(\text{OH})_2$  can be rapidly formed and nucleated on the wall of CNTs by and the composite of NiO and MWNTS is finally achieved.



**Figure 4.13** The fine structure of (a) Low magnification of NiO/Raw-treated MWNTs (b) High magnification TEM image of NiO/Raw-treated MWNTs (c) HRTEM image of NiO/Raw-treated MWNTs nanocomposites

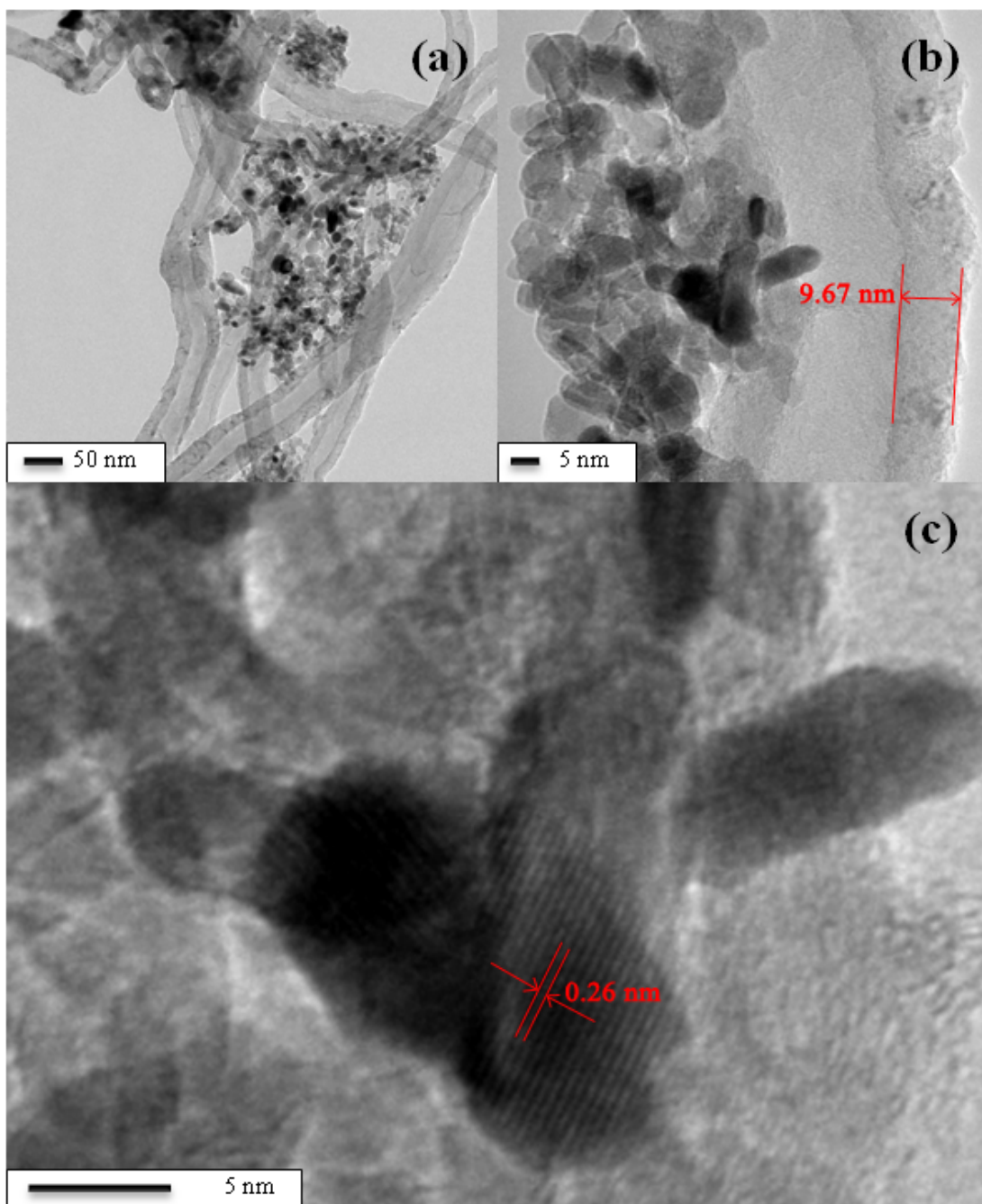


**Figure 4.14** The fine structure of (a) Low magnification of NiO/Acid-treated MWNTs (b) High magnification TEM image of NiO/Acid-treated MWNTs (c) HRTEM image of NiO/Acid-treated MWNTs nanocomposites

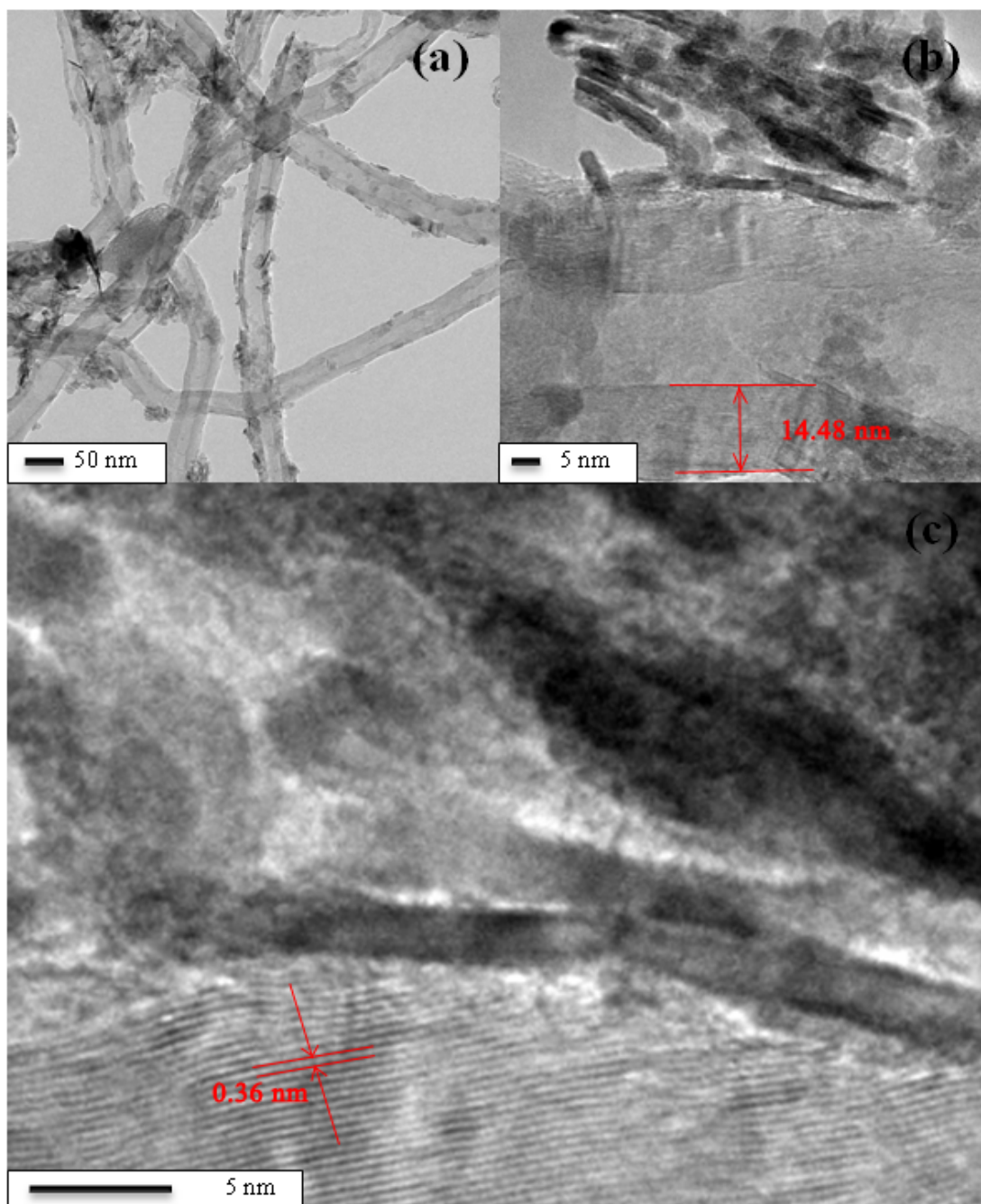


**Figure 4.15** The fine structure of (a) Low magnification of NiO/SDS-treated MWNTs (b) High magnification TEM image of NiO/ SDS -treated MWNTs (c) HRTEM image of NiO/ SDS -treated MWNTs nanocomposites

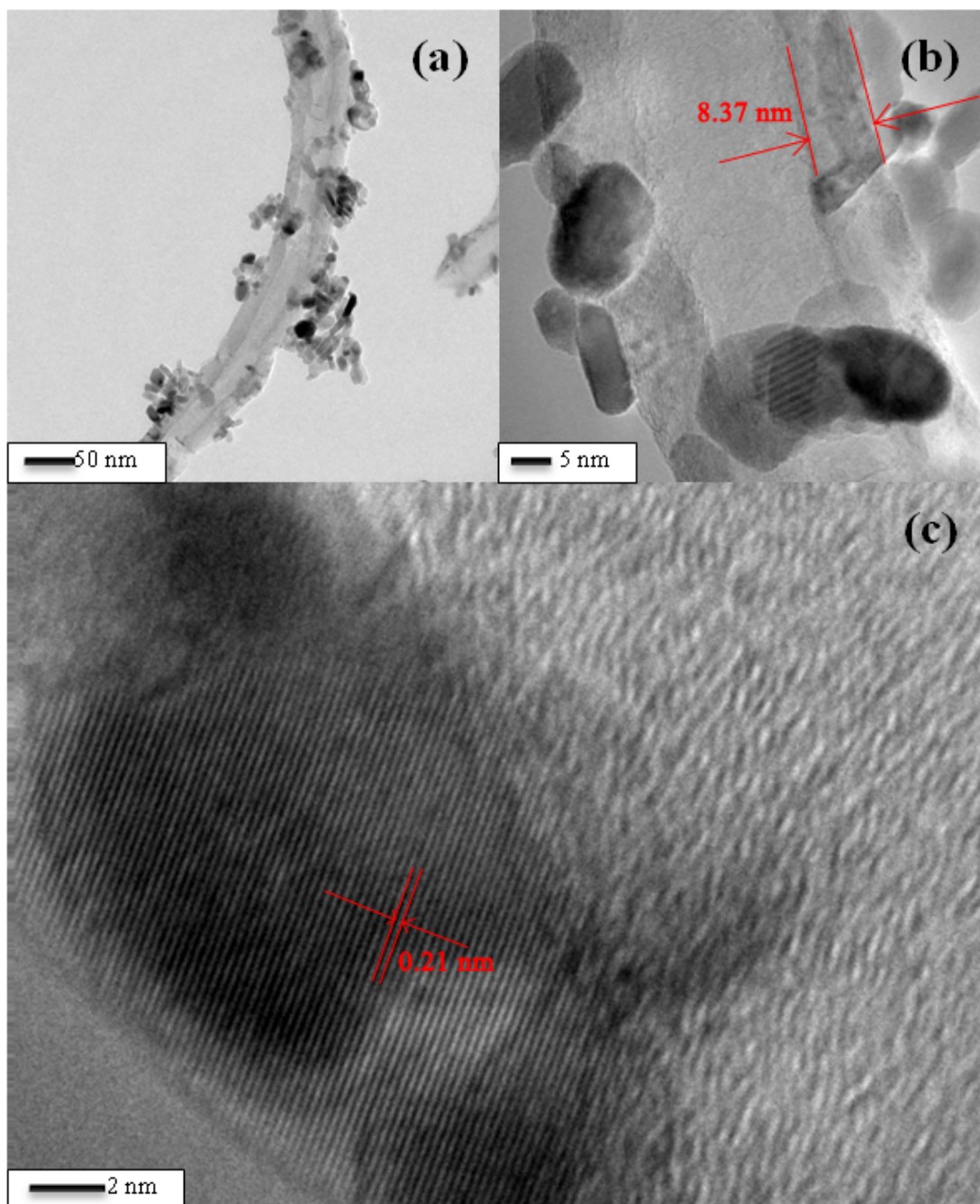


**Figure 4.16** The fine structure of (a) Low magnification of NiO/UV ozone-treated MWNTs (b) High magnification TEM image of NiO/ UV ozone-treated MWNTs (c) HRTEM image of NiO/ UV ozone-treated MWNTs nanocomposites

## **4.2.2. NiO/UV-Ozone treated MWNTs nanocomposites with various irradiation powers**

### **4.2.2.1. XRD results**

As mentioned above, the UV-ozone treatment was chosen as the preliminary process for functionalization of CNTs before the synthesis of the composites. In this section, only this condition was designated for the synthesis of NiO/CNTs composite under various microwave irradiation powers. The XRD patterns of NiO/UV-ozone treated MWNTs nanocomposites are illustrated in Figure. 4.16. As same as Figure. 4.6, the peak situated at  $26.4^\circ$  observed in all samples is referred to (002) *d*-spacing of the CNTs (JCPDS-ICDD No.751621) whereas the peaks at  $44.6^\circ$ ,  $51.9^\circ$  and  $75.7^\circ$  correspond to the FCC structure of the Ni catalyst used in CNTs synthesis process [33]. For as-synthesized composites, the peaks positioned at  $2\theta=37.3^\circ$ ,  $43.1^\circ$ , and  $62.8^\circ$  attribute to (111), (200), and (220) orientation planes of cubic NiO, respectively (JCPDS-ICDD No.895881). XRD results prove that all composites are mixtures of two phases of NiO and CNT. In addition, It is clearly seen that all specific XRD peaks are prominent, indicating high purity of as-synthesized product and high crystallinity of as-obtained NiO particles. It is noticeable that the peak intensity belonging to NiO becomes stronger and more intense as the irradiation power increases, indicating that the crystallinity and formation of NiO nanostructure significantly improve with increasing irradiation power.

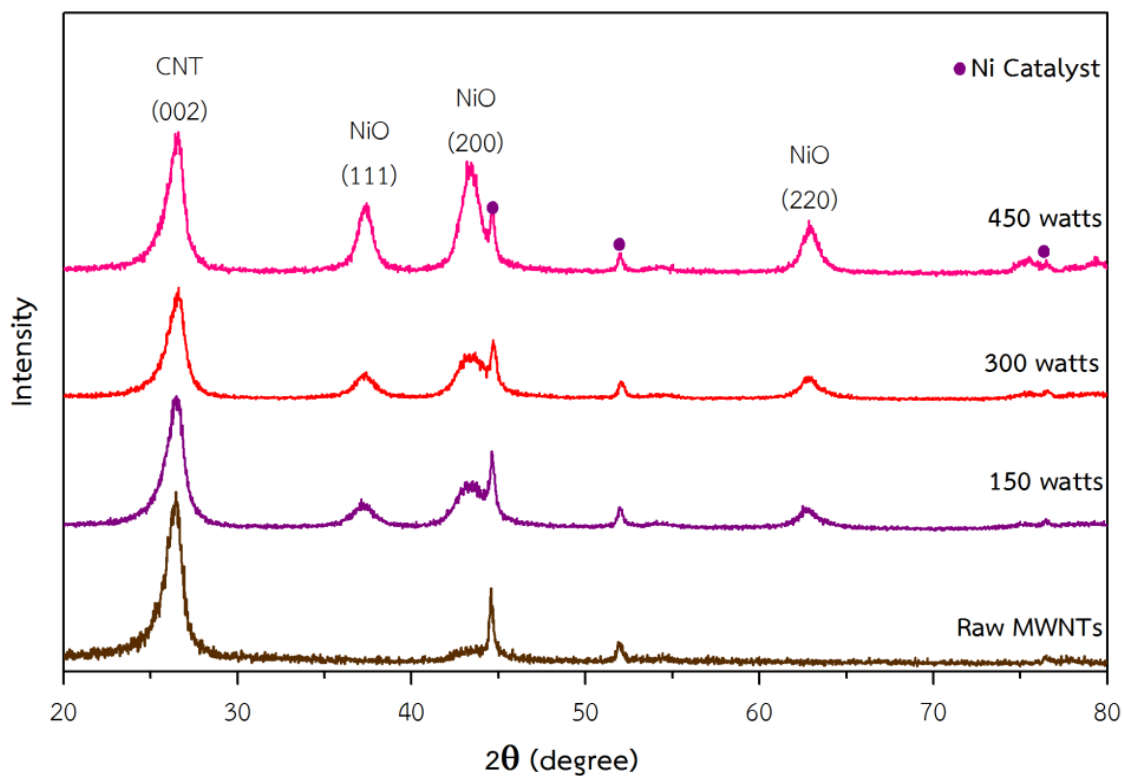


**Figure 4.17** XRD patterns of NiO/MWNTs composites prepared at different microwave irradiation powers

#### 4.2.2.2. The Scanning Electron Microscopy results

The morphologies of NiO/MWNTs with various irradiation powers were investigated by FE-SEM. The morphologies of the composites synthesized by microwave heating at irradiation power of 150, 300 and 450 watt are shown in Figure 4.17, 4.18 and 4.19, respectively. It is clearly seen that a number of NiO particles are tightly attached to the sidewall of MWNTs leading to the well-dispersed network. The amount of NiO nanoparticles attached to the MWNTs surface and distribution uniformity tends to increase in accordance with the increasing of irradiation power. It is also noticed that the MWNTs diameter significantly decrease, comparing to pristine MWNTs, which may be attributable to the dehydration of MWNTs during heating process. The increasing amount of NiO nanoparticles with small sizes can provide greater specific surface area and more active sites for related reactions. The amounts of heat supplied by microwave irradiation increase with increasing irradiation power, which guides in the better formation of NiO and the binding between NiO particles and the sidewall of MWNTs.

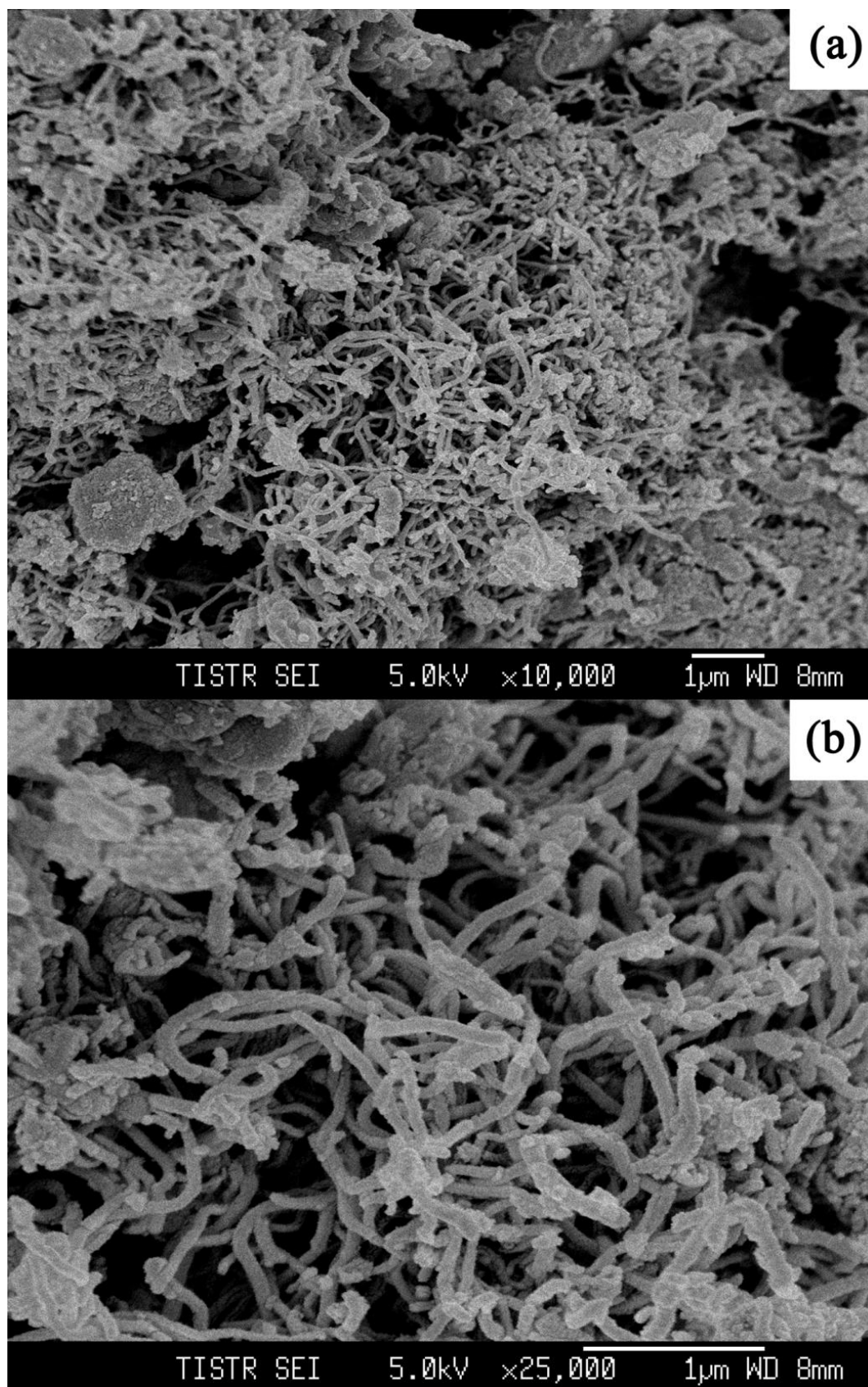


**Figure 4.18** SEM images of NiO/MWNTs nanocomposite prepared at 150 watts

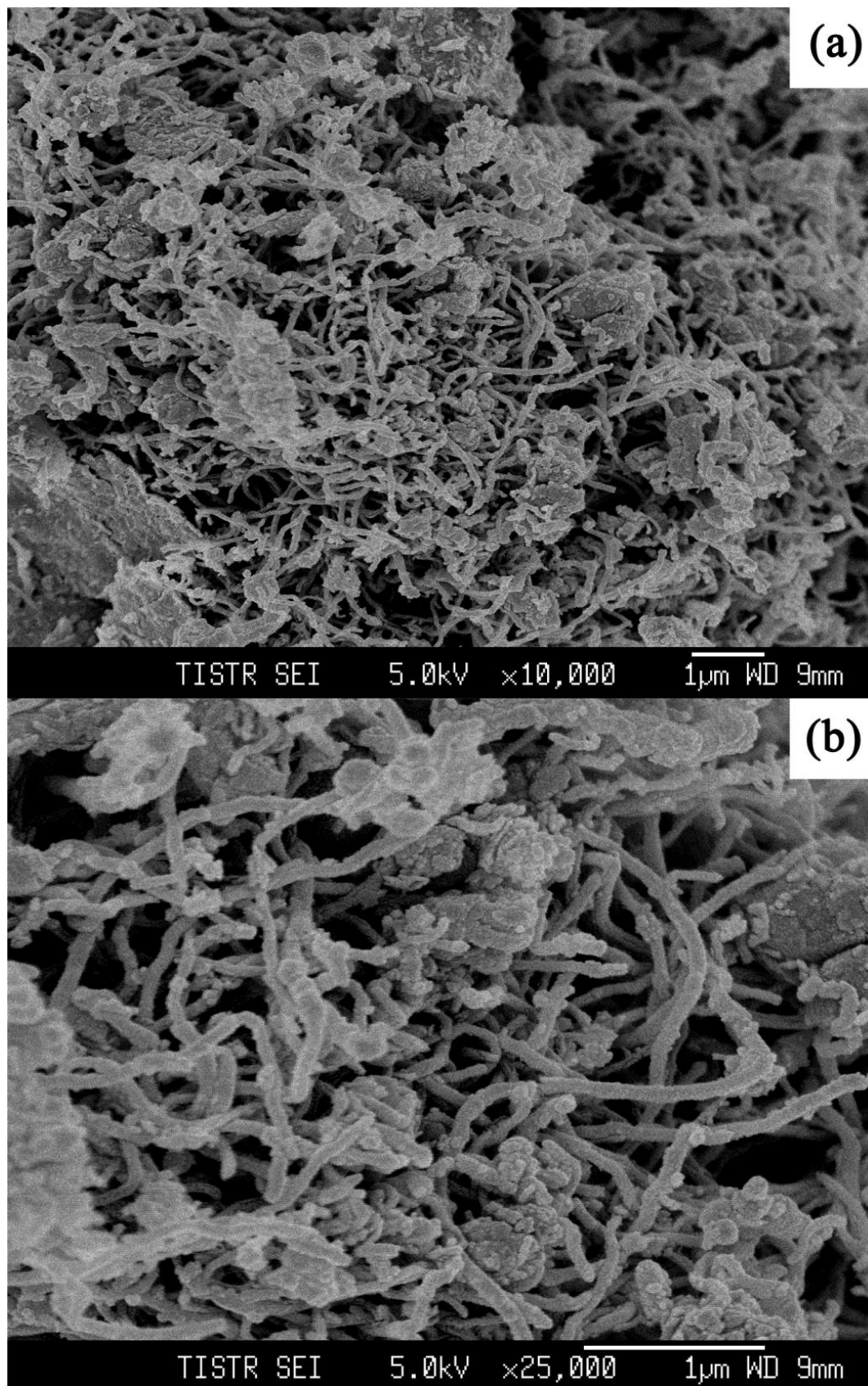


**Figure 4.19** SEM images of NiO/MWNTs nanocomposite prepared at 300 watts

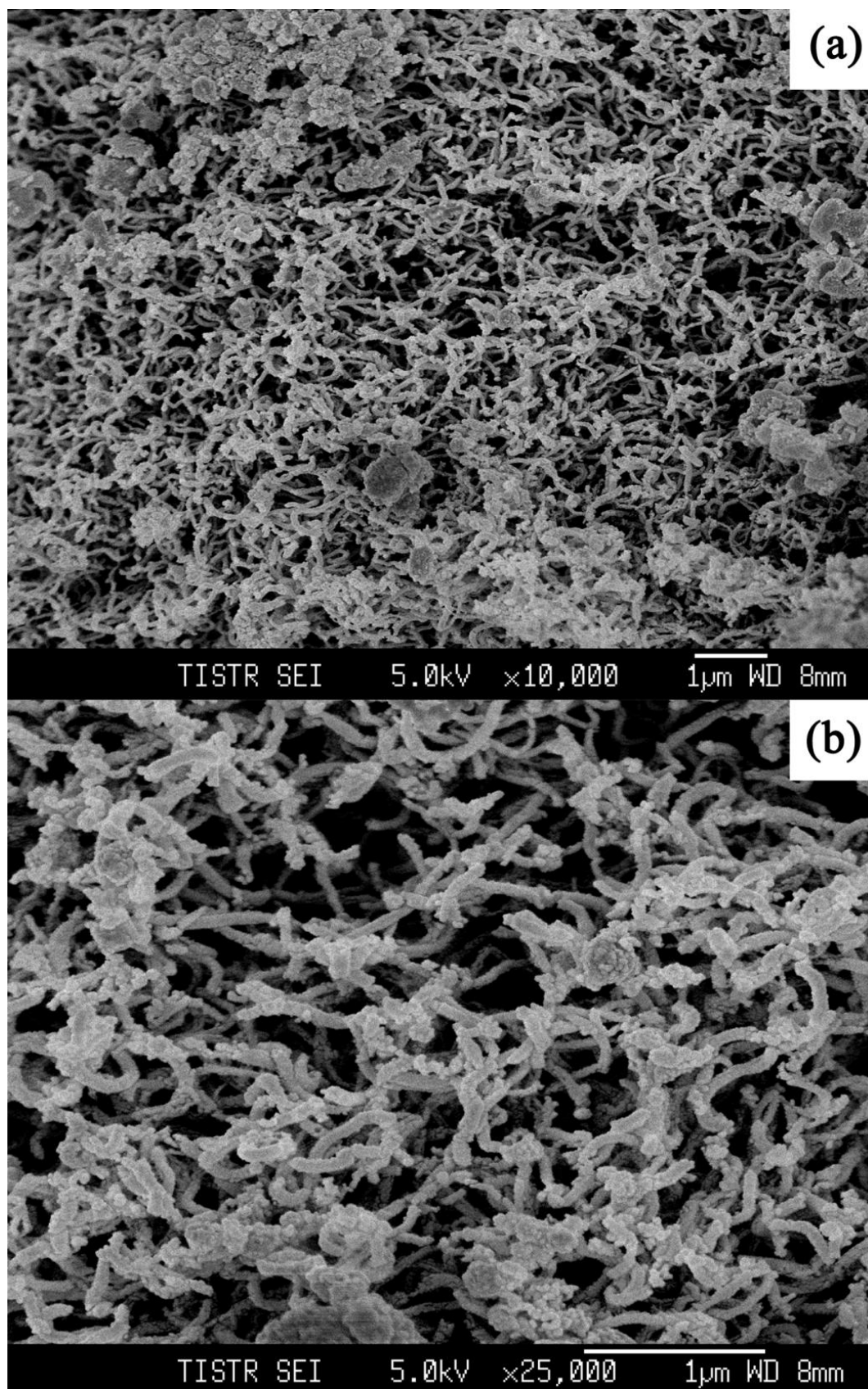


**Figure 4.20** SEM images of NiO/MWNTs nanocomposite prepared at 450 watts

From XRD and SEM results, the amount of Nickel oxide in NiO/ surface modified MWNTs nanocomposite can be speculated. The XRD results indicate that all composites are mixtures of two phases of NiO and CNTs. The intensity of (111), (200), and (220) reflection which is the planes of cubic Nickel oxide of NiO/MWNTs nanocomposite. The intensity of NiO in NiO/ unmodified MWNTs nanocomposite are much higher than that of NiO/ unmodified MWNTs nanocomposite, implying that the amount of NiO nanostructures with better crystallinity increases with increasing irradiation power. In addition, the corresponding SEM results clearly indicate the existence of NiO nanostructure tightly attached to the sidewall of the surface modified MWNTs and reveals that the MWNTs treated with the UV-Ozone have more amount of well-defined and uniformly distributed NiO nanoparticles coated on MWNTs, comparing to the MWNTs treated with either SDS or acid mixture and the amount of NiO nanoparticles also increases with increasing irradiation power. This good appearance and distribution of NiO nanoparticles onto MWNTs obtained by UV-treatment and microwave assistance could result to the increasing of active surface area and significant enhancement of their chemical sensing performance.

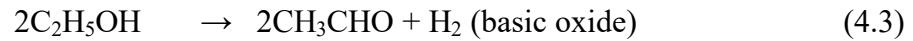
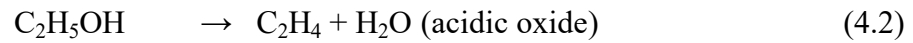
### **4.3.Applications of the NiO/MWNTs composite as chemical sensing materials**

#### **4.3.1. Gas sensing**

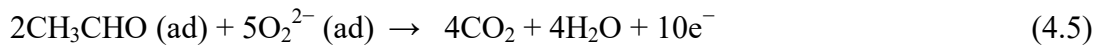
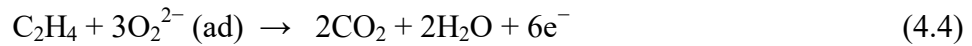
The basic principles of gas sensor usually use an electrical response by adsorption of gas molecules on surface of an active layer (in this case is surface of Nickel oxides) which causes the electron transfer between gas molecules and material, leading to the alternation of conductivity (or resistivity) of the material. The conductivity of semiconductor oxides consisted to the conductivity of bulk, grain boundary and especially on surface. Surface area exposed to the first reaction area to gases. Therefore, the nano-structured have more specific materials area to detected gas molecules.

To compare the sensing properties of MWNTs, NiO and NiO/modified MWNTs nanocomposite, the gas sensing experiment was conducted toward ethanol ( $C_2H_5OH$ ), and methanol ( $CH_3OH$ ) vapor and the sensing performance results are exhibited in Figure 4.20. For MWNTs and NiO/MWNTs nanocomposite, under gas atmosphere, gas molecules are adsorbed on either MWNTs or NiO surface by van der

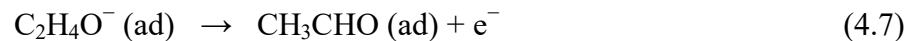
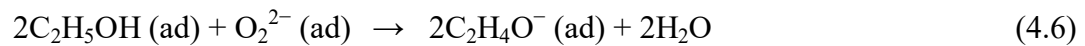
Waals attracting forces, which leads to remarkable changes in their electrical resistance. However, the electrical resistance of NiO/MWNTs nanocomposite was changed abruptly, reflecting dynamically fast response and good recovery. This feature may attribute to the fact that the formation of NiO on the MWNTs surface can provide much greater specific surface areas. It may be also deduced that NiO particles play role on the assistance of the enhancement gas sensing activity meanwhile CNTs matrix can act as both scaffold for the formation of NiO nanoparticles and active sites for gas sensing. There is acknowledged that when NiO particle which is a p-type semiconductor with an energy band gap from 3.6 to 4.0 eV is exposed to alcohol vapor, the gas molecules can adsorbed on the surface of the particle or on the grain boundaries, then generated positive hole on valence band of NiO. This leads to a band bending and depletion region so called space-charge layer in the surface region of the particle. This feature consequently results to a higher surface potential barrier and higher resistance. The alternation of band bending and electrical resistance could be occurred under gas and air atmosphere, leading to the feasibility of gas sensing of these composites. Figure 4.21 shows the sensing performance of NiO/surface modified MWNTs nanocomposites. The results indicated that the NiO/UV-ozone treated MWNTs nanocomposites shows higher response due to the formation of NiO on the surface of MWNTs. This may be resulted from the truth that NiO/UV-ozone treated MWNTs nanocomposites have greater specific surface area and more active sites for vapor detection. The sensing performance of NiO/UV-ozone treated MWNTs nanocomposites with various irradiation powers are illustrated in Figure 4.22. The corresponding sensing response increases as the irradiation power elevates from 150 W to 450 W. The result indicated that the increase in heating provided to the system by increasing irradiation power can result to the better formation of NiO onto the MWNTs surface. This increment in specific areas which take responsibility to the better sensing performance can provide more active sites to alcohol sensing reaction. NiO is a p-type semiconductor which readily covered with chemisorbed oxygen. Thus, at the sensing temperature, the adsorption of negatively charged oxygen can generate the holes for conduction. The target gas (ethanol) may undergo different reactions, and then can take two routes of decomposition reaction, i.e., dehydration and dehydrogenation as described by following equations:



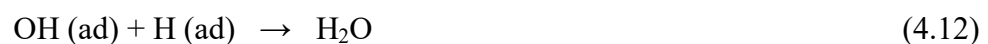
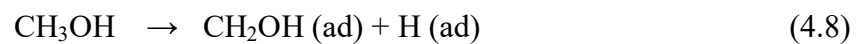
These primary products thus formed are consecutively oxidized to CO, CO<sub>2</sub> and H<sub>2</sub>O.



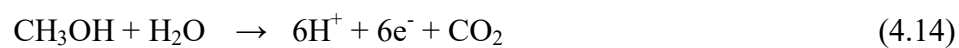
Under sensing condition, target ethanol gas could favorably experience dehydrogenation and Acetaldehyde (CH<sub>3</sub>CHO) was obtained [39], the reaction of the sensing process was explained by equation:



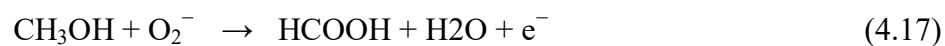
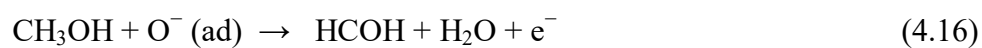
For methanol gas, the sensor is exposed to methanol molecules that can react with the adsorbed surface oxygen or with the moisture present in air and then decompose to hydrogen atoms on the catalytic gate electrode surface. The reaction of the sensing process can be explained by following equations:



In presence of moisture, the following reactions are possible:



However, another possibility is the decomposition of methanol to formaldehyde and formic acid by reacting with the chemisorbed oxygen on the oxide surface.



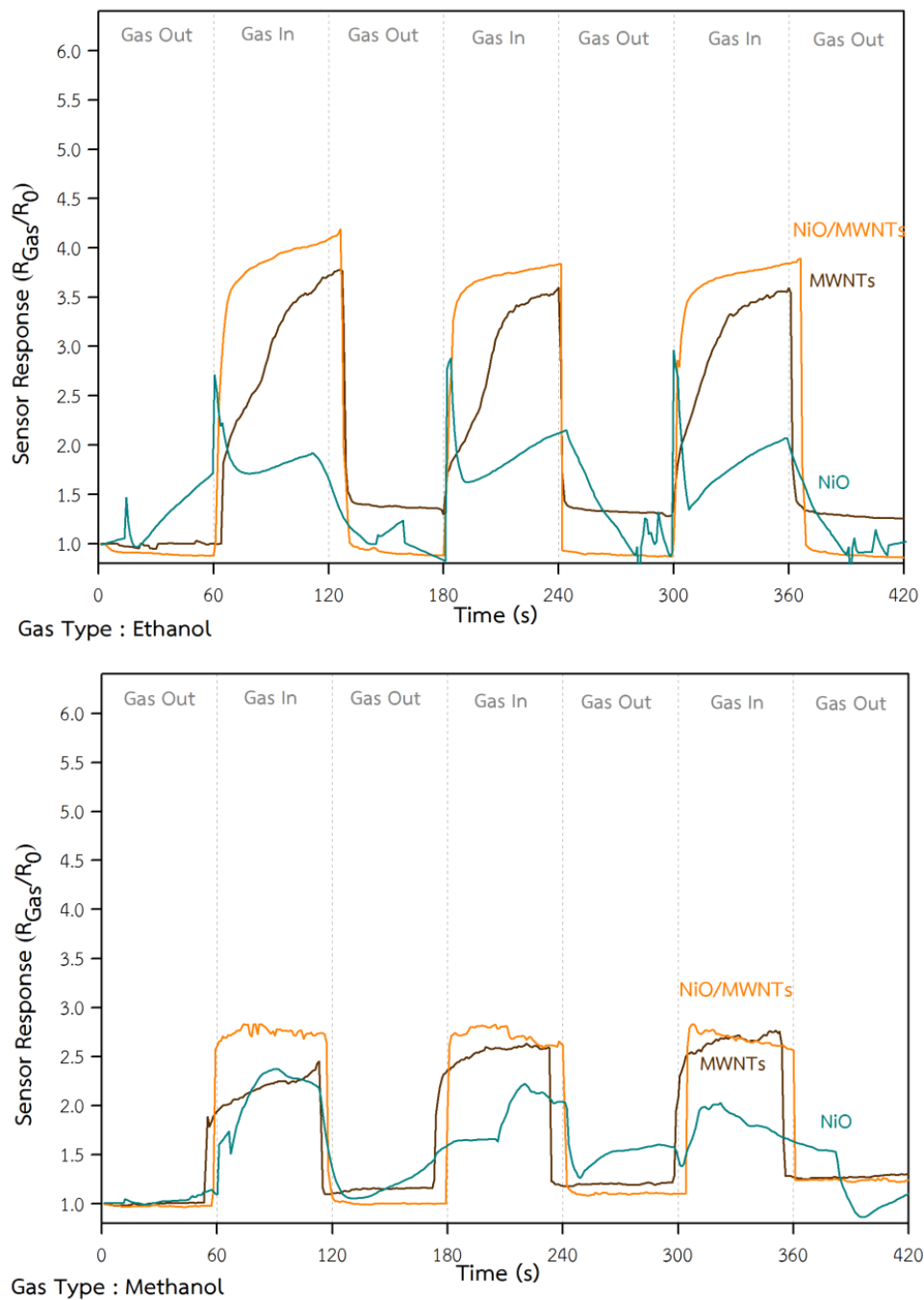


**Figure 4.21** Sensing Performance of MWNTs, NiO and NiO/MWNTs nanocomposite.

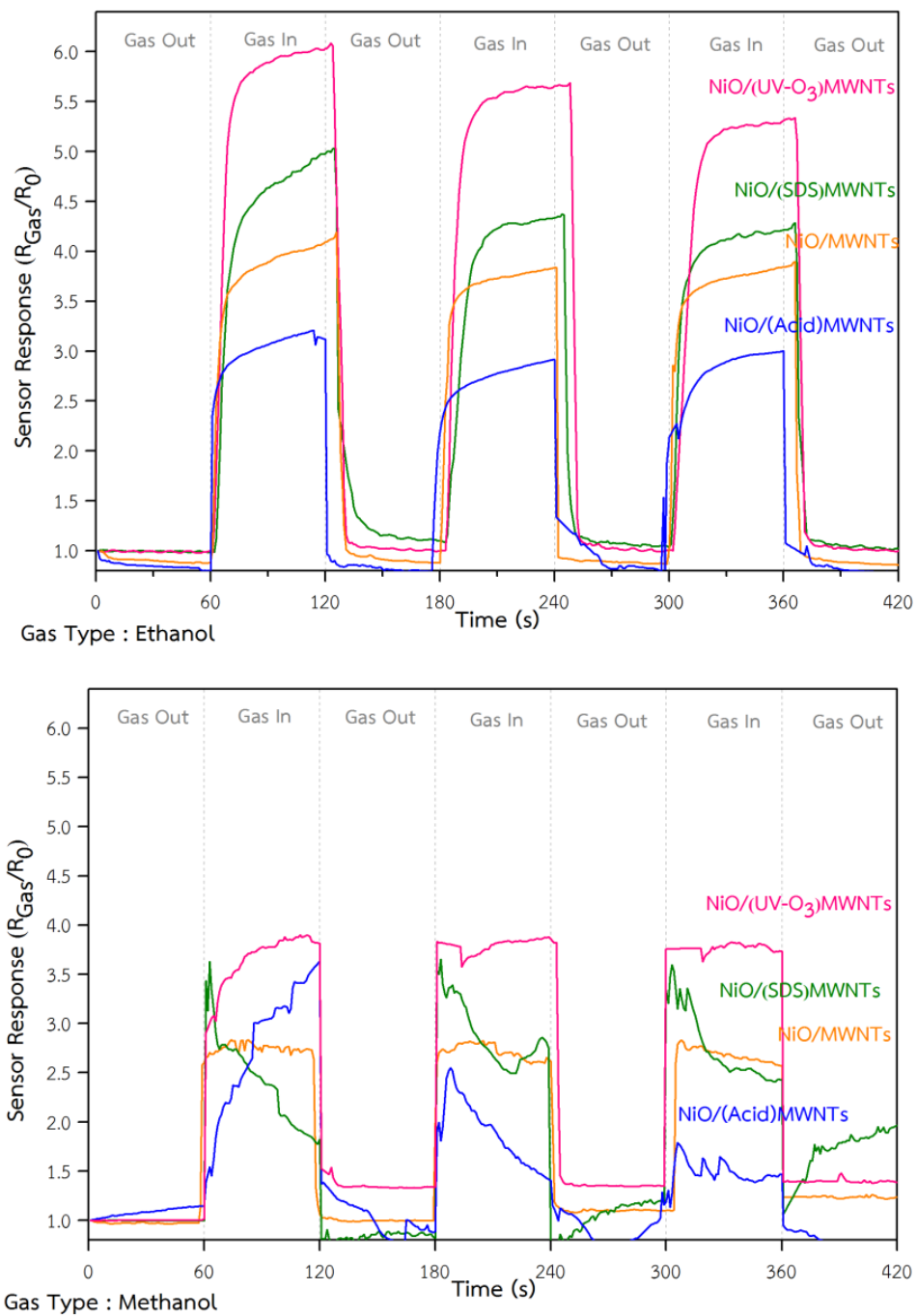


**Figure 4.21** Sensing Performance of NiO/surface modified MWNTs nanocomposites.

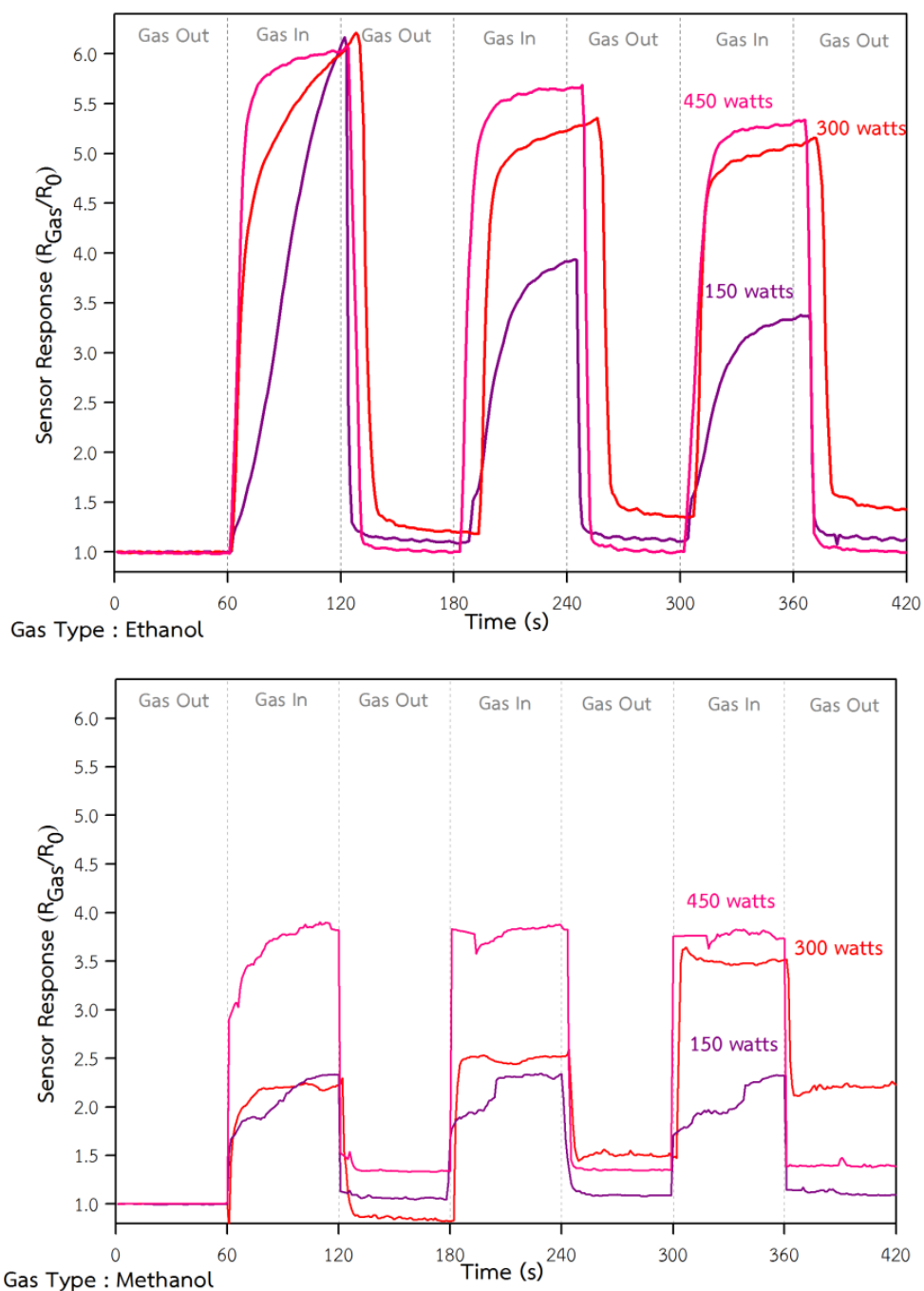


**Figure 4.22** Sensing Performance of NiO/UV-O<sub>3</sub> treated MWNTs nanocomposites with various irradiation powers.

### 4.3.2. Modified electrode

#### 4.3.2.1. Cyclic Voltammetry measurement of NiO/MWNTs/FTO modified electrode

To investigate the electrochemical and electrocatalytic performance of NiO/MWNTs composites, modified working electrode using as-synthesized

composite as modified sensing material were carried out by cyclic voltammetry measurement. The cyclic voltammograms performed for the electrodes in 1 mM  $K_3Fe(CN)_6$  at a scanning rate of 50 mV/s is illustrated in Figure. 4.23. The electrode potential was scanned between  $-0.4$  V to 1 V and the anodic and cathodic current responses were measured. The higher anodic and lower cathodic peak were observed indicated that the current responses of electrode modified by NiO/MWNTs composite is more efficient than unmodified electrode. This enhanced characteristic performance may be resulted from the fact that the NiO particles with smaller sizes should be beneficial for higher specific surface area and more active sites for redox action of the NiO. Each curve is composed of capacitive current, which originates from the phase of active materials, resulting from a uniform NiO coating layer on MWNTs with larger specific surface area. For the modified electrode, an obvious anodic oxidation peak was observed. CV results suggest that the performance of working electrode can be enhanced by modification with NiO/MWNTs nanocomposites. The optimized preparation condition of the composite was also notified. The peak shifts to higher potential values (about 300 mV) due to the increased of specific area and kinetic effect of NiO/MWNTs/FTO modified electrode.

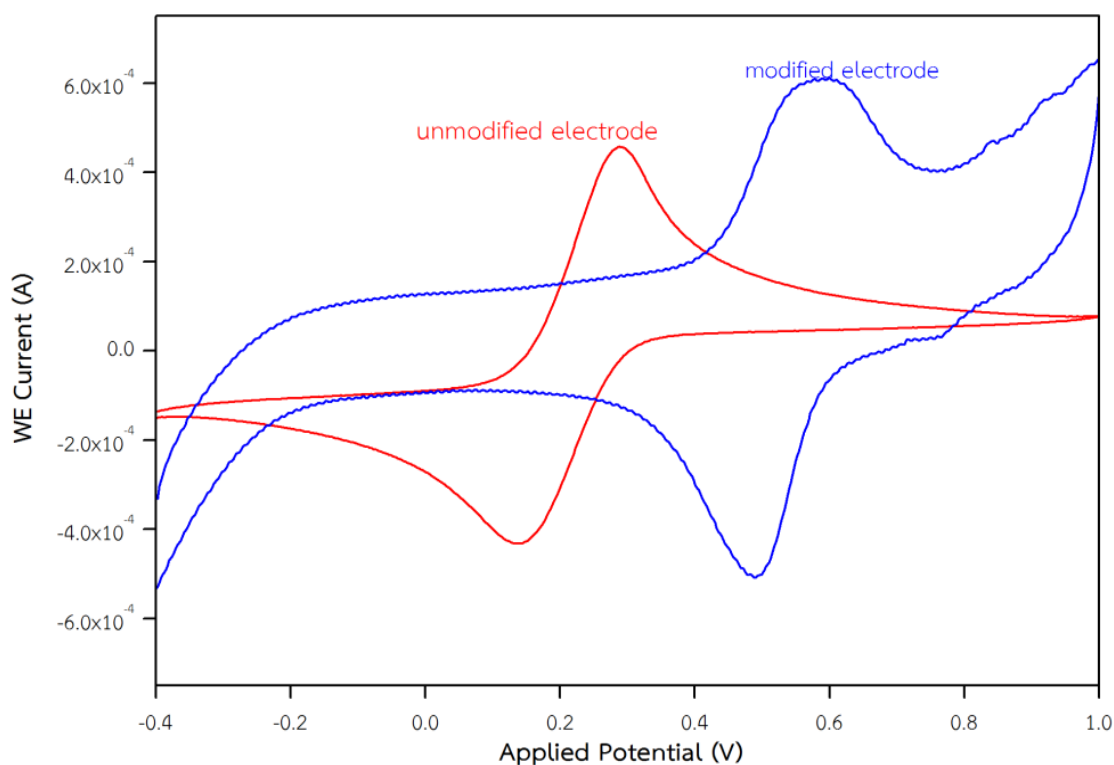


**Figure 4.24** Cyclic voltammograms of bare electrode and modified electrode heat with irradiation powers

#### 4.3.2.2. The electrocatalytic reduction of NiO/MWNTs/FTO modified electrode

The electrocatalytic reduction of hydrogen peroxide ( $\text{H}_2\text{O}_2$ ) at NiO/MWNTs/FTO modified electrode was studied by amperometry, which is one of the most widely used techniques for biosensor. Amperometric batch measurements were conducted in a stirred 0.1M phosphate buffer solution (pH 7) by applying a potential of 0.5V. The current–time responses of the modified electrodes to 10  $\mu\text{L}$  additions of  $\text{H}_2\text{O}_2$  at the applied potential are shown in Figure 4.24. Comparing to the bare FTO electrode, the response of NiO/MWNTs/FTO modified electrode increases in accordance with the increasing of irradiation power. Referring to previous results revealed by XRD and SEM, The electrodes modified by the composite prepared at 450 watt provides larger surface area which give the highest electrocatalytic activity towards  $\text{H}_2\text{O}_2$ . This feature indicates that the increase of irradiation power during microwave irradiation can provide the amount of NiO cluster which can increase the specific surface area and the active sites for reaction.

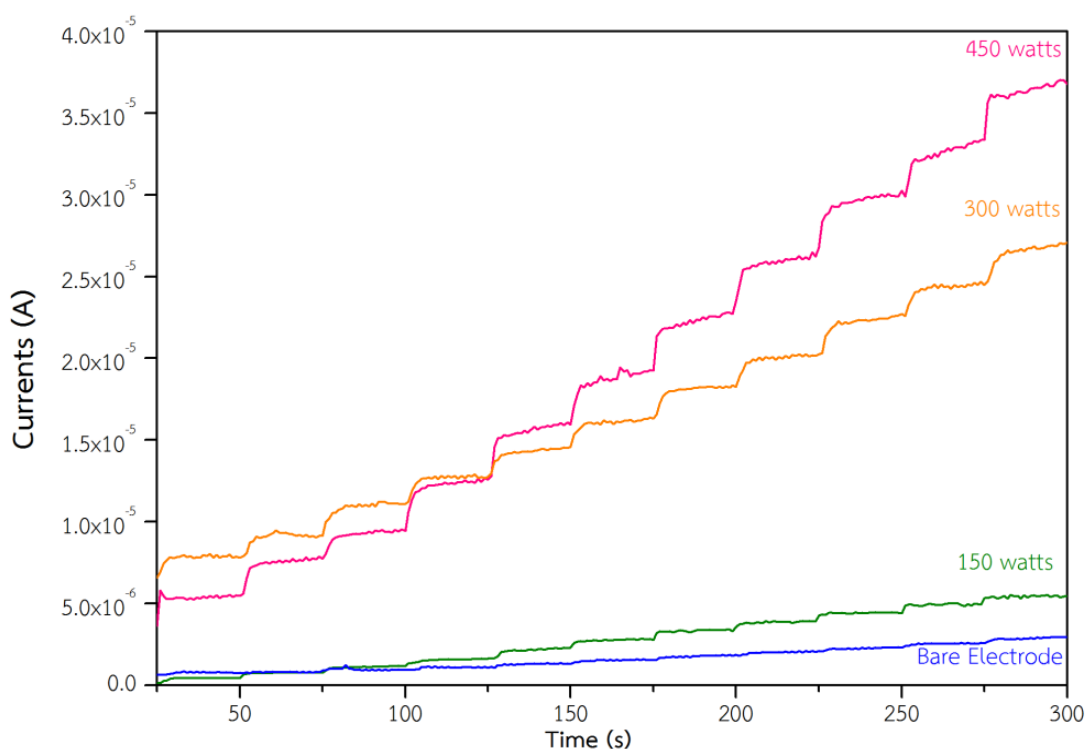


**Figure 4.25** Amperometric response of the FTO electrode and NiO/MWCNT/FTO modified electrodes from successive 10mL additions of  $\text{H}_2\text{O}_2$  at 0.5V in 0.1M phosphate buffer solution with a stirring rate of  $\sim 300$  rpm.

## CHAPTER 5

# CONCLUSIONS

### 5.1. Surface Modification of Multiwall Carbon nanotubes

This work is aimed at the comparison of three different functionalization methods of CNTs for increasing their dispersion stability and developing high-performance of NiO/MWNTs nanocomposites. The results showed that the surface modification of the CNTs has a strong influence on the deposition of the NiO/CNTs composites. Raman spectra of the MWNTs possess two distinct bands located at  $1339\text{ cm}^{-1}$  and  $1570\text{ cm}^{-1}$  which indicates the formation of defects on MWNTs achieved by surface modification which highly affect to the composition of nanoparticles on the surface of MWNTs. It can be concluded that, among three treatment methods, the UV-ozone treatment of CNTs greatly improves the dispersion stability. The FTIR results of UV/ozone-treated MWNTs suggested that the MWNTs are functionalized with the hydroxyl groups and carboxyl group resulting to the induction of the formation of NiO particles on the CNT surface. In addition, this method did not produce any severe morphological damage, such as shortening or sharp bending, compared to acid method. The deposition of NiO on UV-treated CNTs wall was clearly improved, comparing to a surfactant method.

### 5.2. NiO/MWNTs Nanocomposites

NiO/surface modified MWNTs nanocomposites were successfully synthesized by a simple and effective microwave-assisted route via a mixture precursor of  $\text{NiCl}_2 \cdot 6\text{H}_2\text{O}$  and MWNTs. The previous results suggested that the UV-Ozone treatment is suitable as a potential method to functionalized MWNTs. The SEM image reveals that the UV ozone-treated MWNTs have more uniform coating ability of NiO, comparing to the other methods. The XRD and EDX results exhibited that as-prepared composites are composed of two phases of MWNTs and NiO and confirms that nanoparticles absorbed on MWNTs are NiO nanoparticles. SEM and TEM results inform that NiO nanostructures with their size of less than 12 nm are firmly adhered on the surface of CNT and the amount of NiO nanostructures increases with the increase of irradiation power.

### 5.3. Applications

The NiO/MWNTs nanocomposites synthesized by microwave irradiation was utilized as modified material of gas sensor, electrochemical working electrode and its electrocatalytic activities towards hydrogen peroxide were performed.

The gas sensing property of the CNTs is applicable to many kinds of applications due to the fact that CNTs have nanosize, leading to the high sensitivity and rapid gas adsorption. By taking ethanol, methanol and acetone sensing as an example, the sensing stability of the NiO/MWNTs nanocomposite indicates that the NiO/MWNTs modified gas sensor prepared by UV-Ozone treatment at 450 watts of microwave irradiation powers exhibits superiority in sensor response compared to the other treatment methods and other microwave irradiation powers.

The significant improvement interpreted from cyclic voltammogram results. The higher anodic and lower cathodic peak were observed, indicating that the current responses of electrode modified by NiO/MWNTs composite is more efficient than unmodified electrode. It is deduced that the performance of working electrode can be enhanced by modification with NiO/MWNTs nanocomposites. The electrocatalytic reduction of hydrogen peroxide ( $H_2O_2$ ) at NiO/MWNTs/FTO modified electrode was studied by amperometry which compare to the bare FTO electrode, the response of NiO/MWNTs/FTO modified electrode increases in accordance with the increasing of irradiation power, indicating that the increasing of irradiation power can provide greater amount of small NiO cluster which can increase the specific surface area and the active sites for chemical reaction.

## REFERENCES

- [1] Odom, T.W., Huang, J.L., Kim, P. and Lieber, C.M. 2000 “Structure and Electronic Properties of Carbon Nanotubes” **Journal of Physical Chemistry B**. 13(104) : 2794-2809
- [2] McCarthy, M. 2009. **Single-walled Carbon Nanotube**. [Online]. Available : <http://www.istockphoto.com/stock-photo-10936011-single-walled-carbon-nanotube.php>.
- [3] McCarthy, M. 2009. **Multi-walled Carbon Nanotube**. [Online]. Available : <http://www.istockphoto.com/stock-photo-10935590-multi-walled-carbon-nanotube.php>.
- [4] Daenen, M. 2003. **Wondrous World of Carbon Nanotubes**. [Online]. Available : <http://http://students.chem.tue.nl/ifp03/introduction.html>
- [5] Demoncey, N., Stephan, O., Brun, N., Colliex, C. Loiseau, A. and Pascard, H. 1998 “Filling carbon nanotubes with metals by the arc-discharge method: the key role of sulfur” **European Physical journal B**. 4(2) : 147-157
- [6] Nobuta, Y. Yokoyama, K., Kanazawa, J., Yamauchi, Y., Hino, T., Suzuki, S., Ezato, K., Enoda, M. and Akiba M. 2011 “Deuterium concentration of co-deposited carbon layer produced at gap of wall tiles” **Journal of Nuclear Materials** 417(1–3) : 607–611
- [7] Scott, C.D., Arepalli, S., Nikolaev, P. and Smalley, R.E. 2001 “Growth mechanisms for single-wall carbon nanotubes in a laser-ablation process” **Applied Physics A-Materials Science & Processing**. 72(5) : 573–580
- [8] Rummeli, H. 2008. **Synthesis of Single Wall Carbon Nanotubes by Laser Evaporation**. [Online]. Available : <http://www.ifw-dresden.de/institutes/iff/research/Carbon/CNT/laser-ablation/>.

- [9] Sinnott, S.B., Andrews, R., Qian, D., Rao, A.M., Mao, Z., Dickey, E.C. and Derbyshire, F. 1999 “Model of carbon nanotube growth through chemical vapor deposition” **Chemical Physics Letters**. 1(315) : 25–30
- [10] Saveliev, A.V., Kennedy, L. and Jimenez, W.C. 2010 “Combustion synthesis of carbon nanotubes and related nanostructures” **Progress in Energy and Combustion Science**. 6(36) : 696–727
- [11] Li, J., Stevens, R., Delzeit, L., Hou T.N., Cassell, A., Han, J. and Meyyappan M. 2002 “Electronic properties of multiwalled carbon nanotubes in an embedded vertical array” **Applied Physics Letters**. 5(81) : 910-912
- [12] Korneva, G. 2008. “**Functionalization of Carbon nanotubes**” Ph.D.Thesis Of Drexel University
- [13] Wang, Y. Zhu, J., Yang, X., Lu, L. and Wang, X. 2005 “Preparation of NiO nanoparticles and their catalytic activity in the thermal decomposition of ammonium perchlorate”, **Thermochimica Acta**. 1(437) : 106–109
- [14] Steele, R.B. 2004. **New Layered Compounds for High Temperature Superconductivity**. [Online]. Available : <http://www.chemexplore.net/ReO3-NiO.htm>.
- [15] Winter, M. 2000. **Nickel compounds: nickel oxide**. [Online]. Available : [http://www.webelements.com/compounds/nickel/nickel\\_oxide.html](http://www.webelements.com/compounds/nickel/nickel_oxide.html)
- [16] Lan, T. 2007. **Nanocomposite Materials for Packaging Applications**. [Online]. Available : [http://www.nanocor.com/tech\\_papers/Antec-Nanocor-Tie%20Lan-5-07.pdf](http://www.nanocor.com/tech_papers/Antec-Nanocor-Tie%20Lan-5-07.pdf)
- [17] Saito, T., Matsushige, K. and Tanaka, K. 2002 “Chemical treatment and modification of multi-walled carbon nanotubes” **Physica B** 1-4(323) : 280–283
- [18] Pang, M., Li, C., Ding, L., Zhang, J., Su, D., Li, W. and Liang C. 2010 “Microwave-Assisted Preparation of Mo<sub>2</sub>C/CNTs Nanocomposites as Efficient Electrocatalyst Supports for Oxygen Reduction Reaction” **Industrial & Engineering Chemistry Research**. 9(49) : 4169–4174

- [19] Clark, C.M. 2007. **Single-crystal X-ray Diffraction.** [Online]. Available : [http://serc.carleton.edu/research\\_education/geochemsheets/techniques/SXD.htm](http://serc.carleton.edu/research_education/geochemsheets/techniques/SXD.htm)
- [20] Yager, K. 2008. **Nanotechnology: A Brief Overview.** [Online]. Available : <http://barrett-group.mcgill.ca/tutorials/nanotechnology/nano02.htm>
- [21] Melbourne, J. 2012. **Seeing is believing.** [Online]. Available : <http://www.experimentation-online.co.uk/article.php?id=1369>
- [22] Nadu, T. 2011. **Fourier transform infrared spectroscopy.** [Online]. Available : <http://nanotechno.webnode.com/nanoparticles/characterization-of-nano-particles/fourier-transform-infrared-spectroscopy/>
- [23] Kast, R. 2010. **“Identification of neuroblastoma and its prognostic markers using Raman spectroscopy.”** Ph.D.Thesis Of Philosophy, Wayne State University
- [24] Andrade, C. 2011 “Biosensors for detection of Low-Density Lipoprotein and its modified forms” **Biosensors for Health, Environment and Biosecurity**, ISBN: 978-953-307-443-6
- [25] Parka, O.K., Jeevananda, T., Kima N.H., Kim, S.I. and J.H. Lee 2009 “Effects of surface modification on the dispersion and electrical conductivity of carbon nanotube/polyaniline composites” **Scripta Materialia.** 7(60) : 551–554
- [26] Najafi, E. Kim, J.Y., Han, S.H. and Shin, K.W. 2006 “UV-ozone treatment of multi-walled carbon nanotubes for enhanced organic solvent dispersion” **Colloids and Surfaces A- physicochemical and engineering Aspect.** 1(284) : 373–378
- [27] Flahaut, E., Peigney, A., Laurent, Ch., Marliere, Ch., Chastel, F. and Rousset, A. 2000 “Carbon nanotubes-Metal oxide nanocomposites : Microstructure, Electrical conductivity and Mechanical properties” **Acta Materialia.** 14(48) : 3803–3812
- [28] Prasek, J. 2007 “Nanopatterned Working Electrode with Carbon Nanotubes Improving Electrochemical Sensors” **Journal of Nanoengineering and Nanosystems.** 3(221) : 115-119

- [29] Xing, W. Lia, F., Yan, Z.F. and Lu, G.Q. 2004 “Synthesis and electrochemical properties of mesoporous nickel oxide” **Journal of Power Sources**. 2(134) : 324–330
- [30] Liao, X.N., Hub, C.Y., Wanga, Q.L. and Lid, F.Y. 2009 “Preparation of NiO/MWNTs nanocomposites by a simple chemical precipitation method” **Journal of Chinese Chemical Society**. 3(56) : 475-479
- [31] Lee, J.Y., Liang, K., An, K.H. and Lee, Y.H. “Nickel oxide/carbon nanotubes nanocomposite for electrochemical capacitance” **Synthetic Metals**. 2(150) : 153–157
- [32] Zhao, Y., Liu, H., Wang, F., Liu, J.J., Park, K.C. and Endo. M. 2009 “A simple route to synthesize carbon-nanotube/cadmium-sulfide hybrid heterostructures and their optical properties” **Journal of Solid State Chemistry**. 4(182) : 875-880
- [33] Singjai, P., Changsarn, S. and Thongtem S. 2007 “Electrical resistivity of bulk multi-walled carbon nanotubes synthesized by an infusion chemical vapor deposition method” **Materials Science and Engineering A**. 1(443) : 42–46
- [34] Wepasnick, K.A., Smith B.A., Bitter J.L. and Fairbrother, H.D. 2010 “Chemical and structural characterization of carbon nanotube surfaces” **Analytical and Bioanalytical Chemistry**. 3(396) : 1003-1014
- [35] Trana, P.A., Zhang, L. and Webster T.J. 2009 “Carbon nanofibers and carbon nanotubes in regenerative medicine” **Advanced Drug Delivery Reviews**. 12(61) : 1097–1114
- [36] Saito, T., Matsushige, K. and Tanaka, K. 2002 “Chemical treatment and modification of multi-walled carbon nanotubes” **Physica B** 1-4(323) : 280–283
- [37] Li, W., Xie, S., Liu, W., Zhao, R., Zhang, Y., Zhou, W., Wang G. and Qian, L. 1999 “A structure model and growth mechanism for novel carbon nanotubes” **Journal of Materials science**. 11(34) : 2745 – 2749

- [38] Carreno, N.L.V., Nunes, M.R., Garcia, I.T.S., Orlandi, M.O., Fajardo, H.V. and Longo, E. 2009 “Carbon-coated SnO<sub>2</sub> nanobelts and nanoparticles by single catalytic step” **Journal of Nanoparticle Research**. 4(11) : 955–963

## Microwave-Assisted Synthesis of NiO/CNTs Nanocomposites for functional electrochemical working electrode

Papitchaya Woointranont<sup>1,2\*</sup>, Russameeruk Noonuruk<sup>1,2</sup>,  
Boonsong Jandai<sup>3</sup>, Suwan Chaiyasitch<sup>3</sup> and Wisanu Pecharapa<sup>1,2</sup>

<sup>1</sup> College of KMITL Nanotechnology, King Mongkut's Institute of  
Technology Ladkrabang, Bangkok 10520, Thailand

<sup>2</sup> ThEP Center, CHE, 328 Siayutthaya Rd., Bangkok 10400

<sup>3</sup> Department of Chemistry, Faculty of Science, King Mongkut's Institute of  
Technology Ladkrabang, Bangkok 10520, Thailand

\*Corresponding author: p.woointranont@gmail.com

### Abstract

In this work, nickel oxide/carbon nanotubes (NiO/CNTs) nanocomposites were prepared by chemically depositing nickel hydroxide onto carbon nanotubes under microwave irradiation and thermal annealing process. The CNTs were functionalized with 1% sodium dodecyl sulfate (SDS) and stabilized with deionized water before dried at 100 °C for an hour. A series of NiO/CNTs composites with different microwave irradiation powers were extensively characterized by Scanning Electron Microscopy (SEM), X-ray Diffractometer (XRD) and Fourier transform infrared spectroscopy (FT-IR) in order to investigate the physical properties of composites. The SEM results indicated that NiO nanoparticles are well distributed on the surface of CNTs. Cyclic voltammetry was used to investigate current responses of the modified electrode using NiO/CNTs nanocomposites.

**Keywords:** Microwave, Nickel Oxide, Carbon Nanotubes, Nanocomposites, electrochemical electrode

## 1. INTRODUCTION

Carbon nanotubes (CNTs) have attracted worldwide attention since their discovery. Due to their high conductivity and stability at high temperatures, CNTs have been used as a support material for the dispersion and stabilization of metal and semiconductor nanoparticles [1]. It has been reported that CNTs properties can be influenced by surface modification with nanoparticle [2] and metal oxide nanostructure [3]. However, due to the chemically stable and highly hydrophobic nature of carbon nanotubes, surface modification of CNTs is the first step to integrate CNTs to a wide scope of materials. Recently, noncovalent modification with common surfactants is widely used to obtain well-dispersed nanoparticles on CNTs [4]. In this work, sodium dodecyl sulfate (SDS) was chosen to functionalize multi-wall carbon nanotubes (MWNTs) through noncovalent method. Among functional metal oxide materials, Nickel oxide (NiO) is one of cheap transition metal oxides with p-type semi-conductivity, which has stable and wide band gap. It can be prepared by several methods such as sol-gel method and liquid-phase process [5]. However, low specific surface area of NiO is still its major drawback for working electrode application. Combination of NiO and CNT, with the high conductivity and large specific surface area, is expected to provide a chance to improve the performance of pure NiO particles. A simple and rapid synthesis method for metal catalysts using microwave irradiation energy has been suggested [6]. The Microwave Assisted Process (MAP) is a high speed method used to selectively extract target compounds from various raw materials. The advantage of the microwave irradiation is that it transfers heat to the substance uniformly and shorter crystallization time compared to conventional heating.

## 2. EXPERIMENTAL DETAILS

### 2.1 Materials

Pristine multiwall carbon nanotubes (MWCNTs) with nanotube diameters of 20-50 nm synthesized by an infusion

chemical vapor deposition were supported by Research Laboratory for Excellence in Nano and Smart Materials (Chiang Mai University). Further details of CNT synthesis were described elsewhere [7]. Nickel chloride hexahydrate (NiCl<sub>2</sub>•6H<sub>2</sub>O) were purchased from Sigma Aldrich Co., Ltd. NaOH, acetone and deionized (DI) water were used for washing and treatment processes.

### 2.2 Equipment

In the modification of MWCNTs, heater with stirrer was used for the surface modification process and the centrifuge was used for the separation. Thermogravimetric Analysis (TGA), Scanning Electron Microscopy (SEM), X-ray Diffractometer (XRD) Fourier transform infrared spectroscopy (FT-IR) and Cyclic Voltammetry (CV) were used to investigate the physical and electrochemical properties of the composites.

### 2.3 Methodology

NiO/CNT composite were carried out as following procedures. First of all, multiwall carbon nanotubes (2 g) were dispersed in 1 wt% SDS aqueous solution to modify the MWNTs surface by ultrasonication for 1 h. The interaction between MWNTs and SDS due to hydrophobic interactions through the -CH<sub>3</sub> groups is identified to be effective for modifying the surface of MWNTs. After that, the MWNTs were washed with deionized water and separated by centrifuge before dried in oven at 100°C for an hour. The treated MWNTs were immersed in 0.1 M Nickel chloride hexahydrate (NiCl<sub>2</sub>•6H<sub>2</sub>O) solution under stirring at room temperature (~25°C). 0.1 M NaOH solution was then added dropwise to the mixture until the pH 12.00 was reached. After reaction of 24 hours, products were repeatedly rinsed. After that, the mixture was heated at 150 watt for 5 mins in microwave. Finally, the Ni(OH)<sub>2</sub>/CNTs composites were calcined at 300 °C for 2 h to obtain the final product NiO/CNTs. A series of NiO/CNTs composites with different microwave irradiation powers (300 watt and 450 watt) were synthesized by same route. Fluorosilicic acid was mixed with NiO/CNTs

composites before coating on carbon electrode by doctor blade method. Finally, the modified electrode was treated by UV-ozone until dried.

### 3. RESULTS AND DISCUSSION

Thermal-Gravimetric (TG) and Differential-Thermal Analyses (DTA) ascertain the formation of Nickel chloride hexahydrate ( $\text{NiCl}_2 \cdot 6\text{H}_2\text{O}$ ) at a scan rate of  $5^\circ\text{C}/\text{min}$ , in the temperature range  $50\text{--}800^\circ\text{C}$ . Fig.1 shows the TGA and DTA analysis of  $\text{NiCl}_2 \cdot 6\text{H}_2\text{O}$  in air atmosphere. The result indicated that the loss of weight took place in three endothermic peaks at  $83.6$ ,  $190.03$  and  $602.43^\circ\text{C}$  [8]. The regular weight loss starts at about  $190^\circ\text{C}$ , which is due to the transformation of nickel chloride into nickel oxide. This continues up to  $614^\circ\text{C}$ . The calculation of the amount of residue ( $32.2\%$ ) clearly indicates the formation of NiO phase, which remains stable up to about  $800^\circ\text{C}$ .

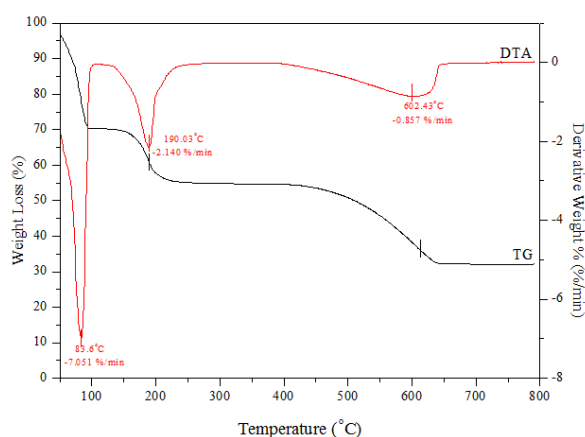


Fig. 1 Typical TG-DTA curve of  $\text{NiCl}_2 \cdot 6\text{H}_2\text{O}$  in the range of temperature  $50\text{--}800^\circ\text{C}$

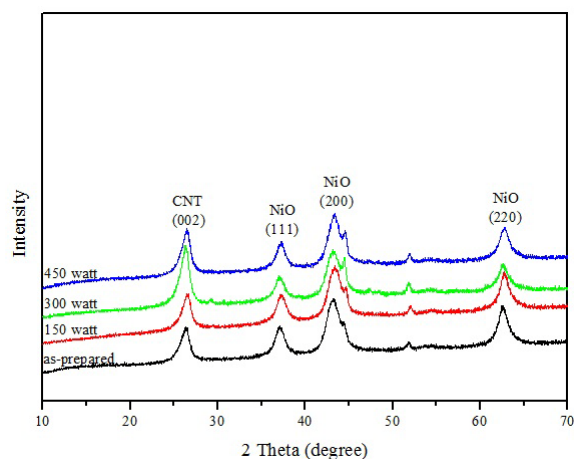


Fig. 2 XRD patterns of NiO/CNT composites annealed at  $300^\circ\text{C}$  with different microwave irradiation powers

Fig. 2 shows the XRD patterns of NiO/CNT nanocomposites prepared at various irradiation power. The diffraction angles at  $2\theta = 37.34^\circ$ ,  $43.38^\circ$  and  $62.66^\circ$  are assigned to (111), (200), (220) planes of the cubic structure of NiO. The peak at  $26.26^\circ$  is nicely indexed to the (002) plane of MWCNTs. From XRD results, it is clear that all composites are mixtures of two phases of wurzite NiO and MWCNTs. The grain size of the crystallites was calculated for major reflex (2 0 0) using the well-known Scherrer's formula:

$$D = \frac{K\lambda}{\beta \cos \theta} \quad (1)$$

Where  $D$  is the grain diameter,  $K$  is the shape factor (0.9),  $\lambda$  is the X-ray wavelength ( $1.5406 \times 10^{-10}$  m),  $\beta$  is the full-width at half maximum and  $\theta$  is the Bragg angle. The calculated average particle sizes of NiO obtained by microwave heating are approximately  $4.7\text{--}4.9$  nm.

The morphology of the NiO/CNT nanocomposites were investigated with SEM. Fig. 3 shows the morphology of the composites prepared by microwave heating with different irradiation power of 150, 300 and 450 watts. The surface of MWNTs were randomly coated by NiO nanoparticles. In addition, there is a part of NiO still existing as grain forms. Amount of NiO nanoparticles attached to the CNT surface and distribution uniformity seem to increase in accordance with the increasing of irradiation power.

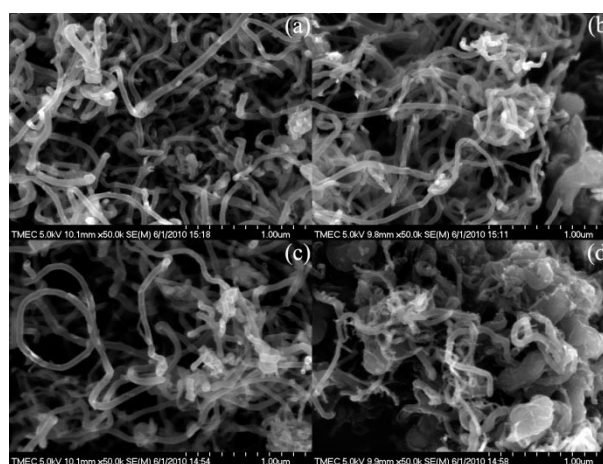


Fig. 3 SEM images of NiO/CNT composites (a) as-prepared (b) 150 watt (c) 300 watt (d) 450 watt

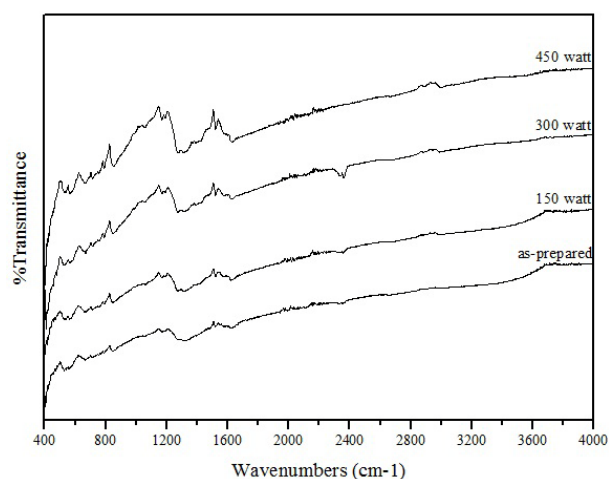


Fig. 4 FTIR spectrum of NiO/CNT composites with different microwave irradiation powers

Fig.4 shows the FT-IR spectra of NiO/CNTs composites prepared at different microwave irradiation powers. The measurement was conducted in the range of  $400\text{--}4000\text{ cm}^{-1}$ . Fundamental  $\text{CO}_2$  vibrations are evident at  $2350\text{ cm}^{-1}$ . The symmetric stretching vibration of  $\text{CO}_2$  is inactive in infrared because there was immutable in the dipole of the molecule. The FTIR spectrum of Ni-O band appears at  $422\text{ cm}^{-1}$  [9] and the band at about  $849\text{ cm}^{-1}$  can be assigned to the

Ni-O-CO<sub>2</sub> group [10]. From the results indicating that the possible growth mechanisms of NiO on CNTs are generated.

Cyclic voltammetry (CV) was employed to determine the electrochemical properties of the NiO/CNTs electrodes in 30 mM K<sub>3</sub>Fe(CN)<sub>6</sub>. Fig. 5 shows the CV curves of the NiO/CNTs with different method and normal electrodes at scan rates of 50 mV/s. The electrode potential is scanned between -0.6 and 0.8 V, and the anodic and cathodic current responses are measured. As shown in Fig. 5, the voltammetric current responses of electrode which is modified by NiO/CNT composite prepared at 450 watt is more efficient than unmodified electrode. Each curve is composed of capacitive current, which originates from the phase of active materials. Microwave irradiation for CNTs creates sufficient Nickels which can act as nucleation sites for Ni(OH)<sub>2</sub> nucleating, resulting a uniform NiO coating layer on CNTs with larger specific surface area, and thus a significant increase in the charge/discharge storage capacity.

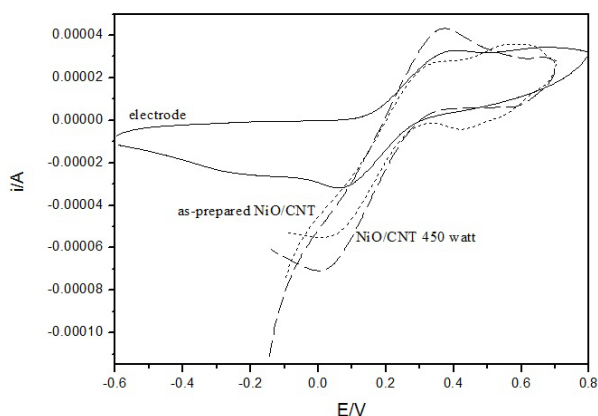


Fig. 5 Cyclic voltammograms of NiO/CNTs with different microwave irradiation powers

#### 4. CONCLUSION

In summary, MWNTs coated with NiO nanoparticles were obtained by a microwave method with the aid of SDS. Comparing to annealing process, microwave irradiation which is simple and quick heating process can effectively assist the formation of NiO nanostructures on CNTs and reduce the synthesized time. The XRD result ensures the formation of NiO nanoparticles on CNTs in form of composites. SEM images reveal that NiO nanoparticles formed by microwave heating are fairly distributed onto the surface of MWCNTs. The CV result indicated that the voltammetric current responses of electrode which is modified by NiO/CNT composite prepared at 450 watt is suitable to be a good factor for make working electrode.

#### 5. ACKNOWLEDGMENTS

This work has partially been supported by the National Nanotechnology Center (NANOTEC), NSTDA, Ministry of Science and Technology, Thailand, through its program of Center of Excellence Network.

#### 6. REFERENCES

- [1] Georgakilas, V., Gournis, D., Tzitzios, V., Pasquato, L., Guldie, D. M. and Prato, M. J. (2007) Decorating carbon nanotubes with metal or semiconductor nanoparticles, *Journal of Materials Chemistry*, 17, pp. 2679-2694
- [2] Zhang, M., Su, L. and Mao, L. (2006) Surfactant functionalization of carbon nanotubes (CNTs) for layer-by-layer assembling of CNT multi-layer films and fabrication of gold nanoparticle/CNT nanohybrid, *Carbon*, 44, pp. 276 – 283
- [3] Wang, X., Xia, B., Zhu, X., Chen, J., Qiu, S. and Li, J. (2008) Controlled modification of multiwalled carbon nanotubes with ZnO nanostructures, *Solid State Chem*, 181, pp. 822 -827
- [4] Kocharova, N., Aaritalo, T., Leiro, J., Kankare, J. and Lukkari, J. (2007) Aqueous Dispersion, Surface Thiolation, and Direct Self-Assembly of Carbon Nanotubes on Gold, *Langmuir*, 23, pp. 3363–3371
- [5] Zhang, FB., Zhou, YK. and Li, HL. (2004) Nanocrystalline NiO as an electrode material for electrochemical capacitor, *Materials Chemistry and Physics*, 83, pp. 260-264
- [6] Tsuji, M., Hashimoto, M., Nishizawa, Y., Kubokawa, M. and Tsuji (2005) Microwave-Assisted Synthesis of Metallic Nanostructures in Solution, *Chemistry - A European Journal*, 11, pp. 440–452.
- [7] Singjai, P., Changsarn, S. and Thongtem, S. (2007) Electrical resistivity of bulk multi-walled carbon nanotubes synthesized by an infusion chemical vapor deposition method, *Materials Science and Engineering*, 443, pp. 42–46
- [8] Al-Hajry, A., Umar, A., Vaseem, M., Al-Assiri, M.S., El-Tantawy, F., Bououdinad, Al-Heniti, M. S. and Hahn, Y.B. (2008) Low-temperature growth and properties of flower-shaped  $\beta$ -Ni(OH)<sub>2</sub> and NiO structures composed of thin nanosheets networks, *Superlattices and Microstructures*, 44, pp. 216-222
- [9] Biju, V. and Abdul Khadar, M.(2003) Fourier transform infrared spectroscopy study of nanostructured nickel oxide, *Spectrochimica Acta*, 59, pp. 121-134
- [10] Yu, P.C. and Lampert, C.M (1987) In-situ Spectroscopic studies of electrochromic hydrated Nickel oxide films, *Optical Materials Technology for Energy Efficiency and solar energy conversion*, 823, pp. 113-123

# Modification of Electrochemical Working Electrode using NiO/MWCNT Nanocomposites Synthesized by Microwave-Assisted Route

Papitchaya Woontranont<sup>1,2\*</sup>, Sirapat Pratontep<sup>1,2</sup>, Wisanu Pecharapa<sup>1,2</sup>

<sup>1</sup> College of KMITL Nanotechnology, King Mongkut's Institute of Technology Ladkrabang, Bangkok, Thailand 10520

<sup>2</sup> ThEP Center, CHE, 328 Siayutthaya Rd., Bangkok, Thailand 10400

\*Corresponding author, e-mail: p.woontranont@gmail.com

## Abstract

The modification of electrochemical working electrode using NiO/CNT nanocomposites was reported in this study. Nickel oxide/carbon nanotubes composites were prepared by chemically depositing nickel hydroxide onto carbon nanotubes under microwave irradiation and thermal annealing process. The as-prepared composites were characterized by Scanning Electron Microscopy and X-ray Diffractometer and the results indicated that NiO nanoparticles are well distributed on the surface of CNT. Current responses of the modified electrode using NiO/CNT nanocomposites demonstrated that the modified electrode with the composite prepared at 450 watt show the superiority in electrocatalytic activity.

## Introduction

Carbon has played a leading role in material science and has become an extensively studied and widely used material. Different forms of carbon ranging from glassy carbon, carbon fibers have been used for diverse electrochemical applications[1]. Nowadays with the investigation of carbon nanotubes (CNT) and their unique electronic, mechanical and chemical properties, CNT has been used as a support material for the dispersion and stabilization of metal and semiconductor nanoparticles[2]. In electrochemical applications the CNT have been usually used as material for metal oxide based composites[3]. Among functional metal oxide materials, Nickel oxide (NiO) is one of cheap transition metal oxides with p-type semi-conductivity, and possesses stable and wide band gap. However, low specific surface area of NiO is still its major drawback for working electrode application. Combination of NiO/CNT, with the high conductivity and large specific surface area, is expected to provide a chance to improve the performance of pure NiO particles. A simple and rapid synthesis method for metal catalysts using microwave irradiation energy has been suggested[4]. The Microwave Assisted Process (MAP) is a high speed dry method. The advantage of the microwave irradiation is that it transfers heat to the substance uniformly and shorter crystallization time compared to conventional heating.

CNT can be also used as a material for working electrodes, because carbon based electrodes are attractive for electrochemical measurements. Among various types of miniaturized electrodes, screen printed electrodes have several advantages including low cost of preparation, easy-to-use and mechanical stability.

## Experiment

Pristine multiwall carbon nanotubes (MWCNT) with nanotube diameters of 20-50 nm synthesized by an infusion chemical vapor deposition were supported by Research Laboratory for Excellence in Nano and Smart Materials, Chiang Mai University, Thailand. The CNT were surface modified by UV-Ozone treatment method for 60 mins to improve the solubility of CNT. The treated MWNTs were immersed in 0.1, 0.5 and 1 M Nickel chloride hexahydrate (NiCl<sub>2</sub>·6H<sub>2</sub>O) solution under stirring at room temperature (~25°C). 0.1 M NaOH solution was then added dropwise to the mixture until the pH 12.00 was reached. After reaction of 24 hours, products were washed with deionized water. After that, the mixture was heated with different microwave irradiation powers at 150, 300 and 450 watts for 5 mins in microwave. Finally, the Ni(OH)<sub>2</sub>/CNT composites were calcined at 300 °C for 2 h to obtain the final product NiO/CNT.

The structure of the samples was determined by powder X-ray diffraction (X'Pert Pro MPD8 PW3040/60). The morphological images were examined by scanning electron microscopy (JSM-6510). The electrodes for electrochemical working electrode were prepared by mixing the prepared powders with Fluorosilicic acid. Then the mixture was coated onto graphite electrode by doctor blade method. Finally, the modified electrode was heat until dried. The working electrode was characterized electrochemically in 1 mM K<sub>3</sub>Fe(CN)<sub>6</sub> solution by potentiostat (PGSTAT302).

## Result and Discussion

As shown in Fig. 1, the XRD patterns of NiO/CNT composites different concentration and microwave irradiation are clearly exhibit typical diffraction peaks of NiO at  $2\theta=35.4^\circ$ ,  $43.7^\circ$ , and  $62.9^\circ$  corresponding to (111), (200), and (220) reflection, respectively. The CNT peak is also seen near  $25.1^\circ$  in different ratio of NiO/CNT composites, which is referred to graphite (002) plane of multi-walled CNT [5]. The small peaks at  $44.8^\circ$ ,  $52.1^\circ$  and  $76.4^\circ$  correspond to the structure of the Ni catalyst. The results have obviously proved that all composites are mixtures of two phases of NiO and CNT. Moreover, the intensity of (200) reflection of NiO becomes stronger as the irradiation power increases suggesting that the crystallinity and formation of NiO onto the CNT surface can be enhanced by sufficient thermal energies supplied to the system via microwave irradiation.

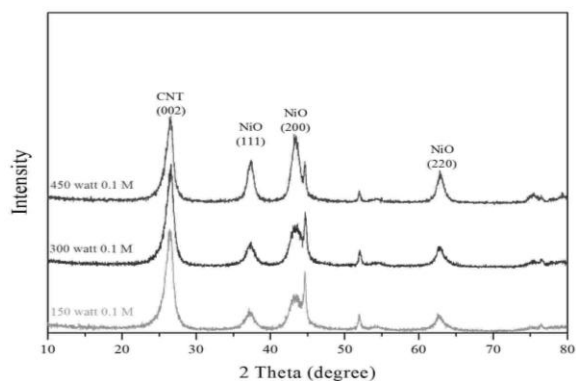


**Fig. 1** XRD patterns of NiO/CNT composites prepared at different microwave irradiation powers and post-annealed at 400°C.

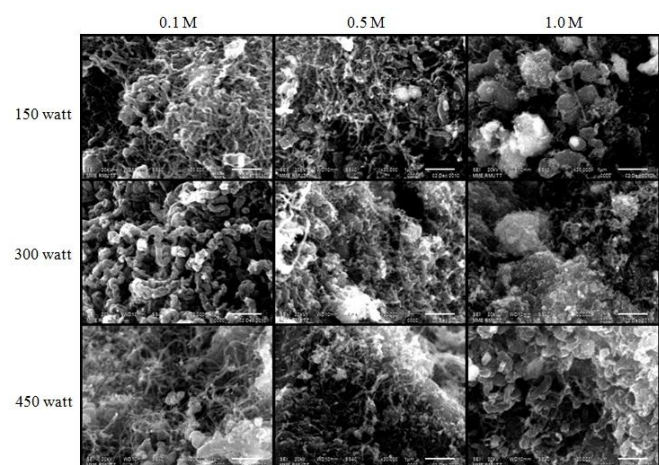


**Fig. 2** SEM images of NiO/CNT composites with different microwave irradiation powers and concentration

The corresponding SEM images as illustrated in figure 2 show the morphology of the composites prepared by microwave heating with different concentration of 0.1, 0.5, 1 M and different irradiation power of 150, 300, 450 watts. The results indicate that the surface of MWNTs were randomly coated by NiO nanoparticles. In addition, there is a part of NiO still existing as grain forms. Amount of NiO nanoparticles attached to the CNT surface and distribution uniformity tends to increase in accordance with the increasing of irradiation power and concentration of precursor.

Cyclic voltammetry measurements were performed to investigate the influence of NiO/CNT composite used as modified materials on the performance of the electrode. The CV measurement was performed in 1 mM  $K_3Fe(CN)_6$  at scan rates of 50 mV/s. The electrode potential was scanned between -1 V to 1 V and the anodic and cathodic current responses are measured. The CV curve indicates that all electrodes have the characteristic of a capacitor with constant charging and discharging rates over a complete cycle. The charging and discharging rates of the modified electrode with NiO/CNT composite is much faster than unmodified electrode. As shown in Fig. 3(a), the voltammetric current responses of electrode modified by NiO/CNT composite prepared at 450 watts is more efficient than unmodified electrode, suggested by the observable higher anodic and lower cathodic peak. Each curve is composed of capacitive current, which originates from the phase of active materials, resulting from a uniform NiO coating layer on CNT with larger

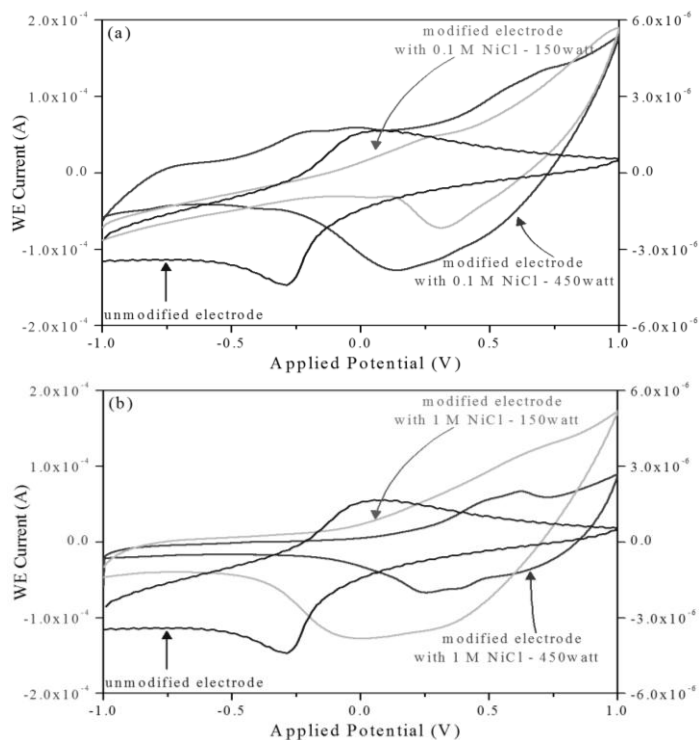


**Fig. 3** Cyclic voltammograms of electrode and modified electrode with (a) different irradiation powers (b) different concentration

specific surface area. For the modified electrode with 0.1 M NiCl heated at 450 watt, an obvious anodic oxidation peak was observed. The anodic peak potential is 142 mV shifting 193 mV toward negative direction compared to modified electrode with 0.1 M NiCl heated at 150 watt. CV results suggest that the performance of working electrode can be enhanced by modification with NiO/CNT composites. The optimized preparation condition of the composite was also notified.

## Conclusion

NiO/CNTs nanocomposites were successfully synthesized by a simple and effective chemical precipitation method and microwave-assisted route. The XRD and SEM results ensured the formation of NiO nanoparticles on CNT in form of composites. The irradiation power and precursor concentration are two main parameters affecting the functional properties of the composite. The significant improvement interpreted from CV results suggest that NiO/CNT composite is suitable as a potential candidate for modified material of electrochemical working electrode.

## Acknowledgements

This work has partially been supported by the National Nanotechnology Center (NANOTEC), NSTDA, Ministry of Science and Technology, Thailand, through its program of Center of Excellence Network.

## References

- [1] J. Prasek, et al., IEEE SENS. J. Korea, pp. 1253-1256. October 2006
- [2] V. Georgakilas, et al., J.Mater Chem 17, pp.2679-2694. 2007
- [3] Y. Zhang, et al., Solid State Ionics 180, pp.1525-1528. 2009
- [4] M. Tsuji, et al., Chem. Eur. J.11, pp. 440-452. 2005
- [5] P. Singjai, et al., Mat Sci Eng A 443, pp. 42-46. 2007

# Study of Acid-Treated Multiwall Carbon Nanotubes by Electron Microscopy and Raman Spectroscopy

Chokchai Kahattha<sup>1\*</sup>, Papitchaya Wointranont<sup>1</sup>, Thanawee Chodjarusawad<sup>1,2</sup> Wisanu Pecharapa<sup>1</sup>

<sup>1</sup>College of KMITL Nanotechnology, King Mongkut's Institute of Technology Ladkrabang, Ladkrabang, Thailand.

<sup>2</sup>Department of Physics, Faculty of Science, Burapha University, Bangsean, Chonburi, Thailand.

\* Corresponding author, e-mail: [choki\\_kung@hotmail.com](mailto:choki_kung@hotmail.com)

## Abstract

In this work, multiwall carbon nanotube (CNT) side-wall surface modification is carried out by treatment in  $H_2SO_4$ ,  $HNO_3$ , and their mixtures. The acid-treated tubes are extensively characterized by mean of transmission electron microscopy (TEM) and Raman spectroscopy. Effects of acid concentration and mixture ratio on their side-wall physical properties were investigated. TEM results show that a number of physical defects are obviously observed on the side walls of the acid-treated CNTs whereas such defects are hardly observed in as-produced CNTs. The results of Raman spectroscopy results suggest that the appropriate mixing ratio between  $HNO_3$  and  $H_2SO_4$  is 1:3 with treatment time of about 60 minutes.

## Background

Because of unique structural, electrical and mechanical properties, carbon nanotubes (CNTs) have been recognized as potential nanomaterials for widespread applications such as biosensors [1], composite materials [2], field emission devices [3] and catalyst supporters [4]. CNTs are acknowledged as an advanced filler for polymers attributed to their outstanding desirable properties, including low density, high tensile strength, high conductivity, and high surface area to volume ratios. In order to improve their functionalized properties and good physical contact, modification of external wall of carbon nanotube is essentially required [5]. Chemical functionalization is one method that improves their functionalized properties to ensure good physical and electrical contact between the tubes and the metal nanoparticles. The functionalization is normally carried out by the pretreatment of the CNTs in HF [5],  $HNO_3$  [6], UV-ozone [7],  $H_2SO_4$  [8] and so on. In this work, the effect of treatment acid including  $HNO_3$  and  $H_2SO_4$  and their mixtures were conducted and interpreted by mean of TEM and Raman spectroscopy measurement.

## Materials and Methods

### Materials

Pristine multiwall carbon nanotubes (MWCNTs) with nanotube diameters of 20-50 nm synthesized by an infusion chemical vapor deposition were supported by Nanomaterials Research Unit (Chiang Mai University). Further details of CNT synthesis were described elsewhere [9]. Sulfuric acid (98 wt%) and nitric acid (70 wt%) were purchased from Labscan Asia Co., Ltd. NaOH, acetone and deionized (DI) water were used for washing and treatment processes.

### Equipment

In the modification of MWCNTs, heater with stirrer was used for the oxidation process and the centrifuge was used for the separation. Raman Spectroscopy and Transmission Electron

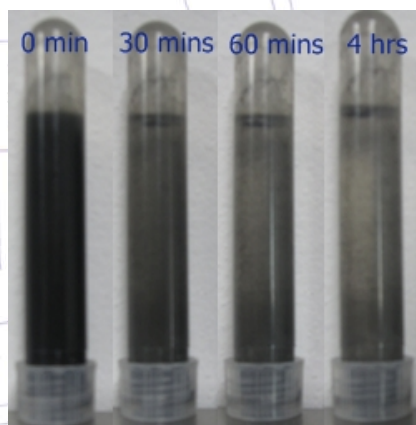


Figure 1 Dispersion stability of Pristine MWCNTs in DI water for various times

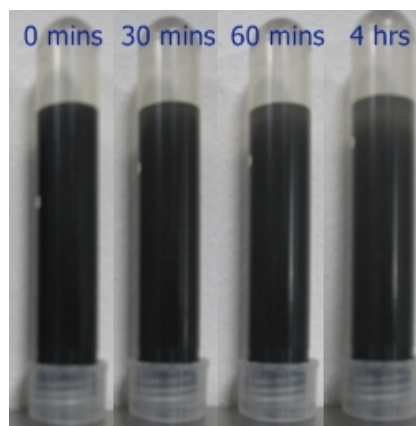
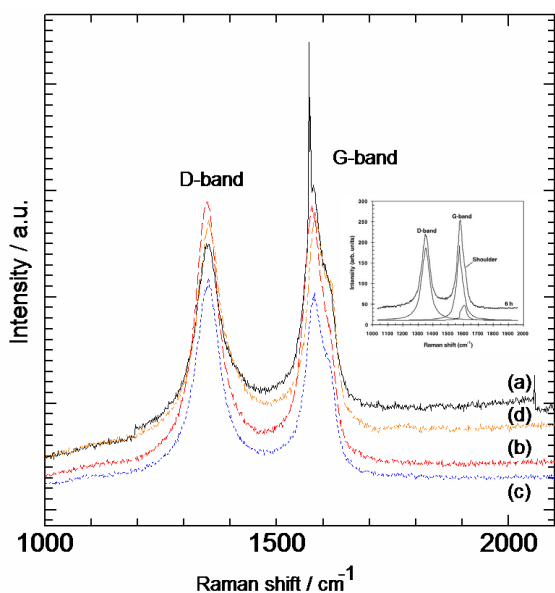


Figure 2 Dispersion stability of treated MWCNTs in DI water for various times



**Figure 3** Raman spectra of MWCNTs treated at the different ratio of HNO<sub>3</sub>/H<sub>2</sub>SO<sub>4</sub> and oxidation time. The inserted image shown Raman spectra of the as-produced MWCNTs without acid treatment process[9]. (a) 1:2 in 30 min (b) 1:3 in 30 min (c) 1:3 in 60 min and (d) 1:3 in 90 min.

Microscopy (TECNAI 20 FEI) were used to investigate the effect of acid modification on the physical properties of MWCNTs.

#### Methodology

Multiwall carbon nanotubes (1.6 g) were washed in acetone and then the filtered MWCNTs was immersed in NaOH for an hour under stirring at room temperature (~25°C). After washing to neutral with DI water and dried at 100°C for an hour, MWCNTs was immersed in 10 mL various types of acid solution which a mixture of HNO<sub>3</sub> and H<sub>2</sub>SO<sub>4</sub>. The suspension was stirred for 15 min before refluxed at 160°C for 60 min. After cooling to room temperature, the MWCNTs were washed with DI water until pH 7 was obtained. The treated MWCNTs were separated by centrifuge and dried in oven at 100°C for 24 hours.

#### Results and Discussion

The dispersion stability of MWNTs in DI water are shown in Figures 1 and 2. In Fig 1, the suspension stability of the pristine CNT agglomerate and lodge to the base of the container. Figure 2 show the dispersion of an acid treated MWNTs. It is obviously seen that, after acid treatment, the dispersion of carbon nanotubes in DI water was improved after the suspension was left for several hours.

Figure 3 shows Raman spectra of the MWCNTs treated at the different ratio of HNO<sub>3</sub>/H<sub>2</sub>SO<sub>4</sub> and oxidation time. Two peaks were observed showing the characteristics of CNTs, the defects of the structure, named D band at 1330 cm<sup>-1</sup> and another bands point is the graphite band at 1580 cm<sup>-1</sup> (G

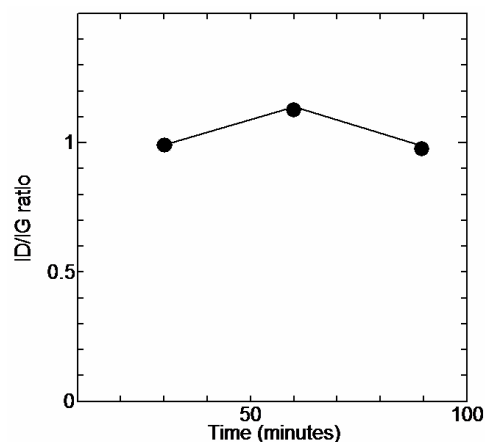


**Figure 4** The ratio between the intensity of the D band and the G band by Acid-treated Method

band). When the acid treatment of CNT was conducted, these observed peaks can still be recognized, indicating that the acid treatment does not destroy the structure of CNT [10]. The ratio between the intensity of the D band and the G band is 0.76, 0.99, 1.13 and 0.98 for CNTs treated by HNO<sub>3</sub>/H<sub>2</sub>SO<sub>4</sub> with ratio of 1:2, HNO<sub>3</sub>/H<sub>2</sub>SO<sub>4</sub> in ratio 1/3 for 30 min, 60 min and 90 min respectively. These results are generally attributed to the presence of more structural defects [11].

Figure 4 shows the  $I_D/I_G$  ratio from Raman spectrum of the MWCNTs treated by HNO<sub>3</sub>/H<sub>2</sub>SO<sub>4</sub> with ratio of 1/3 at 30 min, 60 min and 90 min. This result indicates that the treated MWCNTs in 60 min contain more amount of defects than the MWCNTs treated by other conditions.

Figures 5a and 5b shows TEM images of the as-received MWCNTs and the acid-treated MWCNTs with the mixture of HNO<sub>3</sub>/H<sub>2</sub>SO<sub>4</sub> in ratio 1:3, respectively. In acid treatment process, treating agent can destroy relevant bonds located on surfaces and chemical groups resulting to the existence of physical defects on the side wall of MWCNTs[10]. A number of physical defects on the side wall of acid-treated CNTs are clearly observed meanwhile such defects are hardly observed in as-received CNTs. Furthermore, bending tubes were observed in the pristine MWNTs caused to agglomeration of MWNTs. After oxidation process, the MWNTs were stretched leading to the good dispersion.

In addition, we have synthesized ZnO/CNT composite by microwave-assisted method using acid treated MWNTs. Figure 6 illustrates TEM image of ZnO/CNT composites indicating that ZnO nanoparticles formed by the assistance of microwave heating are firmly attached to the surface of MWCNTs. This feature suggests that acid treatment can modify CNTs with functional groups which are more reactive than the defect-free CNTs and consequently more vulnerable to oxidation [12]. These functional groups consequently initiate the reaction between carbon and ZnO.

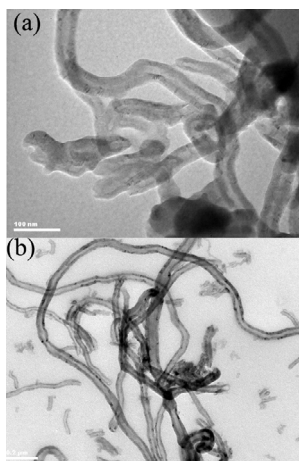


**Figure 5** TEM images of acid-treated MWNTs (a) As -produced CNTs and (b) Acid-treated CNTs with HNO<sub>3</sub>/H<sub>2</sub>SO<sub>4</sub> (1:3 by volume)

### Conclusion

In summary, the side-wall surface modification of MWNTs was accomplished by pretreatment in HNO<sub>3</sub>/H<sub>2</sub>SO<sub>4</sub>. After acid treatment, the dispersion of carbon nanotube in DI water was improved. Raman spectra of the CNTs process to two distinct bands located at 1330 cm<sup>-1</sup> and 1580 cm<sup>-1</sup> which are assigned to D-band and G-band, respectively. The optimized condition interpreted from the ratio between the intensity of the D band and the G band was also obtained. The appearance of functional defects modified by acid treatment can be verified by the formation of ZnO nanoparticles on the side wall of acid-treated CNTs .

### Acknowledgments

This work has partially been supported by the National Nanotechnology Center (NANOTEC), NSTDA, Ministry of Science and Technology, Thailand, through its program of Center of Excellence Network.

### References

1. D. Odaci, A. Telefoncu, S. Timur, Pyranose oxidase biosensor based on carbon nanotube(CNT)-modified carbon paste electrodes, *Sens. Actuators B* 132, 159-165 (2008).
2. J. Gong, J. Sun, and Q. Chen, Micromachined sol-gel carbon nanotube/SnO<sub>2</sub> nanocomposite hydrogen sensor, *Sens. Actuators B*. 130, 829-835 (2008).
3. C.S. Huang, C.Y. Yeh, Y.H. Chang, Y.M. Hsieh, C.Y. Ku, and Q.T. Lai, Field emission properties of CNT-ZnO composite materials, *Diamond Relat. Mater.* 18, 452-456 (2009).
4. H.L. Pang, J.P. Lu, J.H. Chen, C.T. Huang, B. Liu and X.H. Zhang, Preparation of SnO<sub>2</sub>-CNTs supported Pt catalysts and their electrocatalytic properties for ethanol oxidation, *Electrochim. Acta* 54, 2610-2615 (2009).

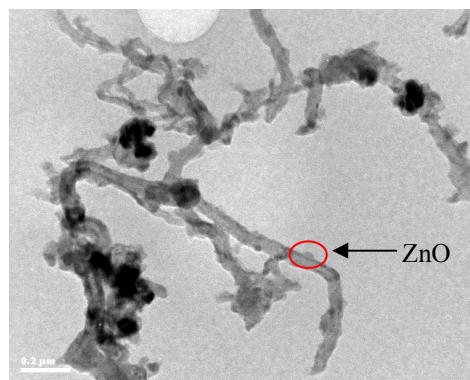


**Figure 6** TEM image of ZnO/CNT composite obtained by microwave irradiation.

5. Yongliang Li, Feng Ping Hu, Xin Wang, Pei Kang Shen, Anchoring metal nanoparticles on hydrofluoric acid treated multiwalled carbon nanotubes as stable electrocatalysts, *Electrochemistry Communications* 10, 1101-1104 (2008).
6. Xiuying Wang, Baiying Xia, Xingfu Zhu, Jiesheng Chen, Shilun Qiu, Jixue Li, Controlled modification of multiwalled carbon nanotubes with ZnO nanostructures, *Journal of Solid State Chemistry* 181, 822-827 (2008).
7. Ebrahim Najafi, Jae-Yong Kim, Song-Hee Han, Kwanwoo Shin, UV-ozone treatment of multi-walled carbon nanotubes for enhanced organic solvent dispersion, *Colloids and Surfaces A: Physicochem. Eng. Aspects* 284-285, 373-378 (2006).
8. Hao Yu, Yuguang Jin, Zhili Li, Feng Peng, Hongjuan Wang, Synthesis and characterization of sulfonated single-walled carbon nanotubes and their performance as solid acid catalyst, *Journal of Solid State Chemistry* 181, 432-438 (2008).
9. P. Singjai, S. Changsarn, S. Thongtem, Electrical resistivity of bulk multi-walled carbon nanotubes synthesized by an infusion chemical vapor deposition method, *Materials Science and Engineering A* 443, 42-46 (2007)
10. A.G.Osorio, I.C.L.Silveira, V.L.Bueno, C.P.Bergmann, H<sub>2</sub>SO<sub>4</sub>/HNO<sub>3</sub>/HCl-Functionalization and its effect on dispersion of carbon nanotubes in aqueous media, *Applied Surface Science* 225, 2485-2489 (2008).
11. Zhi Qun Tian, San Ping Jiang, Yong Min Liang, Pei Kang Shen, Synthesis and Characterization of Platinum Catalysts on Multiwalled Carbon Nanotubes by Intermittent Microwave Irradiation for Fuel Cell Applications, *J. Phys Chem.B* 110, 5343-5350 (2005).
12. X. Jin, W. Zhou, S. Zhang, G.Z. Chen, Nanoscale micro-electrochemical cells on carbon nanotubes, *Small* 3, 1513-1517 (2007).

# Effects of Surface Modification of Carbon Nanotubes on the Deposition of NiO/CNTs Nanocomposites

Papitchaya Wointranont<sup>1,2\*</sup>, Wisanu Pecharapa<sup>1,2</sup>

<sup>1</sup> College of KMITL Nanotechnology, King Mongkut's Institute of Technology Ladkrabang, Bangkok, Thailand

<sup>2</sup> ThEP Center, CHE, 328 Siayutthaya Rd., Bangkok

\*Corresponding author, e-mail: p.wointranont@gmail.com

---

## Abstract

The effect of the surface modification of carbon nanotubes (CNTs) on the formation of nickel oxide/carbon nanotube nanocomposites was investigated. The surface modification was carried out by surfactant treatment, uv-ozone exposure and acid treatment. The nickel oxide/carbon nanotube composites were prepared by chemically depositing nickel hydroxide onto carbon nanotubes under microwave irradiation and a thermal annealing process. Series of composites with various surface modifications were extensively characterized by X-ray diffractometer (XRD) to investigate the crystal structure of the composites. The diffraction angles of XRD results are assigned to the cubic structure of NiO and plane of MWCNTs indicating that the composite is a mixture of two phases of NiO and MWCNTs. The morphology and functional groups of the nanocomposites were observed by Scanning Electron Microscopy (SEM) and Fourier transform infrared spectroscopy (FT-IR), respectively. The results showed that the surface modification of the CNTs has a strong influence on the deposition of the NiO/CNTs composites. It can be concluded that the well-defined formation of NiO/CNT composites was obtained as CNTs were treated by UV-Ozone treatment method.

---

## Background

Carbon nanotubes (CNTs) have been recognized as highly potential sensing materials in many applications according to their unique electrical, optical and mechanical properties. CNTs have been used as a support material for the dispersion and stabilization of metal and semiconductor nanoparticles[1]. It has been reported that CNTs properties can be influenced by incorporated with nanostructured-metal oxide[2]. However, due to the chemical stability and highly hydrophobic nature of CNTs, surface modification of CNTs is the first important step for developing high-performance CNT/metal oxide composites and increasing their dispersion stability. Chemical functionalization is method that can improve their functionalized properties to ensure good physical and electrical contact between the tubes and the metal oxide nanoparticles. Acid-treated CNTs generally contain carboxylic acid and hydroxyl groups, which are the most common functional groups on CNTs [3]. Although this process can increase the dispersion property, it can also have a detrimental effect on the conductivity of the composites because of the morphological damage. Several studies have contributed to study the effects of surfactant on dispersibility and other related properties of CNTs[4-5]. On the other hand, UV-Ozone dry treatment is found to be an effective but relatively simple surface modification process. It has been reported that insignificant severe morphological damages commonly observed in the

case of a conventional acid treatment such as shortening or sharp bending were observed after UV-ozone treatment. In this work, the surface modification of CNTs including acid mixtures, surfactant and UV-Ozone on NiO/CNTs nanocomposites were conducted. The influence of the pre-treatment on the formation of NiO/CNTs composite was investigated by mean of SEM, FTIR and XRD.

## Materials and Methods

### Materials

Pristine multiwall carbon nanotubes (MWCNTs) with tube diameter of 20-50 nm synthesized by an infusion chemical vapor deposition were supplied by Research Laboratory for Excellence in Nano and Smart Materials, Chiang Mai University. Further details of CNT synthesis were described elsewhere[6]. Sulfuric acid (98 wt%) and nitric acid (70 wt%) were purchased from Labscan Asia Co., Ltd. Nickel chloride hexahydrate ( $\text{NiCl}_2 \cdot 6\text{H}_2\text{O}$ ) and Sodium dodecyl sulfate were purchased from Sigma Aldrich Co., Ltd. NaOH, acetone and deionized (DI) water were used for washing and treatment processes.

### Equipment

In the modification of MWCNTs, heater with stirrer was used for the surface modification process. A series of modified NiO/CNTs composites were extensively characterized by X-ray diffractometer (X'Pert Pro MPD PW3040/60)

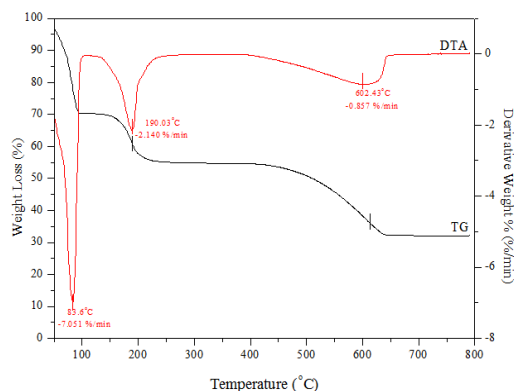


**Figure 1** Typical TG-DTA curve of  $\text{NiCl}_2 \cdot 6\text{H}_2\text{O}$  in the range of temperature 50- 800 °C

which use to investigate the crystal structure of the composites. The fine structure of the composite was investigated by Transmission Electron Microscopy (JEOL JEM-2010). The morphology and functional groups of the nanocomposites were observed by Scanning Electron Microscopy (JSM-6510) and Fourier transform infrared spectroscopy (Spectrum GX FTIR System T904019).

#### Methodology

$\text{NiO}/\text{CNT}$  composites were carried out as following procedures. First of all, multiwall carbon nanotubes (2 g) were dispersed in 1 wt% SDS aqueous solution to modify the CNTs surface under sonication for 1 h. After that, the CNTs were washed with deionized water and separated by centrifuge before being dried in an oven at 100°C for an hour. The raw CNTs were also surface modified with 1:3 mixtures of concentrated  $\text{HNO}_3$  and  $\text{H}_2\text{SO}_4$  at 160 °C for 60 min[3]. In addition, MWNTs treated with UV-Ozone were also prepared ; CNTs were placed in a commercial UV-ozone generator for 60 min. The treated CNTs were immersed in 0.1 M Nickel chloride hexahydrate ( $\text{NiCl}_2 \cdot 6\text{H}_2\text{O}$ ) solution under stirring at room temperature ( $\sim 25^\circ\text{C}$ ). 0.1 M NaOH solution was then added dropwise to the mixture until the pH 12.00 was reached. After reacting of 24 hours, products were repeatedly rinsed. After that, the mixture was heated under microwave irradiation at 450 watt for 5 min. Finally, the  $\text{Ni}(\text{OH})_2/\text{CNTs}$  composites were calcined at 400 °C for 2 h to obtain the final product of  $\text{NiO}/\text{CNTs}$ . The composites formed from CNTs treated with acid mixture, UV-Ozone and SDS were designated as A-Cl, U-Cl and S-Cl, respectively.

#### Results and Discussion

Figure 1 shows the TGA and DTA analysis of Nickel chloride hexahydrate ( $\text{NiCl}_2 \cdot 6\text{H}_2\text{O}$ ) in air atmosphere for ascertain the formation of sample at a scan rate of 5°C/min, in the temperature range 50–800°C. The result indicated that the loss of weight took place in three endothermic peaks at 83.6, 190.03 and 602.43°C. The regular weight loss

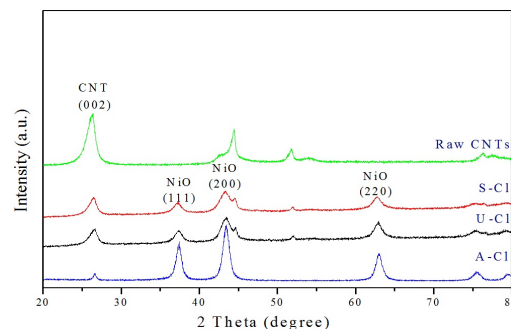
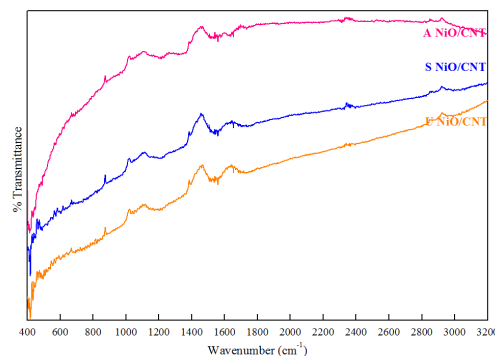


**Figure 2** XRD patterns of  $\text{NiO}/\text{CNT}$  composites annealed at 400°C with different treatment

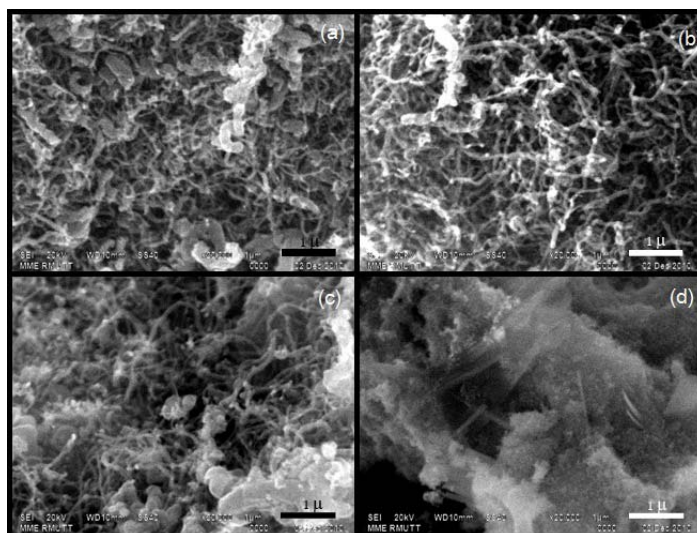
starts at about 190°C, which is due to the transformation of nickel chloride into nickel oxide[6]. This characteristic continues up to 614°C. The calculation of the amount of residue (32.2%) clearly indicates the formation of  $\text{NiO}$  phase, which remains stable up to about 800°C.

Figure 2 shows the XRD patterns of  $\text{NiO}/\text{CNT}$  nanocomposites prepared by different modification method. The diffraction angles at  $2\theta = 37.34^\circ$ ,  $43.38^\circ$  and  $62.66^\circ$  are assigned to (111), (200), (220) planes of the cubic structure of  $\text{NiO}$  (JCPDS-ICDD No.895881). The peak at  $26.26^\circ$  is nicely indexed to the (002) plane of CNTs (JCPDS-ICDD No.751621) and the small peaks at  $44.5^\circ$ ,  $51.8^\circ$  and  $76.4^\circ$  correspond to the structure of the Ni catalyst. These XRD features exhibit that all composites are mixtures of two phases of  $\text{NiO}$  and CNT. Moreover, comparing to U-Cl and S-Cl samples, the intensity of (002) reflection of CNTs of A-Cl sample significantly decreases, implying that acid-treated method may cause the structural destruction of CNTs.

FT-IR measurements of  $\text{NiO}/\text{CNT}$  composites prepared by three different modification methods were carried out in the range of 400-3200  $\text{cm}^{-1}$  and the corresponding results are shown in Fig. 3. The chemical composition of  $\text{NiO}/\text{CNT}$  composite was scrutinized by correlating the developed peaks in the spectrum to the bond, vibration, or stretching of various functional groups. The band located at 408  $\text{cm}^{-1}$  and 885  $\text{cm}^{-1}$  from treated sample can be



**Figure 3** FTIR spectra of surface modified  $\text{NiO}/\text{CNT}$  nanocomposites



**Figure 4** SEM images of (a) surfactant treated NiO/CNT composite (b) UV-ozone treated NiO/CNT composite and (c) acid treated NiO/CNT composite

assigned to nickel oxygen interaction[7] and Ni-O-CO<sub>2</sub> group[8] which indicates the formation of NiO structure. For A-Cl, the band at 1405 cm<sup>-1</sup> can be assigned to the bending vibration of C-H groups[9], which may originate from the strong HNO<sub>3</sub> and H<sub>2</sub>SO<sub>4</sub> treatment resulting to the obstruction of the formation of NiO particles on the CNT surface as shown in SEM image. The noticeable band at about 1520 cm<sup>-1</sup> and 1600 cm<sup>-1</sup> appeared in all samples attributes to the C=C aromatic stretching and the stretching of C=O bond located near the oxygen containing groups[8], respectively. The results indicate the existence of oxygen-containing functional groups such as hydroxyl and carboxyl groups on the CNTs. These functional groups may originate from the UV and surfactant treatment process or the weak oxidation in air. [10].

Fig. 4 shows the SEM images of the surface-treated CNTs and NiO/CNTs composites. The SEM images clearly indicate the NiO deposited over the surface-modified CNTs. The SDS treatment of the raw CNTs does not produce a uniform layer of NiO on their surface as shown in Fig. 4(a). As seen in Fig. 4(b), the SEM image reveals that the CNTs treated with the UV-ozone have more uniform coating ability of NiO compared to the CNTs treated with SDS and acid mixture. Furthermore, the SEM image of acid treated sample exhibits the formation of NiO cluster covering thoroughly the CNT matrix. This ill-defined formation of NiO cluster may originate from the acid induced C-H group on CNT, which obstruct the formation of NiO particles on the CNT surface.

The formation of NiO particles onto the CNT surface can be confirmed by TEM image as shown in Fig. 5. As seen in the figure, the combination of nanorod-like structure and quasi-spherical shape

NiO structures are tightly connected to the CNT walls. The inset of Fig.5 shows the corresponding selected area electron diffraction (SAED) pattern of NiO particle. ED patterns and diffraction rings are well agreeable to XRD peaks, which suggests that the NiO nanoparticles are polycrystalline. The rapid formation and nucleation of NiO onto CNTs may be described from the fact that the dehydration of Ni(OH)<sub>2</sub> resulting to the crystallization of NiO can be obtained by uniformly heating under microwave irradiation [11] and the composite of NiO and MWCNT is finally achieved.

### Conclusion

The surface modification of CNTs is the first step for developing high-performance CNT/metal oxide composites and increases their dispersion stability. The results showed that the surface modification of the CNTs has a strong influence on the deposition of the NiO/CNTs composites. It can

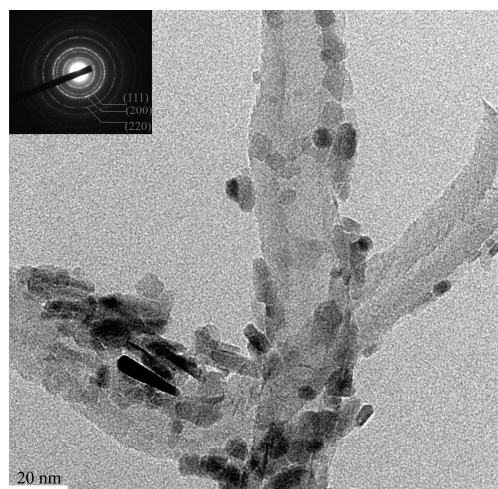


**Figure 5** TEM image of NiO/CNTs composites and the inset is the corresponding SAED pattern

be concluded that, among three treatment methods, the UV-ozone treatment of CNTs greatly improves the dispersion stability. In addition, this method did not produce any severe morphological damage, such as shortening or sharp bending, compared to acid method. The deposition of NiO on UV-treated CNTs wall was clearly improved, compared to a surfactant method. Moreover, Acid treatment may cause the C-H group on the CNT surface leading to the formation of ill-defined NiO cluster.

#### Acknowledgements

This work has partially been supported by the National Nanotechnology Center (NANOTEC), NSTDA, Ministry of Science and Technology, Thailand, through its program of Center of Excellence Network. Authors would like to thank Rajamangala University of Technology Thanyaburi (RMUTT) for XRD and SEM measurement.

#### References

1. V. Georgakilas, D. Gournis, V. Tzitzios, L. Pasquato, D.M. Guldie and M.J. Pratod, Decorating carbon nanotubes with metal or semiconductor nanoparticles, *J. Mater. Chem* 17, 2679-2694 (2007).
2. X. Wang, B. Xia, X. Zhu, J. Chen, S. Qiu and J. Li, Controlled modification of multiwalled carbon nanotubes with ZnO nanostructures, *Solid State Chem* 181, 822 - 827 (2008).
3. C. Kahattha, P. Wointranont, T. Chodjarusawad and W. Pecharapa, Study of Acid-Treated Multiwall Carbon Nanotubes by Electron Microscopy and Raman Spectroscopy, *J. Microsc. Soc. Thailand* 24, 133-135 (2010).
4. L. Vaisman, G. Marom, HD. Wagner, Dispersions of surface - modified carbon nanotubes in water-soluble and water-insoluble polymers, *Adv Funct Mater* 16, 357-363(2006).
5. M.S. Strano, V.C. Moore, M.K. Miller, M.J. Allen, E.H. Haroz, C. Kittrell, The role of surfactant adsorption during ultrasonication in the dispersion of single-walled carbon nanotubes. *J Nanosci Nanotechnol* 3, 81-86(2003).
6. J.K. Dong and G.K. Sun, Morphologies and properties of NiO particles prepared from NiCl<sub>2</sub>·6H<sub>2</sub>O by spray pyrolysis, *J. Chem. Eng. Korean* 26, 1800-1805 (2009).
7. S. Goyanes, G.R. Rubiolo, A. Salazar, A. Jimeno, M.A. Corcuera, and I. Mondragon, Carboxylation treatment of multiwalled carbon nanotubes monitored by infrared and ultraviolet spectroscopies and scanning probe microscopy, *Diam. Relat. Mater* 16, 412-417 (2007).
8. B.P. Das, M. Panneerselvam, and K.J. Rao, A novel microwave route for the preparation of ZrC-SiC composites, *J. Solid State Chem* 173, 196-202 (2003).
9. H.L. Hsu, J.M. Jehng and Y.C. Liu, Synthesis and characterization of carbon nanotubes synthesized over NiO/Na-montmorillonite catalyst and application to a hydrogen peroxide sensor, *Mater. Chem. Phys* 113, 166-171 (2009).
10. E. Najafi, JY.Kim, SH Han and K. Shin, UV-ozone treatment of multi-walled carbon nanotubes for enhanced organic solvent dispersion, *Colloid Surface A* 284, 373-378 (2006).
11. Y. Wang, J. Zhu, X. Yang, L. Lu, X. Wang, Preparation of NiO nanoparticles and their catalytic activity in the thermal decomposition of ammonium perchlorate. *Thermochim Acta* 437: 106-109 (2005).

